ARL 70-0138
AUGUST 1970

Aerospace Research Laboratories

THERMOLUMINESCENCE OF THORIUM OXIDE SINGLE CRYSTALS

ELWARD T. RODINE
SYSTEMS RESEARCH LABORATORIES, INC.
DAYTON, OHIO

CONTRACT NO. AF33615-69-C-1017
PROJECT NO. 7021

This document has been approved for public release and sale; its distribution is unlimited.

AIR FORCE SYSTEMS COMMAND

United States Air Force

NOTICES

When Government drawings, specifications, or other data are used for any purpose other than in connection with a definitely related Government procurement operation, the United States Government thereby incurs no responsibility nor any obligation whatsoever; and the fact that the Government may have formulated, furnished, or in any way supplied the said drawings, specifications, or other data, is not to be regarded by implication or otherwise as in any manner licensing the holder or any other person or corporation, or conveying any rights or permission to manufacture, use, or sell any patented invention that may in any way be related thereto.

Agencies of the Department of Defense, qualified contractors and other government agencies may obtain copies from the

Defense Documentation Center
Cameron Station
Alexandria, Virginia 22314

This document has been released to the

CLEARINGHOUSE
U. S. Department of Commerce
Springfield, Virginia 22151

for sale to the public.

Copies of ARL Technical Documentary Reports should not be returned to Aerospace Research Laboratories unless return is required by security considerations, contractual obligations or notices on a specified document.

300-October 1970-CO105-7-71-130

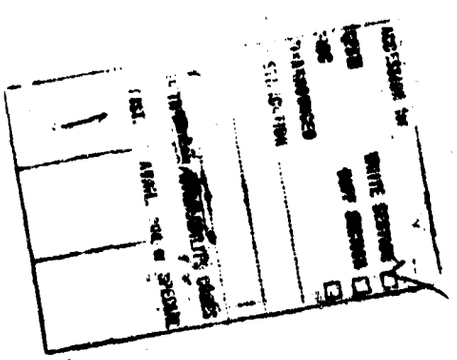

ARL 70-0138

THERMOLUMINESCENCE OF THORIUM OXIDE SINGLE CRYSTALS

ELWARD T. RODINE

SYSTEMS RESEARCH LABORATORIES, INC.
7001 INDIAN RIPPLE ROAD
DAYTON, OHIO 45440

AUGUST 1970

CONTRACT NO. AF33615-69-C-1017
PROJECT NO. 7021

AEROSPACE RESEARCH LABORATORIES
AIR FORCE SYSTEMS COMMAND
UNITED STATES AIR FORCE
WRIGHT-PATTERSON AIR FORCE BASE, OHIO

FOREWORD

This is an interim technical report summarizing the work on the thermoluminescence of ThO_2 completed to this date by Systems Research Laboratories, Inc., Dayton, Ohio, on Contract AF33615-69-C-1017 for the Aerospace Research Laboratories, Office of Aerospace Research, United States Air Force. This contract was initiated under Project 7021, "Structure and Properties of Solids," under the technical cognizance of Dr. Henry Graham of the Metallurgy and Ceramics Research Laboratory of ARL. This report covers work conducted from July 1968 to May 1970.

The experimental work under this project was conducted within the facilities of the Aerospace Research Laboratories, Wright-Patterson Air Force Base, Ohio, with the close technical cooperation of Dr. Peter L. Land of ARL.

ABSTRACT

This report contains the results of measurements of the thermoluminescence between liquid nitrogen temperature and 300°C of a large number of ThO_2 single crystals. These results indicate that the same traps occur commonly in crystals grown by different methods and which differ considerably in purity, although there are substantial differences in apparent trapping densities. The most important glow peaks have maxima at about -160°C, -120° to -100°C, -14°C and 150°C. The maxima of the thermoluminescence excitation spectra and the ultraviolet cutoff are shown to coincide, indicating that some trap excitation involves a band gap transition and that the band gap is 5.75 eV. The thermoluminescence emission spectra observed in this investigation are quite broad in some cases but in other cases they are the sharp line spectra of particular rare earths. The fluorescence emission for some of these ThO_2 crystals appears to be identical to the thermoluminescent emission. Dosage studies on these crystals indicate relative trap densities and show cases of linear and quadratic growth of thermoluminescence with dose. Excitation due to the radioactivity of thorium is observed in some of these crystals. Energy and frequency factor analysis of the trapping states is performed, and comparison is made between the results obtained by applying the methods of initial rise, inflection points, and halfwidths according to monomolecular and bimolecular models. The thermoluminescence experiments discussed in this report are correlated with each other and with EPR measurements. This investigation shows that as few as 10^{10} optical transitions are necessary for a resolvable glow peak and that concentrations of rare earth impurities of less than 1 ppm may result in bright thermoluminescence. No correlation between the thermoluminescent trapping states and specific impurities was determined. There are strong indications that the trapping states are due to intrinsic defects involving oxygen vacancies, and several models are proposed and correlated with the experimental results.

TABLE OF CONTENTS

V EXPERIMENTAL RESULTS (cont)

LIST OF ILLUSTRATIONS

LIST OF TABLES

Section I

INTRODUCTION

The defect structure can influence and in some cases determine the physical properties of a solid. A fundamental understanding of the defect structure is necessary for the characterization of the material and also for the interpretation of many physical properties. The defect structure of a material can, and in fact should, be studied by a number of different methods, such as electrical, mechanical, thermal, optical and magnetic techniques that measure the properties of the defects under a variety of conditions.

A study of the optical properties of relatively wide band gap materials such as ThO_2 at moderate or low temperatures enables one to obtain information about the electronic structure of the defects. The optical transitions are fundamentally related to the energy structure of the host lattice and to the electronic states of the defects which may be in the normally forbidden regions of the energy states. Point defects in the forms of impurities and/or stoichiometric defects can be expected to have stable and metastable excited states between which optical transitions may take place. The study of these defects or impurity states by means of carefully controlled cyclic electronic rearrangement within the defects can lead to a basic understanding of the nature of the defects and to a characterization of the material with its associated defects. Such a study can result not only in the identification and understanding of particular defects but also can lead to techniques which control the defects through enhancement or quenching for suitable applications.

Thermoluminescence is one useful method for studying the cyclic processes among defects, and this has not been fully exploited in previous investigations. The excitation can yield information about the absorption of the crystal and its defects and the emission can yield information about the recombination process. A study of the glow peaks can determine the thermal activation energies, kinetics, and multiplicities of the peaks. Each major stage of the cyclic rearrangement can be at least partially studied by the variation of selected parameters, permitting a more detailed distinction between the various models that are possible.

In this study, the thermoluminescence of thoria has been characterized by means of a number of related experiments. These studies have been correlated with complementary studies of fluorescence, absorption, and spin resonance. The opportunity exists for further correlation with electrical and thermal studies for more complete characterization of the defect structure.

In the following section, we shall consider thermoluminescence theoretically. Some of the basic parameters are defined and suitable forms for the rate equations are developed. These equations are applied to specific models to yield expressions for the glow which can be compared with experimental data. The theoretical ideas are used to define or suggest experimental procedures. Each of the experiments is discussed with regard to the information to be gained concerning the characterization and identification of the processes.

The experimental apparatus used in the laboratory will be discussed and the procedures used in each experiment will be described with particular emphasis on the controlled variation of the many parameters involved. It will be shown that the equipment is quite flexible so that one can perform many experiments with one basic setup. We will discuss some details of the spin resonance experiments in a later section.

Detailed experimental data on the thermoluminescence of thoria are shown and discussed. Data from undoped and rare earth doped single crystals from several sources and grown by several different methods are shown. The crystals used represent a wide variation of impurity content and the role of impurities in the thermoluminescence of thoria is discussed. The data are analyzed with respect to the theoretical concepts developed in the next section and on the basis of the experimental results of other studies made on different materials as well as previous experiments on thoria.

It is shown that each set of measurements places restrictions and requirements on an eventual complete model of the defect structure as well as providing data for the construction of a model. It is shown that each set of measurements can be correlated with the other measurements for a more complete description. Some specific models will be proposed for particular thermoluminescence peaks, and specific requirements on the models in general will be defined. Suggestions are made for future experiments to further define the defect structure and thermoluminescence mechanisms.

Section II

THEORETICAL CONSIDERATIONS

Thermoluminescence and related photoelectronic processes can be phenomenologically described by reference to a band picture, as shown in Figure 1. Such a picture must, of course, be considered as a simplification of the actual situation. In a real crystal, many types of defects and many different models would be expected to occur. A real crystal will generally have local variations of composition, crystal structure, impurity content and surface discontinuities giving a wide variety of defect states and corresponding electronic energies. Also, each electronic rearrangement such as excitation, emission, and trapping causes changes in the levels, spacings, and densities of the energy states. The problem is to represent a dynamic situation with a static diagram. However, particular defects can be discussed in detail with respect to specific models; the parameters can be defined and experiments to measure the parameters can be suggested.

Therefore, while realizing the limitations involved, it is reasonable to consider the band picture in Figure 1. Thoria is an insulator, so the valence band is nearly filled and the conduction band is nearly empty. Defects in the material cause new energy levels to occur in the normally forbidden band gap and these may act as charge sources, traps, and recombination centers. The thermoluminescent process occurs after electrons are excited from the sources to the metastable traps; subsequent heating of the sample causes the electrons to be released from the traps so that they decay into the recombination centers by either radiative or nonradiative transitions. Thermoluminescent glow curves are plots of the radiative intensity vs. time or temperature; each peak generally indicates the emptying of a particular trapping level. The peak temperatures are approximately proportional to the thermal activation energies, i.e., a high temperature peak represents a "deep" trap and has a higher activation energy than a low temperature peak.

SIMPLE MODELS

One of the more simple models that can be envisioned is the photoconducting model shown in Figure 1. This model is characterized by charge transport via the energy bands of the host crystal. Electrons are excited from sources near or in the valence band to the conduction band where they are free to move until they recombine by a luminescent or nonluminescent transition or are captured by a trap. Thermal activation by heating or optical activation by infrared bleaching releases the trapped electrons to the conduction band from where they may make luminescent transitions to the recombination centers or they may be retrapped by either type of recombination. An analogous case can be constructed for hole processes through the valence band. The distinguishing feature of this model is the charge transport by the bands. This implies that photoconductivity may be observed during excitation, and thermally stimulated currents (TSC) may be observed during heating. There is also the possibility of observing thermally stimulated exo-electrons (TSE).

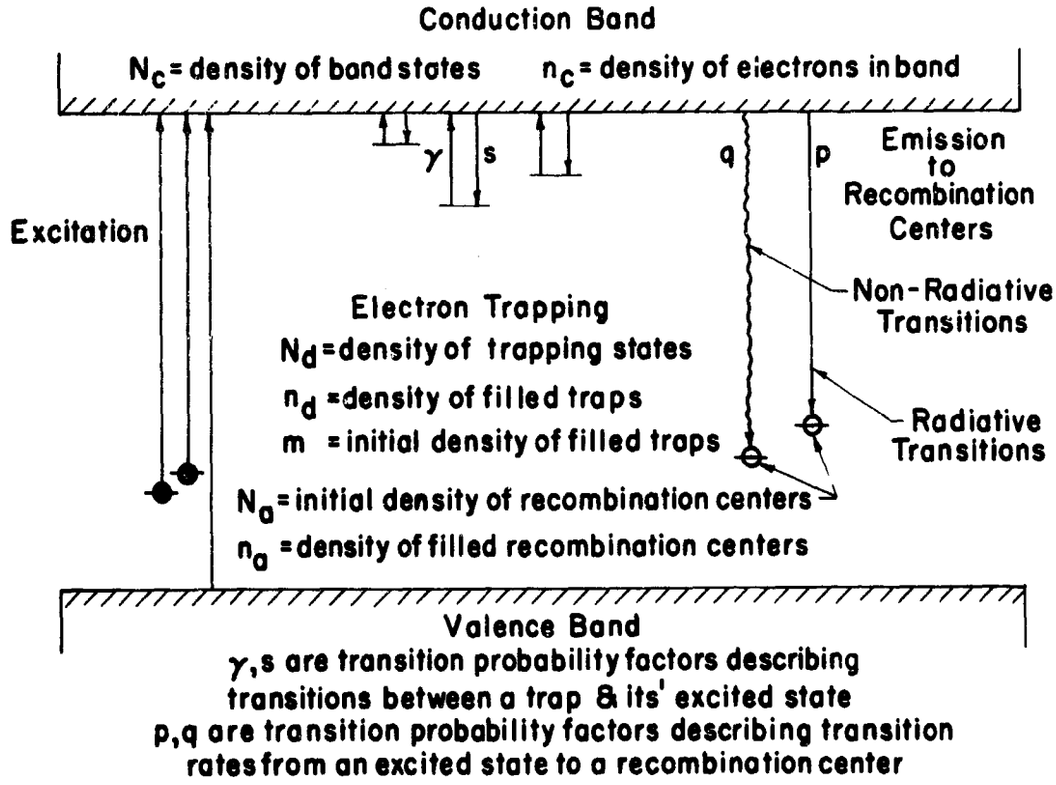

Figure 1. Band picture for photoelectronic processes

Another elementary model is the localized model. In this case, the charge source, trap, and recombination center all belong to one defect and the excitation, trapping, and emission all take place within this defect. There is no charge transport via the bands; hence there is no photoconductivity or thermally stimulated currents. KC1(T1) is a typical example, as are some rare earth doped materials.

There are, of course, variations of these models which might be expected in a real crystal. The excitation process may be through a band, as discussed above, or may be direct to the trapping site. A very reasonable alternate would be that excitation is to an excited state of the trap which may or may not be an excited state of the other traps. The emission may be through the band or through an excited state similar to that for excitation, but possibly at a different energy. Once the carrier has been thermally excited from the trap the recombination may be direct and immediate or the carrier may be retrapped, either by the trap from which it came or by a deeper trap. The strength and type of retrapping has an effect on the shape and peak temperatures of the glow curves and will be discussed below. Nonradiative transitions occur at many stages of the cyclic process and may compete with the radiative transitions. Hence it is impossible to define all steps of the cycle on the basis of optical measurements.

B. EXCITATION

The excitation of thermoluminescence is accomplished by the absorption of energy by electrons in the valence band or in discrete states near the valence band followed by the capture or trapping of the electrons by a metastable state near the conduction band. The intermediate states through which the electrons pass depends on the particular model. Figure 1 shows the process for the photoconduction or band model: for the localized model the excitation would have to be to an excited state of the trap. The actual trapping may be by one or more low energy luminescent transitions or by thermal relaxation.

The spectral dependence of excitation is a measure of the energy difference between the charge source and the excited states of the traps or the conduction band and may be a measure of the width of the energy states involved. The observation of photoconductivity during the excitation of thermoluminescence would be a good indication of a band gap transition. The coincidence of the ultraviolet cutoff with the excitation efficiency maximum would also indicate a band-to-band transition. The excitation may be through absorption bands caused by impurities or stoichiometric defects, in which case the excitation spectra of the thermoluminescence would not be coincident with the ultraviolet cutoff or peaks in the photoconductivity. The excitation of the thermoluminescence need not be identical for all glow peaks. Preferential excitation of particular traps may indicate a localized process and permit the study of individual traps in a manner independent of the other traps. The excitation spectra of the thermoluminescence can sometimes be understood more clearly by comparing it with the excitation spectra of the fluorescence. Both phenomena are consequences of the allowed optical transitions in a material.

The coincidence of or differences between the two types of measurement may help in the identification of the states utilized in the thermoluminescence excitation. For example, large spectral differences between the two measurements would indicate that the ions participating in the fluorescence do not contribute to the thermoluminescence excitation. A degradation of the fluorescence as a function of time could indicate the participation of the fluorescing ions in the excitation of the thermoluminescent traps.

Thermoluminescence can also be excited by the use of high energy radiation or particles such that atomic displacement or very deep energy states are utilized. This investigation is concerned primarily with the study of electronic levels in or near the band gap; hence excitation was performed with ultraviolet light.

C. DOSAGE

The amount and character of the thermoluminescent glow also depend on the time of excitation. The maximum glow possible from a crystal, as well as the amount of glow for a given dose, depends on the total number of charge sources available and the total number of trapping states available. The number of sources and traps available are not necessarily equal. Saturation can be achieved by a depletion of charge sources, by the filling of available traps, by the depletion of recombination centers, or by the establishment of an equilibrium between excitation and optical bleaching.

An assumption which is usually made and appears to be quite reasonable is that the total glow (the area under the glow curve) is proportional to the number of charges trapped. The proportionality may change with irradiation dose because of a change in retrapping, a depletion of available recombination centers, or an increase of nonradiative transitions. Assuming a constant proportionality between the number of charges trapped and the total glow, one can speculate as to the number of charges trapped as a function of irradiation time. Halperin[1] has proposed that a plot of the total glow vs. dose on a log-log plot will yield a straight line of integer slopes, i.e., for low dose conditions,

$$n_d \propto t^x \qquad (1)$$

where n_d = number of charges trapped
t = time of excitation
x = integer

The intercept of a log-log plot of Eq (1) would specify a complicated proportionality factor that is dependent on the wavelength, the densities of states of the sources and traps, and the transition probabilities.

Halperin[1] has observed for diamond a linear (x=1) growth rate with excitation near the band edge and a superlinear growth rate (x=2 or 3) with excitation far from the band edge. Halperin proposed that the latter is due to a two or three step excitation process. A linear growth rate is commonly observed in dosimetry studies on CaF_2[2] or LiF[3] with high energy excitation (x-rays, gamma rays, high energy electrons). Also observed in dosimetry studies[4] is a superlinear growth rate which is attributed either to the creation of traps or recombination centers or to the action of deep traps. In this investigation, we have observed primarily linear growth rates and also some sublinear and superlinear behavior including non-integer values of x.

Deep traps which are not emptied between excitations can absorb much of the excitation energy. If the deep traps are not emptied they become inactive after a few runs and succeeding runs are characteristic of a new set of cyclic conditions. This would be observed as a long term degradation of thermoluminescent efficiency which could be restored by high temperature annealing. Halperin[5] has observed such behavior in KC1. This could also cause apparent saturation if absorption by the deep traps caused the sources to be depleted so there could be no further growth of the shallower traps even if they were unfilled.

From dosage studies, one is able to extract useful information about the thermoluminescence. At saturation conditions, the areas under the individual peaks give a good measure of the relative strengths of the peaks and may imply the total number of trapping states or defects in the crystal. The rate of growth, shape of growth curve, dose necessary for saturation, final saturated strength, and changes of peak temperature and shape can be used to characterize the peaks, identify the principal peaks, and contribute to the construction of a model.

Dosage curves are also useful when determining the experimental conditions for other experiments. For example, an excitation spectrum is determined using monochromatic light and the total dose level is usually very much less than saturation conditions. There will be variations of total dose for the different wavelengths used in the many runs needed for a complete spectra, so it is important that conditions be selected such that the dosage curves are all as straight and parallel as possible to minimize the effect of changing dose levels.

D. THERMAL ACTIVATION

One can describe the analysis of the thermoluminescent glow with the aid of the quantities shown in Figure 1. Particular attention is called to the electron traps and the three densities of states shown, the recombination centers and their densities of states, and the band states. Also to be noted are the transition probability factors γ, s, p, q. These quantities assume slightly different meaning for different models. It is often advantageous to consider the localized model, in which case an excited state of the trap is considered instead of the transport through the conduction band. In this treatment is is assumed that excitation has ceased and that the trapped electrons are "frozen" into the metastable traps. Also, only one trapping state, one excited state, and one recombination center will be considered, so that resulting glow curve would consist of just one isolated peak.

One can generate theroretical glow curves from simple models like that in Figure 1. The basic assumption for all models is that the trapped charge is thermally activated, and that

$$\gamma = se^{-E/kT} \tag{2}$$

where E is the thermal activation energy, k is the Boltzmann constant and T is the temperature in degrees Kelvin. Equations can be written for a model that relate the time derivatives of the occupation numbers for the states assumed in a model and that allow for conservation of charge. The solutions to the time derivative equations have simple analytical forms in general only for localized models, but, with specific conditions, band models or overlap transfer models do permit simple analytical forms.

The rate equations where $\dot{n} = dn/dt$ and t = time, for monomolecular kinetics (mono implies a linear equation) is,

$$\dot{n}_d = -n_d \gamma \tag{3}$$

where again n_d is the number of trapped electrons.

Since the thermoluminescent intensity $I(T) = dn_d/dt$ and the heating rate $\beta = dT/dt$, solution of the above equation yields,

$$I(T) = m\varphi e^{-E/kT} \exp\left[-\int_{T_i}^{T} \varphi e^{-E/kT} \frac{dT}{\beta}\right] \tag{4}$$

where m is the initial density of filled traps. The frequency factor φ is determined by variables like s, p, m, N_d, N_a according to the particular model. It is often thought of as an "attempt frequency" for the electrons in the trap.

Bimolecular kinetics implies a quadratic equation, so

$$\frac{dn_d}{dt} = -n_d^2 \gamma \tag{5}$$

which yields,

$$I(T) = \frac{m\varphi e^{-E/kT}}{\left[1 + \int_{T_i}^{T} \varphi e^{-E/kT} \frac{dT}{\beta}\right]^2} \qquad (6)$$

If we have transport through a band, we must consider the rms velocity in the band which is proportional to $T^{1/2}$ and the density of states in the band which is proportional to $T^{3/2}$. This has the effect of replacing φ in Eq (4) and (6) by $\Phi\ T^2$ where Φ is a quantity similar to φ but with different units.

The simple analytical forms depend on two "fixed" parameters, E and φ. Thus the interpretation of experimental glow curves in terms of these forms can be made from two points on a curve, although confirmation of a consistent fit may require a check at several pairs of points.

Data points frequently used in evaluating the parameters E and φ are the maximum together with either of the points of half-intensity[6,7] or together with either of the inflection points.[8,9] The method of initial rise utilizes two points on the leading edge (below 10% of I_{max}) of a glow curve where both the monomolecular and bimolecular forms, given by Eqs (4) and (6) reduce to

$$I(T) = m\phi \exp(-E/kT) = F\exp(-E/kT) \qquad (7)$$

Equation 7 is a pure exponential, since m is a constant and φ is considered to be constant or at least nearly so. Exact fits for all points on the leading edge can be made by using computer calculations.[8,9] This form of analysis was usually used in calculating E and φ from experimental data.

If a glow curve is properly described by a theoretical form the analysis by any pair of points should agree with that of any other pair. More often than not, what appears as a single glow peak in a curve may be complex or may contain significant overlap from a neighboring peak. Thus the peak will be broadened and an analysis using the inflection points or half-intensity points will

yield energy values which tend to be low. The initial part (exponential rise region) of a glow curve, on the other hand, will tend to yield energy values which are too high under these conditions although generally to a lesser degree.

One usas the exponential rise analysis on data which is generated by making a series of heating and cooling cycles where the maximum temperature for each cycle is increased in increments depending on the width and amplitude of each glow peak. The analysis of each such cycle provides an average for E and φ and these values are plotted vs. the maximum temperature of the cycle. The resulting plot is a series of more or less well defined steps, and each step is taken as the energy or frequency factor for the peak which it procedes in temperature.

The initial rise technique "decays" the peak being investigated since the amount of charge in the corresponding trap is reduced during each heating cycle and essentially eliminates the contribution from peaks which occur at a lower temperature. If a peak has a nonanalytic form initially and if it results from a single trap, then the peak will tend toward an analytical form as the peak is decayed.[8,9] Of course, at the same time , the effects of overlap of a higher temperature peak become more important. There is therefore an optimum amount of decay which can be made, which may provide for an analytical form when one heats through a peak, and which still does not contain significant overlap from a higher temperature peak. This is the optimum condition of "peak cleaning," which is commonly used in generating data for analysis in terms of the inflection points or half-intensity points, and this optimum condition of "decay" should provide the closest agreement in values for E and φ calculated by the different methods.

One can obtain a better understanding of the source of the mathematical forms shown in Eqs (4) and (6) by a more thorough formulation of the equations. Using the quantities defined in Figure 1, one can write as the rate equation for a localized model,

$$\dot{n}_d = -\gamma n_d + s n_c \tag{8}$$

$$\dot{n}_c = n_d - (s + p) n_c \tag{9}$$

$$\dot{n}_a = p n_c \tag{10}$$

It is stipulated that,

$$n_d + n_c + n_a = m$$

and that,

$$I(T) = \dot{n}_a$$

It is usually argued that $\dot{n}_c$ is small compared to the other terms, so

$$n_c \simeq n_d \gamma / (s + p)$$

Furthermore, it is assumed that

$$\gamma = s e^{-E/kT}, \quad n_d \simeq m - n_a$$

Therefore,

$$\dot{n}_a = p(m - n_a)\gamma / (s + p) \tag{11}$$

which is the standard form of the monomolecular glow curve with

$$\varphi = \frac{ps}{s + p}$$

This expression permits more physical insight into the meaning or origin of the frequency factor φ.

In the case of a band model, these equations become,

$$\dot{n}_d = -\gamma n_d (N_d - n_c) + s'(N_d - n_d) n_c \tag{12}$$

$$\dot{n}_c = \gamma' n_d (N_c - n_c) - \left[s'(N_d - n_d) + p'(N_a - n_a) \right] n_c \tag{13}$$

$$\dot{n}_a = p'(N_a - n_a) n_c \tag{14}$$

These equations assume that only one trapping state, one band and one recombination center are active at a time and that there are no nonradiative transitions. Also assumed is that $n_a = 0$ initially and that $n_c = 0$ initially.

Since $N_c \gg n_c$ then $N_c - n_c \longrightarrow N_c$

Treatment similar to that performed for the localized model above yields

$$\dot{n}_a = \frac{p' \gamma' N_c \quad (N_a - n_a)\ (m - n_a)}{s' - p' \qquad n_a + G} \tag{15}$$

where

$$G = s' (N_d - m) + p' N_a / (s' - p')$$

With these equations it is now possible to see that we have a set of competing processes. We see that the densities of electrons in the trap, the excited state, and the recombination center are variable funtions dependent on each other and on the transition probabilities between states. The solution of Eq (15) does not permit an explicit form for the thermoluminescence in general except at the beginning and end of the glow curve, which are described by different frequency factors. In special cases depending on the ratios m/N_a and p/s, however, the glow curves are described by a single analytical form which may be either monomolecular or bimolecular. The details have been treated by Land.[8,9]

It is also possible to see the relationship between the thermoluminescent glow (TL) and thermally stimulated currents (TSC) in the band model. One sees that,

$$\sigma (T) \propto n_c = \dot{n}_a / p \quad N_a \text{ if } N_a \gg m \tag{16}$$

Again, the exact forms of these equations depend on assumptions about the model and the relative population densities. Land[8,9] shows that if $N_a \gg m$ the TL and TSC have coincident peak temperatures; if $N_a = m$ the peaks differ by a predictable amount and if $m \gg N_a$ the TSC will show no peak but only an exponential rise.

Also, with the rate equations it is possible to examine more fully the case of reduced dose. The details will not be discussed here but are discussed by Land.[8,9] The study is carried out by varying the ratios of m/N_a for given p/s and generating the resultant glow curves to determine changes of shape and peak temperature. It will suffice to say here that the theoretical knowledge gained is to be compared with the experimental dosage curves to help in determining the model and relative population densities of the defects in the crystal. One of the more interesting conclusions and one that is illustrated in the work below is that the peak temperature for TL and TSC always increases with a reduction of dose if $N_a \propto m$.

E. EMISSION

The spectral analysis of the thermoluminescent emission can yield considerable information about the recombination process and, to an extent, information about the trapping states. The emission analysis is usually performed at low or moderate resolution, partly because of experimental problems such as lack of intensity and partly because in many cases the emission spectra are quite broad. A major difficulty is that the spectrum must be scanned rapidly as the sample is being heated. In situations where the glow is strong, the overlap of the peaks is weak, and the spectra are fairly narrow, high resolution data can be obtained. High resolution data may result in the positive identification of the recombination mechanism. It will be shown below that the emission from many ThO_2 crystals is due to specific rare earth impurity ions and that the recombination mechanism apparently involves other defects which can exchange energy with rare earth ions. The governing parameters for recombination are the capture cross section of the recombination centers and the transition probabilities p and q which are rather complex quantum mechanical matrix elements based on the wavefunctions of the upper and lower states. The transition probabilities are temperature dependent and possibly dependent on the population densities of the initial, excited, and final states.

It is possible for one to characterize and define the glow peaks by their emission properties. Individual glow peaks or glow peaks in a particular temperature region may have unique emission spectra because of the changing population densities and recombination probabilities permitting association of particular peaks with different defects.

Glow peaks that are superimposed with respect to time or spectral content can frequently be resolved by a study of the emission spectra. A peak which appears singular to the photomultiplier may have two distinct peaks at different wavelengths when observed with good resolution. The upper and lower sides of a peak may have very different spectral properties even though the peak is not clearly resolved into two peaks. A detailed emission analysis can be used to detect the presence of previously undetected submerged peaks or shoulders.

In some cases it is possible to identify the thermoluminescent emission by measuring the fluorescence emission. The fluorescence, measured at a particular temperature, can be measured with higher resolution and accuracy than is generally possible for thermoluminescence and can often be compared accurately with the literature. Merz[10] and others have identified defects and classified them according to their symmetry properties by a study of the fluorescence and then, by comparison with the thermoluminescence emission were able to associate glow peaks with particular defects.

Section III

EXPERIMENTAL CONDITIONS

The first modern development of thermoluminescence techniques was by Randall and Wilkins[11] in 1945. Curie[12] and Garlick[13] have discussed thermoluminescence in review articles, and Prof. A. Halperin has contributed to the experimental techniques and procedures in numerous papers. Recent interest in thermoluminescence as a tool for radiation dosimetry in the fields of health physics and geology has resulted in many contributions of experimental methods to the literature and also has resulted in the commercial availability of thermoluminescent materials and readout instruments. Two recent volumes dealing primarily with thermoluminescence are: (1) *The Proceedings of the 2nd International Conference on Luminescent Dosimetry,* [14] and (2) *Thermoluminescence of Geological Materials.* [15] Both volumes provide a wealth of information and extensive bibliographies.

A. EQUIPMENT

The equipment used in this laboratory is similar to that described by Crawford[16]. A description of the present setup with more complete construction details has been reported by Land and Wysong.[17] Figures 2, 3, and 4 are photographs of the basic equipment used.

The central piece of apparatus is the rotatable variable temperature optical cryochamber shown in Figure 2. On the sides of the brass block are three windows and a pumping port. The three windows are 2.625 inches in diameter and are of ultraviolet quality quartz. Two of the windows (opposite each other) are held in place against "O" rings by teflon gaskets and screw-in retainer rings made of brass. These window ports are threaded to a depth of 3/8 inch so the photomultiplier housings, filter wheel, and retainer rings holding filters and diaphrams can be screwed directly into the block in a light-tight manner. The third window is held in place by a brass retainer and can be covered by a brass plug as shown in Figure 2. The pumping port leads to a Varian 8 liter/sec Vaclon pump for normal operation or a mechanical pump for initial pumpdown. A baffle in the pumping line prevents any glow of the Vaclon pump from entering the sample chamber. The stainless steel coldfinger with copper sample block fits into the top of the brass block through an "O" ring seal and rests on a teflon gasket on the top of the block. Thus the coldfinger is easily rotatable.

The thermocouple and heater wires are brought out through Conax feedthroughs which are made of stainless steel with teflon cores. An extra feedthrough is available for a second thermocouple or electrical leads for conductivity studies.

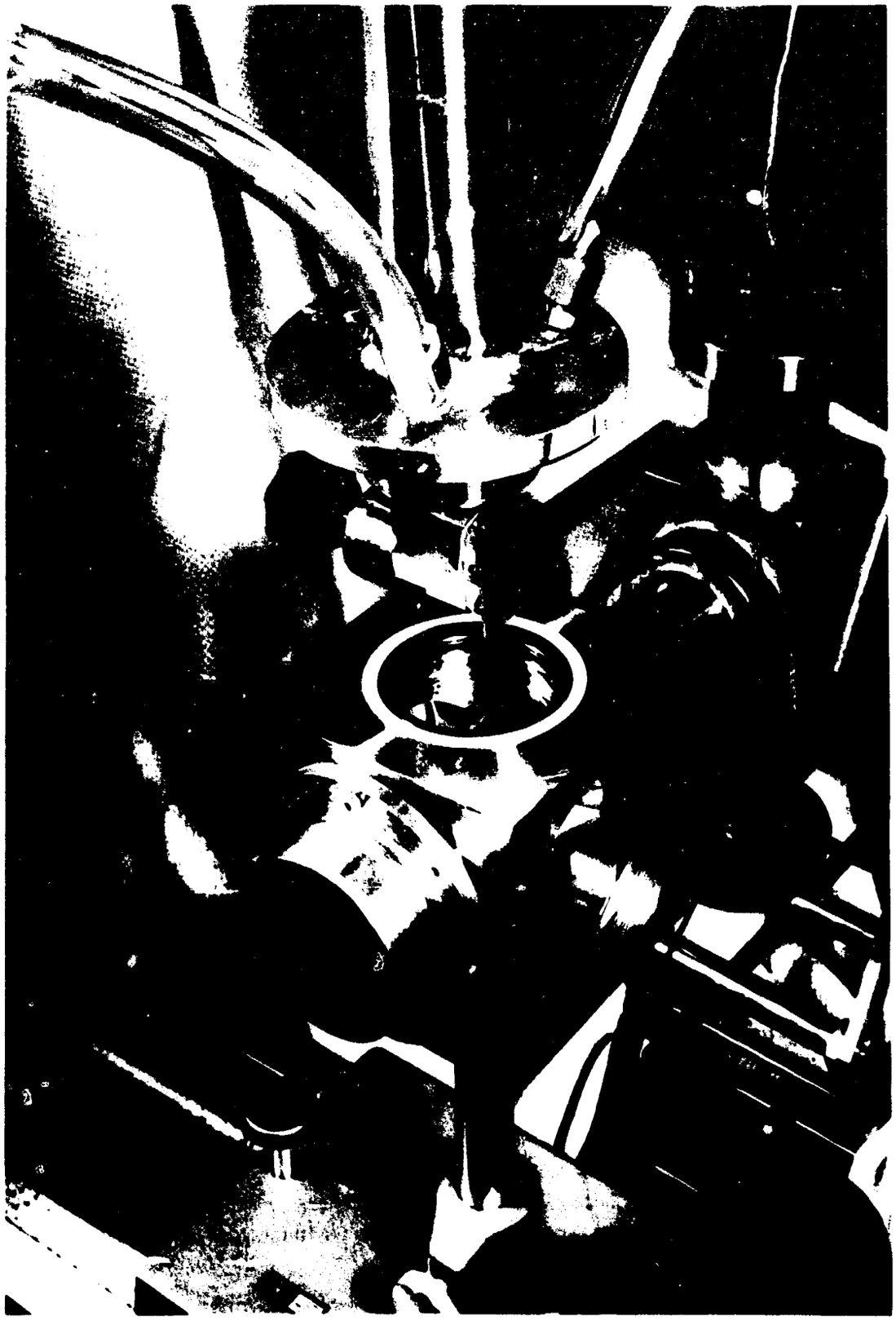

Figure 2. Photograph of variable temperature rotatable optical cryochamber

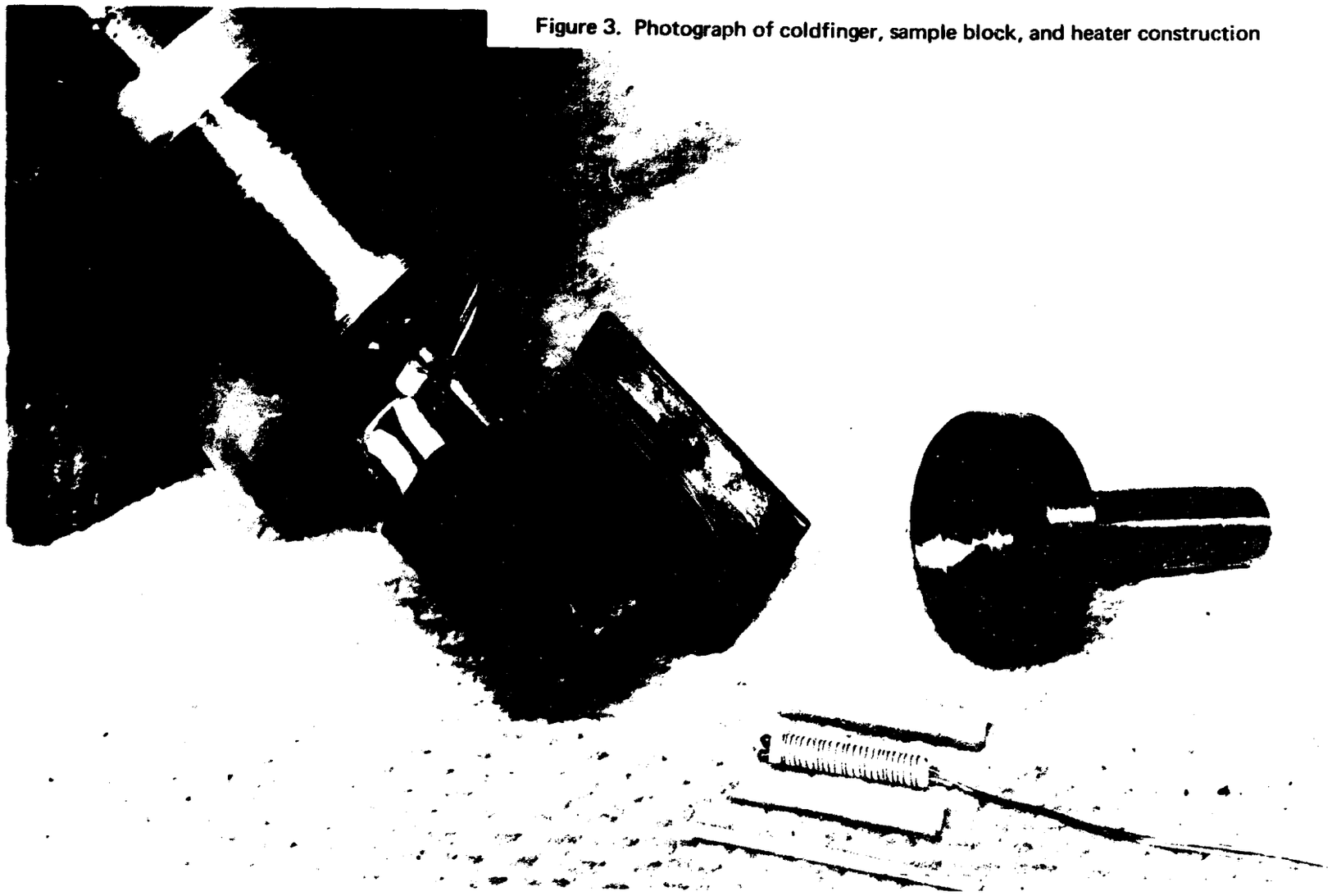

Figure 3. Photograph of coldfinger, sample block, and heater construction

Figure 4. Photograph of variable temperature rotatable optical cryochamber with vacuum system, monochromator, filter wheel and photomultiplier

The helium cryochamber (not shown) is basically a Sulfrian Selectostat with a specially designed tail such that it fits into the brass block and is rotatable like the nitrogen coldfinger. A variety of sample holders were constructed so transmission, fluorescence, and thermoluminescence measurements could be made. Heaters are available for all holders.

Details of the sample block, coldfinger tail, and heater are shown in Figure 3. As seen from the spare on the right of the photograph, the coldfinger tail is hollow to accept liquid nitrogen and extends through the copper sample block. The tail is heliarced to the inside wall of the coldfinger. The sample block is silver soldered to the tail.

Heating is accomplished with a platinum wire resistance heater, wound on a ceramic core, covered by a ceramic tube and imbedded in the sample block. The heater is inserted into the sample block from the bottom so that the sample block does not have to be separated from the coldfinger to replace the heater. The heater and ceramic core are dipped in Sauereisen No. 78 cement for good thermal contact. The leads are passed up through the block (in ceramic sleeves) and are covered with ceramic spacers above the block to prevent the glow of the wires from reaching the photomultiplier. Because survey runs are often made with a sample on the front and samples on the sides of the block, the face of the block is oversize to prevent the glow of the side mounted samples from affecting the measurements on the front sample.

The nominal resistance of the heater is about 5 ohms. A reproducible linear heating rate is accomplished by use of a circuit consisting of adjustable resistors and thermistors.[17] Adjustment of the resistors and the delay effect of the thermistors permit a reasonably linear heating rate from liquid nitrogen temperature to 100°C. The heating rate over most of the temperature range is about 30°C per minute and drops to about 15°C per minute by 300°C. A more complex thermistor circuit or a commercially available system with a programmed heating rate could provide a more linear heating rate over a greater temperature range. This is not necessary since the analysis requires only that the heating rate be linear during each peak and that the rate be reproducible. Reproducibility is easily satisfied because each run begins with the thermistors at room temperature and the sample block at liquid nitrogen temperature.

The copper-constantan thermocouple junction is held against the copper block by the screw just behind the normal sample position. The thermocouple wire is wrapped around the block to reduce thermal gradients near the junction.

Several light sources were used for the experiments. The most frequently used light source was a Sylvania DE50 deuterium arc lamp operated at 32 watts. This lamp is one of the sources available for the Bausch & Lomb High Intensity Grating Monochromator. When used with the

ultraviolet grating of the monochromator a continuous spectrum from 180 nm to 400 nm was available. The peak output was at 260 nm. For high excitation the deuterium lamp was used without the monochromator, in which case the light was focused by a quartz lens from the monochromator and provided an intensity at the sample of approximately 13 m W/cm^2. The duration of the excitation was controlled by a camera shutter. The modular construction of the monochromator permitted visible and infrared gratings to be used with the Bausch & Lomb tungsten source for special experiments. The monochromator was equipped with several sets of slits permitting a variety of slit widths to be used; hence the bandpass was adjustable.

The basic emission detector was an RCA-1P28 photomultiplier, which is an S-5 tube. The wavelengths at which its response had fallen to 10% of its peak value were about 200 nm and 600 nm. This range covers the emission spectra for most of the samples studied. The dark current of this tube was between 2 and 4 nanoamperes. In some cases it was desirable to extend the coverage to longer wavelengths. For these studies an EMI-9558Q photomultiplier was used which had a response to beyond 800 nm. This tube also had the advantages of greater sensitivity, a larger signal-to-noise ratio, and an end-on photocathode. A metal housing was constructed for the EMI tube such that it could be screwed directly into the sample chamber or used with the filter wheel as shown in Figure 4.

The anode current of the photomultiplier was fed to a Keithley 600A electrometer. The 0-1 volt output of the electrometer was recorded on a Varian G-14 strip chart recorder which had a potentiometric input and chart speeds of one inch and four inches per minute. The thermocouple voltage was partially bucked by a potentiometer and the remainder (0-1 mV) was recorded on an identical Varian recorder. An event marker permitted synchronization of the temperature and photomultiplier response records.

The emission spectra in most cases were measured with a rotating filter wheel.[17] A similar device was first proposed by Rohner and Strutt.[18] The filter wheel consists of a metal disk, nine inches in diameter, mounted on the shaft of a 15 rpm Apcon electric motor. Gears mounted on the motor permit the selection of output speeds ranging from 15 rpm to 1/4 rpm in 6 steps. Eight circular holes, 1.75 inches in diameter, were cut near the circumference of the metal disk, and the disk was machined so an interference filter and diaphragm could be mounted over each opening. The disk was enclosed in a housing so that the entire assembly could be mounted between the sample chamber and the photomultiplier in a light-tight manner. All parts were black anodized to reduce stray light.

The filters used were Optics Technology interference filters. These filters have a narrow bandpass (about 3.5% of the peak transmission wavelength) and are available with central

transmission wavelengths ranging from the ultraviolet to the infrared. The filter wheel is rotated at an appropriate speed (7.5 rpm) while the sample is warmed in the usual manner, and the output of the photomultiplier is recorded. The trace is made up of a series of sharp peaks of various intensities corresponding to the transmission of each of the filters as it passes between the sample and photomultiplier. The peak response for each filter can be connected to give a glow curve for that filter resulting in the generation of 8 simultaneous glow curves. In order to obtain an emission spectrum for any temperature, the recorded responses are corrected for the relative transmission of each filter, the spectral response of the photomultiplier, and the transmission of the quartz window in the sample chamber.

Figure 4 is a photograph of the equipment in place for thermoluminescence emission spectra measurements. The entire apparatus is mounted on a heavy optical bench to permit reproducible alignment of all components. The monochromator and the deuterium light source are mounted to the left of the cryochamber and the filter wheel and EMI photomultiplier are mounted to the right. The monochromator and light source can be easily separated and replaced with other units. The gratings, attached to the top of the unit, can also be easily removed and replaced. The normal procedure is to irradiate the sample at liquid nitrogen temperature through one window, rotate the coldfinger 180 degrees, and measure the emission through the opposite window. The third window is used for visual inspection or bleaching experiments.

The light sources, monochromator gratings, and photomultipliers were calibrated with a Hilger-Watts thermopile, used in conjunction with a light chopper and phase lock amplifier. The details of the calibration techniques and the results have been reported.[19]

B. SAMPLE MOUNTING

Prior to mounting, the samples were washed in HCl to remove flux residue and then in NH_4OH. They were rinsed in distilled water in the ultrasonic cleaner and inspected for cleanliness under a microscope.

The method of attaching the samples to the sample block received considerable attention. Silicone vacuum grease was used during the initial stages of the investigation mainly because of the ease with which samples could be attached or removed. However, it was discovered that vacuum grease gave off a small but measurable thermoluminescent glow that had peaks at temperatures similar to the thoria glow. Also, a film that absorbed ultraviolet light was deposited on the windows by the vacuum grease at high temperatures. Investigation revealed that a number of materials that would otherwise be suitable bonding agents exhibited thermoluminescence, fluorescence, or excessive vapor pressure. Sauereisen[20] Super Sealing Varnish No. 66 was found

to have good mechanical strength over the temperature range required and to have minimal optical activity. Proper curing eliminated any vapor pressure problems. The varnish can be removed with acetone. Survey runs were still conducted using the vacuum grease and this can be removed by washing in kerosene or trichloroethalene.

We took special care to insure that the samples were in good thermal contact with the sample block. The samples were either ground to have a flat surface or were mounted on a naturally occurring flat surface. The thermal contact was checked in one typical case by mounting a thermocouple on the face of a polycrystalline sample of Y_2O_3 and measuring the temperature difference between the front face and the back surface of the sample. The temperature difference near liquid nitrogen temperature was about $2^{o}C$ (the sample face being warmer); at $0^{o}C$ the temperature difference was negligible, and at $300^{o}C$ the temperature difference was about $10^{o}C$ (the sample face being cooler). It was concluded by Land[8,9] that the temperature gradient between the sample face and the mount was not sufficiently large to cause significant errors in the analysis. The gradient was reproducible as indicated by the reproducibility of temperature of peak glow.

C. PROCEDURES OF MEASUREMENT

1. Dosage and Excitation Data

Dosage curves were generated simply by exciting the sample for a variety of excitation times and measuring the areas under the resultant glow peaks. The times of excitation were controlled by a camera shutter and timer and varied from 0.01 seconds to several hours. In most cases the deuterium source was used without the monochromator in order to achieve saturation in a reasonable amount of time. In some cases the monochromator was used to check spectral variations of the dosage characteristics. Data were taken in a random order to minimize the effects of possible systematic variations of light source output, fatigue of photomultiplier, coating of windows, or the effects of deep traps. These effects are not believed to be significant in the data presented.

The excitation spectra of some selected samples were obtained by measuring the areas under the glow peaks as a function of excitation wavelength. The time of excitation at each wavelength was determined such that the same number of photons was incident on the sample for each wavelength. That is, if I is the intensity of the monochromator beam (as measured by the thermopile) at a particular wavelength λ, then

$$It = \frac{nhc}{\lambda} = \frac{G}{\lambda}$$

where n = number of photons
h = Planck's constant
c = velocity of light
G = constant
t = time

Therefore,

$$t = \frac{G}{I\lambda}$$

so the product of the wavelength and the thermopile voltage at that wavelength is inversely proportional to the time of excitation. The resultant plot of area under the glow peaks vs. wavelength is a measure of the excitation efficiency.

The large variation of output of the monochromator as a function of wavelength dictates a large variation of excitation times in order to maintain the same number of photons at each wavelength. Typical excitation times over most of the region of interest were of the order of minutes while at wavelengths below 200 nm where the output of the light source was very low the excitation times had to be of the order of several hours.

Bleaching experiments were conducted by exciting the sample to saturation with ultraviolet in the usual manner then irradiating with infrared or visible light through the side window. The resultant glow curve was compared with the unbleached glow. The dosage of infrared light was determined by a schedule giving the same number of photons at each wavelength similar to that used for the excitation spectra

2. Emission Data

The emission spectra were measured by several different methods. The intensity of the thermoluminescence for many of the thoria samples was too weak for analysis by means of a spectrometer or similar piece of equipment. The interference filters used in the filter wheel described above had a peak transmission of up to 50% and a bandpass of several hundred angstroms, so the filter wheel in effect became a low resolution, high sensitivity, scanning spectrometer. The filter wheel, by recording 8 glow curves per run, minimized the effects of variation in excitation conditions, photomultiplier fatigue, filming of the windows, etc., between successive runs, and also reduced the number of runs required to obtain complete spectra.

Usually, two overlapping sets of filters were used on identical, successive runs to cover a broader spectrum. The filter wheel permitted one to study the differences of spectral content between peaks or between the low and high temperature portions of peaks. In cases where line spectra were apparently present the emission was further resolved by either a Bausch & Lomb monochromator or a SPEX spectrometer. In a number of cases, the monochromator was placed between the sample and the photomultiplier and manually scanned while the sample was being warmed.

3. Fluorescence Data

The fluorescence of some thoria crystals was measured with a SPEX Model 1700 grating spectrometer. The fluorescence of one sample (OR2) was measured with the sample mounted in air directly in front of the spectrometer, using the deuterium source and the ultraviolet monochromator for excitation. The fluorescence of some crystals doped with rare earths was measured with the samples mounted on the tail of the helium dewar in the cryochamber such that the spectra could be measured as a function of temperature. Appropriate filters were used to eliminate visible light from the excitation beam and second order ultraviolet light from the emission. A resolution of 1 Å could be attained by adjusting the slits.

4. Transmission Data

The optical transmission of a thoria crystal was measured at room temperature with a Cary 14 spectrophotometer. The crystal was quite small so identical masks were placed in the sample and reference chambers. The sample was glued to one of the masks for support. The transmission was measured from 1,800 nm to 200 nm. Considerable difficulty was encountered in setting a reasonable baseline in the ultraviolet region. This was apparently because the beams were not exactly coincident on the photocathode. This has little effect when the beams are not masked but becomes important when crystals only 2 mm in diameter are used. It has been shown[21] that for a 1P28 photomultiplier, which is used in the Cary 14, the response of the photocathode can vary as much as two orders of magnitude between two spots an eighth of an inch apart.

Section IV

THORIUM OXIDE

A large number of materials exhibit thermoluminescence. Among the reasons for selecting thorium oxide for this study were the availability of good single crystals and the simple crystal structure. The use of single crystals of a material with a simple crystal structure reduces the number of possible defect models and hence induces and encourages other studies with the possibility of coordinating the results.

We also determined that thorium oxide was a suitable material for a detailed study of the thermoluminescent processes on the basis of preliminary measurements. Initial measurements indicated that the thermoluminescence was bright, the peaks were well separated, and there was a relatively small number of peaks in the temperature range of interest.

A. PHYSICAL PROPERTIES

Thoria is a refractory oxide that has a number of interesting properties. Much of the previous work on thoria has involved the study of thoriated tungsten cathodes. Danforth[22] has reviewed the work before 1953 on thoria, concentrating primarily on its technological development and its use as a thermionic emitter.

Campbell[23] discussed a number of the physical properties of polycrystalline thoria. Thoria has a very low vapor pressure at high temperatures, poor shock resistance, and a low thermal conductivity. Thoria has the highest melting point of the refractory oxides, i.e., $3300^{o}C \pm 100^{o}C$. It is sometimes used in crucibles for melting metals since it has a very low reactivity to metals.

The electrical properties of thoria have been investigated by a number of people and there is a wide variation in the published data. Norton[24] has stated that a reasonable value of the electrical resistivity at room temperature is of the order of 10^{13} ohm-cm and at 1200^{o} it is of the order of 10^{4} ohm-cm.

Wachtman[25] studied the mechanical and electrical relaxation processes of calcium doped polycrystalline thoria. The calcium entered the lattice by replacing a thorium atom, simultaneously creating an oxygen vacancy that was tightly bound to the calcium atom. The oxygen

vacancy, in the absence of stress fields, occupied with equal probability the 8 nearest neighbor oxygen sites. The relaxation times were calculated theoretically and verified by measurement of the internal friction and dielectric loss.

Danforth[22] and Weinreich and Danforth[26] have investigated some of the optical properties of fused crystalline thoria with an estimated purity of 99.9%. Polycrystalline or fused crystalline thoria may be red, yellow, or colorless. A red coloration implies an excess of oxygen. A colorless crystal heated to 1000°C in an oxygen or air atmosphere became red, and reheating to 1800°C in vacuum or hydrogen bleached all coloration. The fundamental band gap was quoted at 370 nm as determined by the sharp cutoff of the absorption spectra. After heating to high temperatures in vacuum, the absorption cutoff dropped to 320 nm and a broad absorption peak occurred at about 400 nm that was attributed to an oxygen deficiency. A weight change of 10^{-3} percent was observed during the bleaching and coloration.

Bates[27] measured the optical absorption of some thoria single crystals and polycrystalline samples that had been thermally treated to achieve various degrees of oxidation or reduction. He reported an ultraviolet cutoff of about 250 nm. Linares[28] measured the transmission of some thoria crystals that he had grown by a lead flux technique. Coloration and shifts of the absorption spectra that he observed as a function of dopants will be discussed below.

A rather cursory study of the thermoluminescence of powdered thoria has been reported by Greener et al.[29] Weak peaks were observed at 65°C and 198°C after room temperature irradiation with Co^{60} gamma rays. Linares[28] ran some glow curves on his single crystals but did not show the details of the experiment. Finch et al[30] have studied some thermoluminescence above room temperature of thoria crystals doped with a variety of rare earths. The work of Finch et al will be compared with the results of the present investigation in a later section.

The fluorescence spectra of a number of rare earth ions in thoria have been reported by Trofimov[31] Comparison with this investigation will be made in a later section. Linares[28] has also reported some fluorescent properties of thoria as a function of the charge compensation of rare earth dopants.

The electron paramagnetic resonance of thoria, doped and undoped, has been studied by a number of workers. Considerable effort has been made to correlate the thermoluminescnce discussed here with the EPR work of G.S. Tint and A. Neaves[32]. This work will be discussed in detail in Section VI.

Abraham et al have studied the EPR of thoria doped with Yb^{3+} and Er^{3+} [33], Gd^{3+} [34], Cm^{3+} [35], and Eu^{2+} [36]. Marshall[37] and Low [38] have studied the FPR of Gd^{3+} in thoria also. Nealy et al[39] reported the presence of an F center in thoria as determined by EPR. Comments on this interpretation will be deferred until a later section.

B. CRYSTAL GROWTH, SAMPLE DESCRIPTION, AND NOMENCLATURE

Thoria crystallizes with the fluorite structure which has face centered cubic symmetry and four molecules per unit cell. Each thorium atom is at the center of 8 oxygen atoms that are located at the corners of a cube. Each oxygen atom is at the center of a tetrahedron of thorium atoms.

Thorium oxide crystals were obtained from a variety of sources representing several methods of growth and many degrees of sample purity. Over 40 crystals and one batch of high purity powder were examined on at least an exploratory basis; some of these were selected for detailed study. Twelve crystals from ten batches were selected for impurity analysis.

Table I describes some of the physical characteristics of the samples used. The first column gives the sample number of the principal crystal to be discussed and also the numbers of other crystals from the same batch which have similar properties. The other columns describe the crystals physically, and the last column lists a few selected optical properties. Note that the numbering system specifies the source of the samples.

Most of the crystals used in this investigation were grown by Dr. Cabell Finch and Dr. G. Wayne Clark of the Oak Ridge National Laboratory from a lithium ditungstate solvent.[40] The crystal growth was primarily by solution transfer from a thoria nutrient at about 1300°C to seeds in regions 20°C to 75°C cooler. In some cases, the growth rate was increased by the addition of 1% B_2O_3 to the solvent. In some batches lithium remained as a major contaminant although in most cases the crystals were surprisingly free of lithium, tungsten, or boron. The crystals in some batches were extremely pure. The crystals had well developed octahedral facets that were very smooth and highly reflective.

Batch No. 1 was grown undoped and provided a number of crystals that were studied extensively. The samples from this batch were very pure. The thermoluminescent characteristics of these crystals from batch No. 1 indicated that they could be classified into two groups. The details of the classification are summarized in Table I and will be discussed below. The principal crystals from this batch were OR1, OR2, OR7, and OR8.

Table I

Physical characteristics of some ThO_2 samples

Sample No.	Source	Physical Appearance	Growth Method Dopant	Distinguishing Optical Properties
ORl (3, 11)	Oak Ridge Natn'l Labs Batch #1	less than 3mm on edge jagged with facets clear, colorless	$Li_2O \cdot 2WO_3$ pure	bright TL green emission (Er)
OR2 (7, 8, 9, 10)	same	same	same	bright TL, line emission sharp excitation, absorp. cutoff at 215nm
OR4 (5, 6)	same Batch #2	same	same Ca doped	weak TL narrow excitation additional peaks
FI 1	Franklin Institute	1 x .5 x .3 cm polished faces light brown	arc grown	Bright TL emission towards red
FI 2	same	1 x .5 x .3 cm polished faces colorless	same	bright TL blue and red emission
PE2 (PE1)	Perkin-Elmer, Inc.	.5 x .5 x .3 cm polished faces tan color	lead flux	overlapping TL peaks broad emission
ESP1	Electronic Space Products	white powder	less than 10 ppm impurities	broad, overlapping TL peaks
N 1 (N?)	Norton Company	1 x 1 x .2 cm polished light brown	arc grown reactor grade starting material	self-excitation red shift emission
OR12, 13 14, 15	Oak Ridge Natn'l Labs	clear, colorless	$Li_2O \cdot 2WO_3$-B_2O_3 Er	bright TL Er line emission
OR16, 17 18	same	red	-- Pr	weak TL
OR19, 20	same	very small red	-- Tb	negligible TL green fluorescence
OR21, 22 23	same	clear, colorless	-- Eu	bright TL red emission
OR24, 25 26	same	colorless, cloudy easily shattered large	$Li_2O \cdot 2WO_3$ Dy	bright TL line emission
OR27, 28 29	same	very small yellow	-- Nd(Gd)	weak TL
OR30, 31 32	same	clear, colorless	$Li_2O \cdot 2WO_3$-B_2O_3 Yb	moderate TL emission:two broad bands
OR33, 34 35	same	clear, colorless	-- Tm	moderate TL broad emission

Batch No. 2 was grown with the hope of doping the crystals with Ca. Only a small amount of Ca was incorporated into the lattice. The crystals were similar in appearance to the original batch but the thermoluminescence had some obvious differences as will be shown below. The principal crystals from this batch were OR4, OR5, and OR6.

Eight batches of single crystals, each batch doped with a different rare earth, were also obtained from Dr. Finch. Each batch consisted of many crystals of various sizes. In two batches, ThO_2:Tb and ThO_2: Nd(Gd), all of the crystals were very small. The colors of the crystals are listed in Table I.

A number of large, reddish colored chunks of crystalline thoria were obtained from Dr. Robert Linares of Perkin-Elmer, Inc. These crystals were grown by a lead flux technique[28] and were quite rough and irregular with many cleavage planes. Several fairly transparent samples were cut from these chunks and polished. The lead content in these crystals was quite high. The samples from this batch are labelled PE1 and PE2.

Another technique for growing thoria single crystals, and the only method available until the development of the flux techniques, is the arc method. In this case, single crystals are separated from a large boule of material that has been melted in an arc. Two large arc grown crystals were obtained from the Franklin Institute and were reported to be similar to the crystals used by Danforth in earlier studies.[22,26] Both crystals were translucent with optical faults and one had a reddish-brown coloration. These crystals are labelled FI1 and FI2. Some large chunks of crystalline thoria, arc grown from reactor grade powder, were purchased from the Norton Company.[41] They were mostly opaque and appeared black except for several sections which were translucent with a light brown color. Several samples were cut from the translucent material and will be referred to as N1 and N2. The samples grown by the arc method were quite pure except for a few impurities that were present in high concentrations.

The powder sample (ESP 1) was formed by mixing some high purity thoria powder with silicone vacuum grease. The powder was obtained from Electronic Space Products, Inc.[42] The powder was reported by the company to have a total impurity content of less than 10 ppm but had been handled a number of times since receipt, so the impurity content was undoubtedly somewhat higher.

C. IMPURITY ANALYSIS (GENERAL REMARKS)

Twelve single crystals were sent to the Battelle Memorial Institute in Columbus, Ohio for impurity analysis. The crystals were selected to be representative of each batch. In all cases,

sufficient thermoluminescence data were taken from each sample to establish the optical characteristics before it was sent in for analysis. The samples were analyzed by spark-source mass spectrographic analysis and, when possible, by optical emission spectrographic analysis. The larger samples were directly sparked opposite a gold counter electrode while the smaller samples were ground up and briquetted with graphite before analysis. A major problem with the impurity analysis is that the samples were extremely small; their size was on the borderline of acceptability for the technique. Typically, the accuracy of mass spectrographic analysis for small concentrations is a multiplicative factor of 2 or 3. One of the samples (OR7) weighed 34 mg.; most other samples were lighter.

Table VI in Section VII shows the results of these impurity analyses. Detailed discussion will be deferred until Section VII when specific impurity levels can be related to the optical properties to be presented below. A few brief comments should be made about the results of the impurity analyses before a detailed description of the thermoluminescence. In general, the impurity levels found in these crystals are very low. In most cases, the inequality signs indicate the sensitivity limits of the method of analysis. All of the Oak Ridge crystals were grown from a lithium ditungstate solvent, so it would be reasonable to expect significant concentrations of Li and W. This was found to be true in only three cases.

The column labeled PE in Table VI represents a large chunk of thoria grown in a lead flux and obtained from Perkin-Elmer, Inc. on which two analyses were made. The results shown here represent a clear portion of the sample. Analysis of a portion which was cloudy and had an occlusion revealed very high concentrations (up to 10,000 ppm) of Be, F, Na, S, and Ta and almost as much Pb as Th. The analysis of that section is not given in the table.

Note also that the rare earths are almost totally missing from these crystals. There are exceptions to this, such as the high amount of Nd in the Perkin-Elmer crystals, and the specific dopants. It will be established below that when rare earths are present the thermoluminescent emission is characteristic of the rare earth and that only sub-parts per million concentrations of rare earths are necessary for bright thermoluminescence.

Section V

EXPERIMENTAL RESULTS

A. GLOW CURVES AND PRELIMINARY REMARKS

1. Composite Glow Curves

The many samples used in this investigation were classified in the preceding section by their source, method of growth, appearance, and some optical properties. It is also useful to compare the glow curves of the various samples. Figures 5, 6 and 7 are composite drawings that show the glow curves from a number of samples. Excitation conditions were similar in all cases (although not identical) and represent, in most cases, saturation conditions. The intensity scales have been adjusted so the glow curves from very bright samples could be shown with relatively weak samples. During a normal run the electrometer scale is changed frequently so small peaks barely appearing in the composite curves can be studied in detail.

Figure 5 shows the glow curves for crystals from the first two batches of Oak Ridge crystals, the Franklin Institute, the Norton Company, and Perkin-Elmer, Inc. These are the glow curves from the undoped samples.

Figures 6 and 7 show the glow curves from six batches of rare earth doped thoria crystals. The glow from the crystals doped with Tb and Pr was not strong enough to be included.

A number of similarities and differences between the crystals can be immediately noted. For each crystal the peaks are well separated and clean without a great deal of overlap and without the presence of many "shoulders". The PE2 is an exception of this, and the OR2 is the most dramatic example of peak purity and separation. Some of the peaks which appear pure and singular will be shown to be complex. For example, at high dose levels one component may dominate, yielding the appearance of a singular peak.

Nearly all of the samples have major peaks at -100°C to -120°C and at -10°C to -20°C. There are exceptions to this, i.e., the ThO_2: Eu sample has a major peak at -135°C and ThO_2: Tm has a peak at -85°C. Smaller peaks at -150°C and --70°C are also common. Many crystals, particularly those doped with rare earths, have a high temperature peak at about 140°C and a smaller peak at about 57°C. Some of the particular peaks will be discussed in detail below. The samples doped with Eu, Dy, and Er are very similar to each other and are also very similar to the

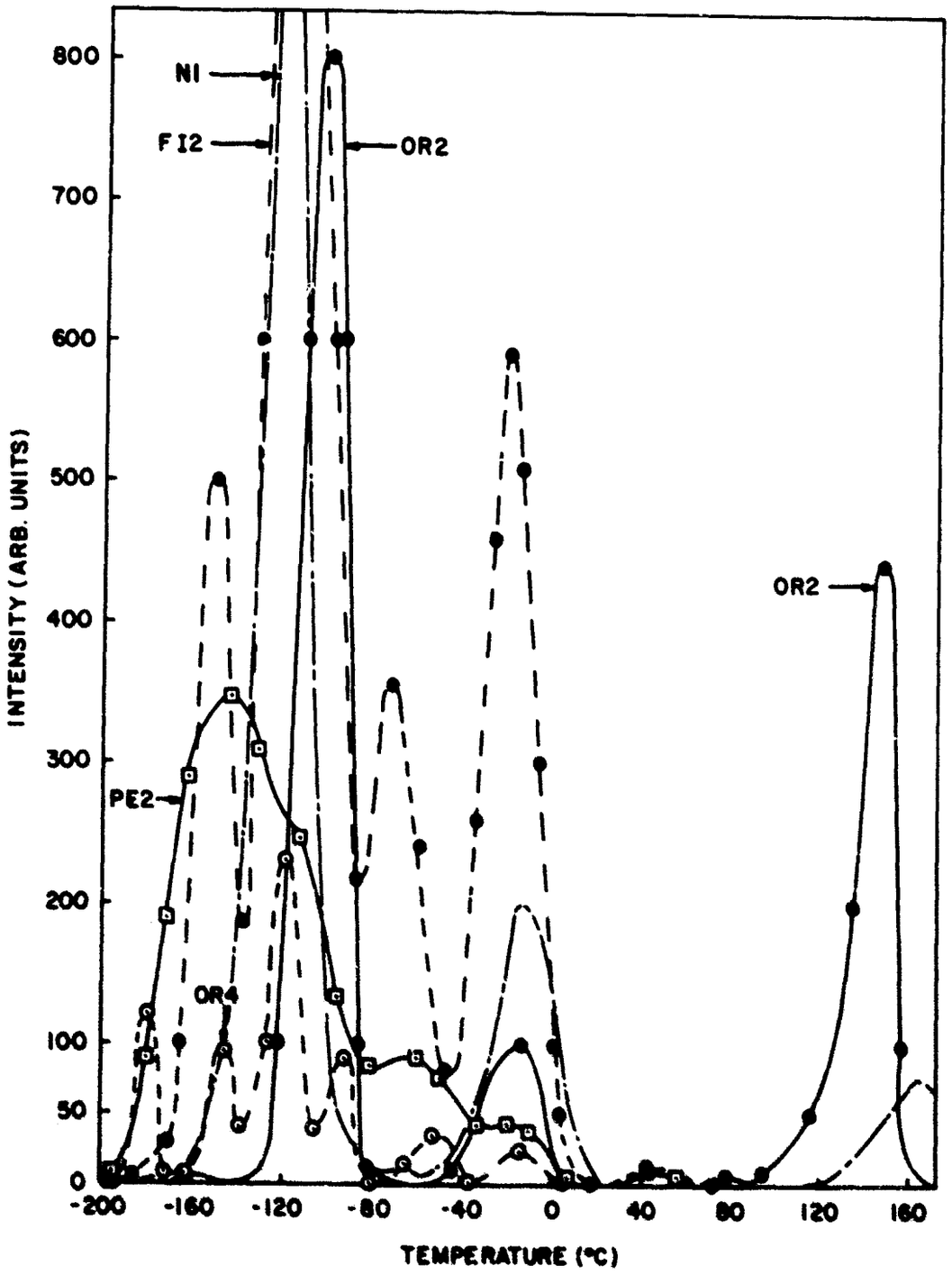

Figure 5 Composite glow curves of some undoped ThO_2 single crystals

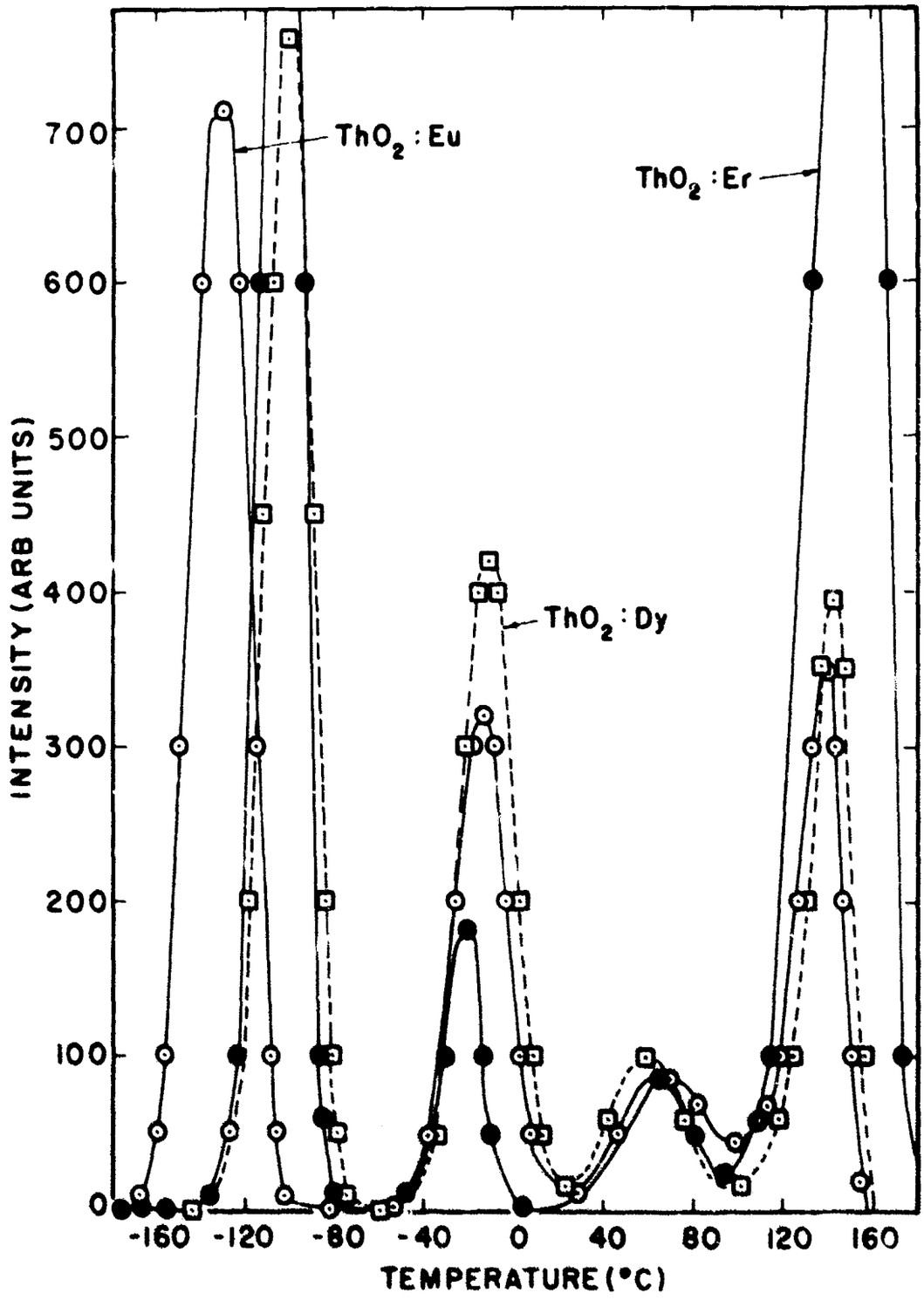

Figure 8. Composite glow curves of ThO_2 single crystals doped with Eu, Dy, and Er

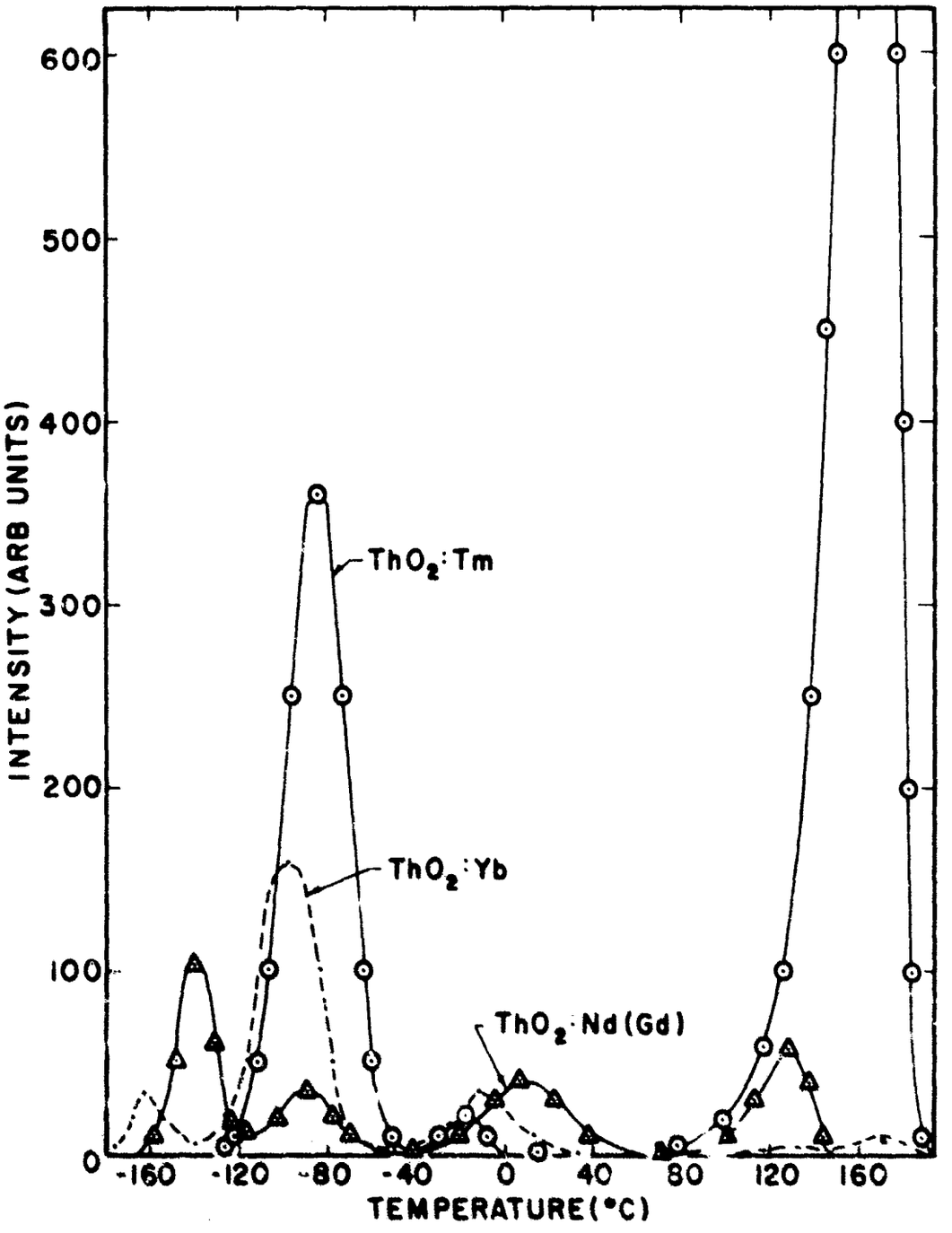

Figure 7. Composite glow curves of ThO_2 single crystals doped with Tm, Yb, and Nd (Gd)

undoped samples in Figure 5. The samples doped with Tm, Yb, and Nd(Gd) are somewhat similar to each other but exhibit more departure from the glow curves seen in Figures 5 and 6. Complete dosage curves were not generated for the rare earth doped crystals so it is not certain that the curves shown in Figuras 6 and 7 represent saturation conditions. This could account for some of the variations of peak temperature. The glow curves from other samples in each batch were very similar to the curves shown in the figures with some differences in relative intensity.

Figures 5, 6, and 7 show that the peak temperatures and the relative intensities of the peaks from the Oak Ridge crystals are essentially independent of the rare earth dopant and are to a large extent identical among samples. Many of the crystals not obtained from Oak Ridge have glow curves which show a strong correlation and similarity to the Oak Ridge crystals. It will be shown below that the emission spectra depend very strongly on the rare earth content of the crystals. It can be concluded that the trapping states in these crystals are very similar in all crystals and are independent of the rare earths. The trapping and the recombination are the results of seperated defect states. These conclusions will be elaborated and extended in the following discussions.

2. Comparison of Total Glow

An additional comparison of samples can be made by considering the amount of total glow from each sample. For the dosage studies, excitation spectra, and bleaching spectra, the amount of glow was measured in square centimeters on the data charts and scaled to a response on the 10^{-7} ampere range of the electrometer. The heating rate was the same for all runs and an upper limit of the temperature was employed so the raw data can be used to compare the response levels of the different crystals.

The total areas under the glow curves for six crystals at saturation conditions are shown in Table II.

Table II

Areas Under Glow Curves at Saturation (Undoped Samples)

Sample	Total Area
OR1	300 cm^2
OR2	4500
OR4	65
OR7	2300
OR8	1500
N 1	2900

The total areas under the glow curves for some other crystals are shown in Table III. These crystals were excited for about the same times as the crystals in Table II but dosage curves were not generated for these crystals, so it is not known if saturation conditions are represented.

Table III

Areas Under Glow Curves (Mostly Doped Samples)

Sample	Dopant	Total Area
OR12	Er	13420 cm^2
OR22	Eu	34020
OR24	Dy	4920
OR31	Yb	62
OR34	Tm	540
FI 1	-	289
FI 2	-	9321

The areas in Tables II and III can be converted to the number of photons emitted from the sample at a particular wavelength. This will be shown and discussed in Section VII A.

B. DOSAGE STUDIES

Dosage studies were generated for six thoria crystals: OR1, OR2, OR4, OR7, OR8, and N 1. The full deuterium source was used for the excitation of all samples and the monochromator set at 210 nm was used for a second set of curves on OR2. Saturation was attained for all samples with the full source. All dosage curves are plotted on a common log-log scale of area under the peaks vs. time of excitation. On all of the dosage plots, each unit of area corresponds to one square centimeter of area on the data charts, adjusted to the 10^{-7} ampere scale of the electrometer.

1. Dosage of OR2 (Comparison of Full Source and Monochromatic Excitation)

The dosage curves for the crystal OR2 are shown in Figures 8 and 9. Figure 8 shows the dosage curves after excitation with the full deuterium source, and Figure 9 shows the dosage curves after excitation with the monochromator set at 210 nm. The times of excitation are considerably different due to the large difference of intensity between the full source and the monochromator. The scale shift between the two figures is approximately what would be expected because of the narrow peak of excitation efficienty at 210 nm (to be shown later). Far fewer runs were made with the monochromator than with the full source, and virtually no check runs were made, so the scatter in the data is somewhat unknown. The data obtained after full source excitation were quite reproducible although a few runs were discarded as anomalous and the very low dose data showed some strong variations.

The data obtained by the two methods of excitation have strong similarities although the slopes coincide in only a few cases. In both figures, the growth curves for the total glow are initially straight and linear with slopes of 0.92 for full source excitation and 1.00 for monochromatic excitation. In Figure 9, the knee of the curve may indicate the onset of saturation. The -103°C peak has two segments in both figures; one at low dose which is quadratic, or nearly so, and one which is sublinear. The 147°C peak also has two segments in each figure: one at low dose which is quadratic and a second segment whose slope is less (1.00 and 1.43) The -14°C (-18°C) peak is initially linear, or slightly sublinear in both figures. With full source excitation this peak has a straight sublinear segment before saturation while the monochromatic data seem to saturate. The 80°C peak is initially quadratic (or nearly so) in both figures and the 174°C peak is nearly linear initially in both cases. The -160°C peak is initially quadratic after monochromatic excitation and superlinear after full source excitation.

Large differences between the two methods of excitation were seen in only two cases. The high dose portion of the dosage curves for the 145°C peak has a slope of 1.00 for full source excitation and 1.43 for monochromatic excitation. This difference may be due to the lack of high dose data in the latter case. The -160°C peak appears to be quadratic for monochromatic excitation and more nearly linear for full source excitation. This is the largest difference observed. The dosage curve for full source excitation is S shaped and the nearly linear region is really a transition between high and low dose plateaus. Again, the lack of data for monochromatic excitation may cause erroneous conclusions. Careful examination of the data points indicate the possibility of S shaped behavior.

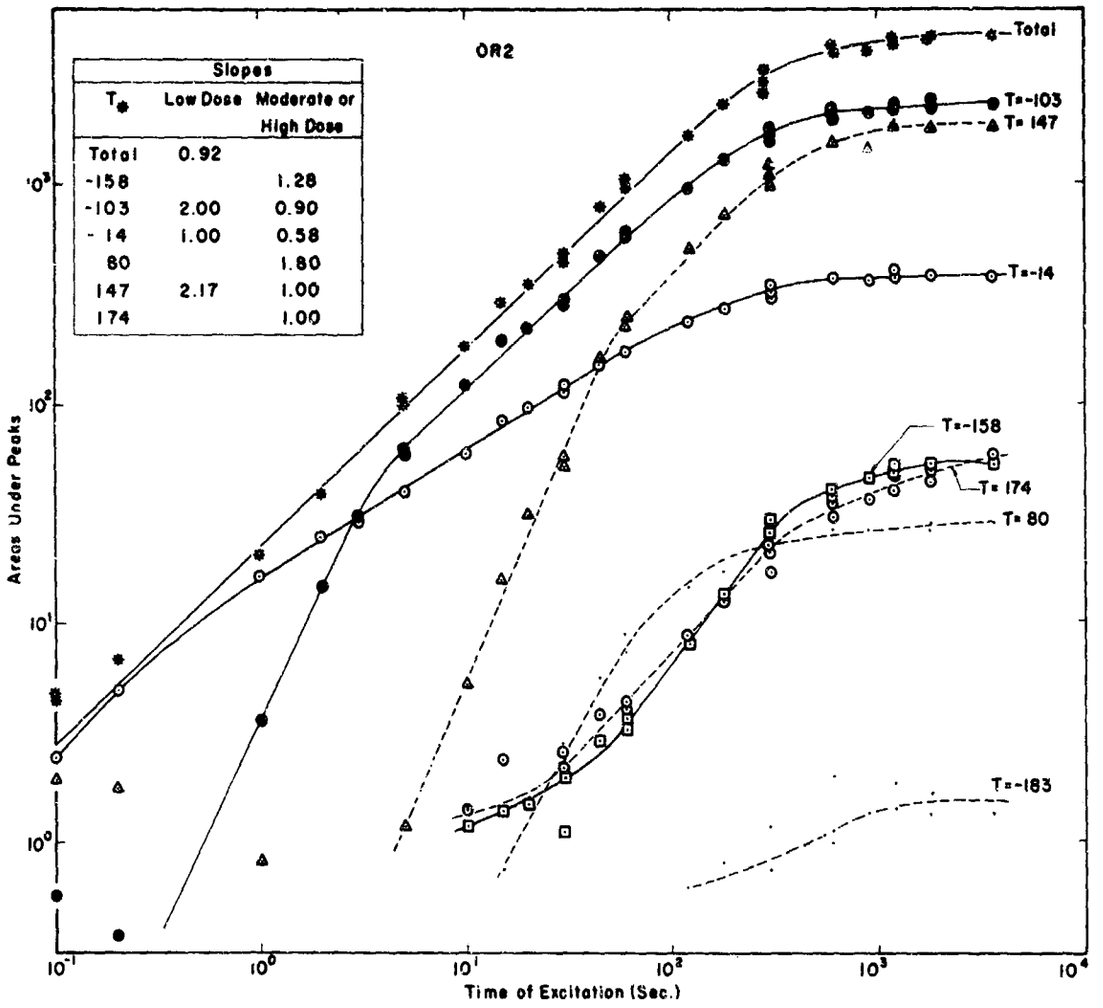

Figure 8. Dosage curves for ThO_2: OR2 (Full Source Excitation)

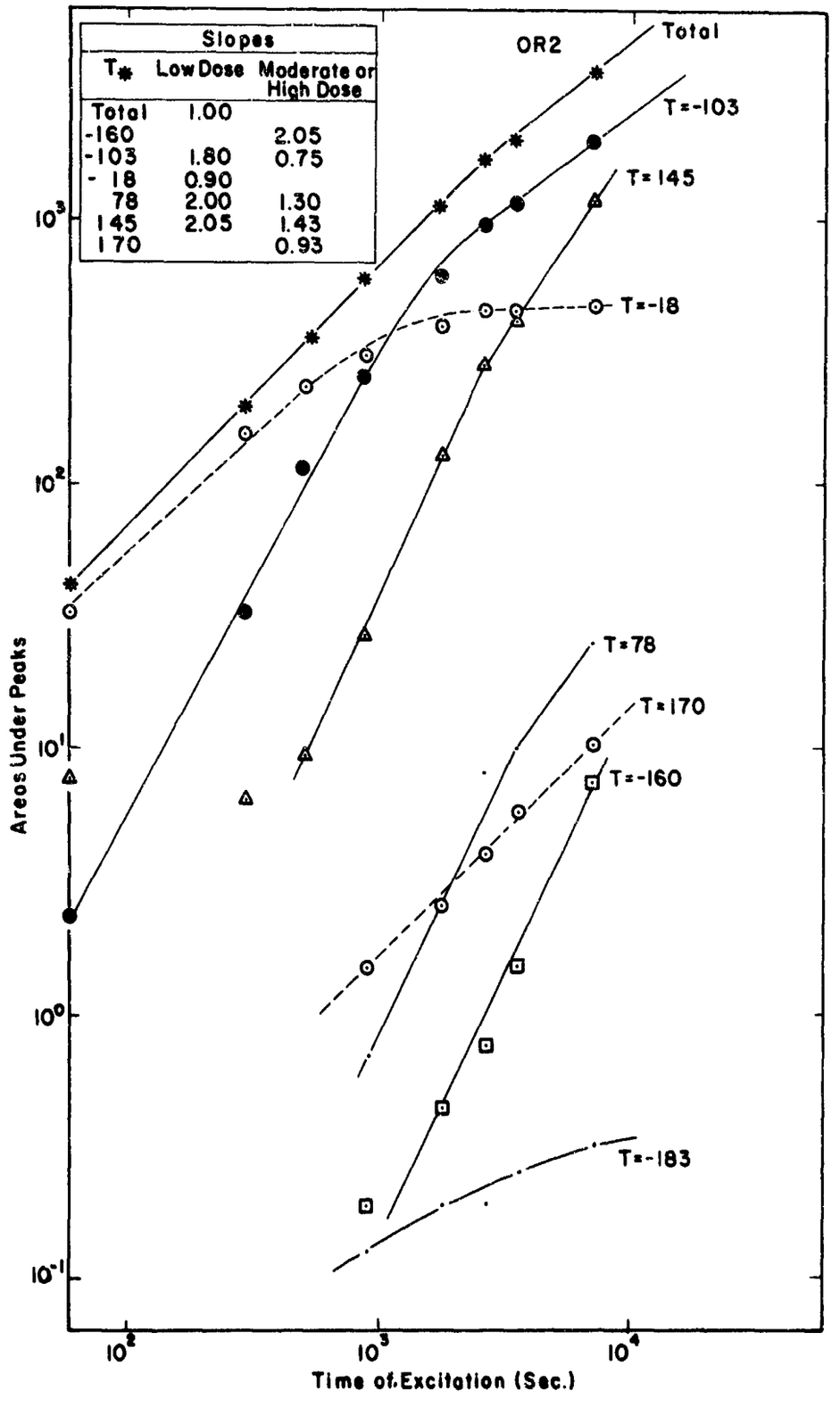

Figure 9. Dosage curves for ThO_2: (Monochromatic Excitation)

2. Shift of T_* with Dose (Retrapping)

In Section II it was pointed out that a decrease of peak temperature with increasing dose indicated a strong self-retrapping process: it was predicted that the decrease of peak temperature would be a straight line if plotted against the log of the excitation time. We observed such behavior with the OR2 crystal. The temperatures of the peaks after 60 minutes of excitation with the full source (saturation conditions) were chosen as a reference, and variations were plotted as a function of excitation time on a semilog plot in Figure 10. The initial behavior of the -15°C peak and the moderate dose behavior of the -103°C peak exhibit the decrease of peak temperature due to strong self-retrapping. The kinetics of these peaks will be discussed in more detail later in this section under Thermal Activation Energies.

The information in Figure 10 can be correlated with the dosage curves in Figure 8 in several ways. As seen from the dosage curves, the 149°C peak did not appear at low dose levels; instead, a peak at about 115°C was observed. Figure 10 shows the regions (high and low dose) of relatively constant peak temperature (149°C and 115°C) and a smooth transition region. Also, note that for an excitation time of about 5 sec the growth curve for the -103°C peak has a sharp change of slope and the ΔT_* vs. t curve in Figure 10 also shows a marked change in behavior. For the -103°C peak this could be due to peak multiplicity as in the case of the 149°C peak. The -103°C peak was observed to be a double peak at very low dose levels in other crystals.

3. Dosage Curves of Other Oak Ridge Crystals

Figure 11 shows the dosage curves for OR1, a crystal from the same batch as OR2. The total glow was somewhat less than for OR2. Several additional peaks occurred, although the peaks that appeared in OR2 were also in OR1, and there were some temperature differences. The initial regions for the total glow, -111°C and -90°C peaks, are quite straight and slightly superlinear with slopes of about 1.2 on the log-log plot. There is apparent saturation after 15 minutes. The curve for the -12°C peak is again bowed and has the added feature that it shows a decrease at high dose levels. The 153°C peak appears only to approach saturation. Shifts of the peak temperatures were only slight. A possible explanation for the decrease of the -12°C and -90°C peaks at very high excitation times would be that the long wavelength light in the deuterium source is bleaching the filled traps at a time when the available sources are significantly reduced in number. The -14°C peak of OR2 showed similar behavior but to a lesser extent. Bleaching will be discussed more fully below.

Figures 12 and 13 show the dosage curves of OR7 and OR8. These crystals were from the same batch as OR1 and OR2 and all thermoluminescent properties exhibited were much more

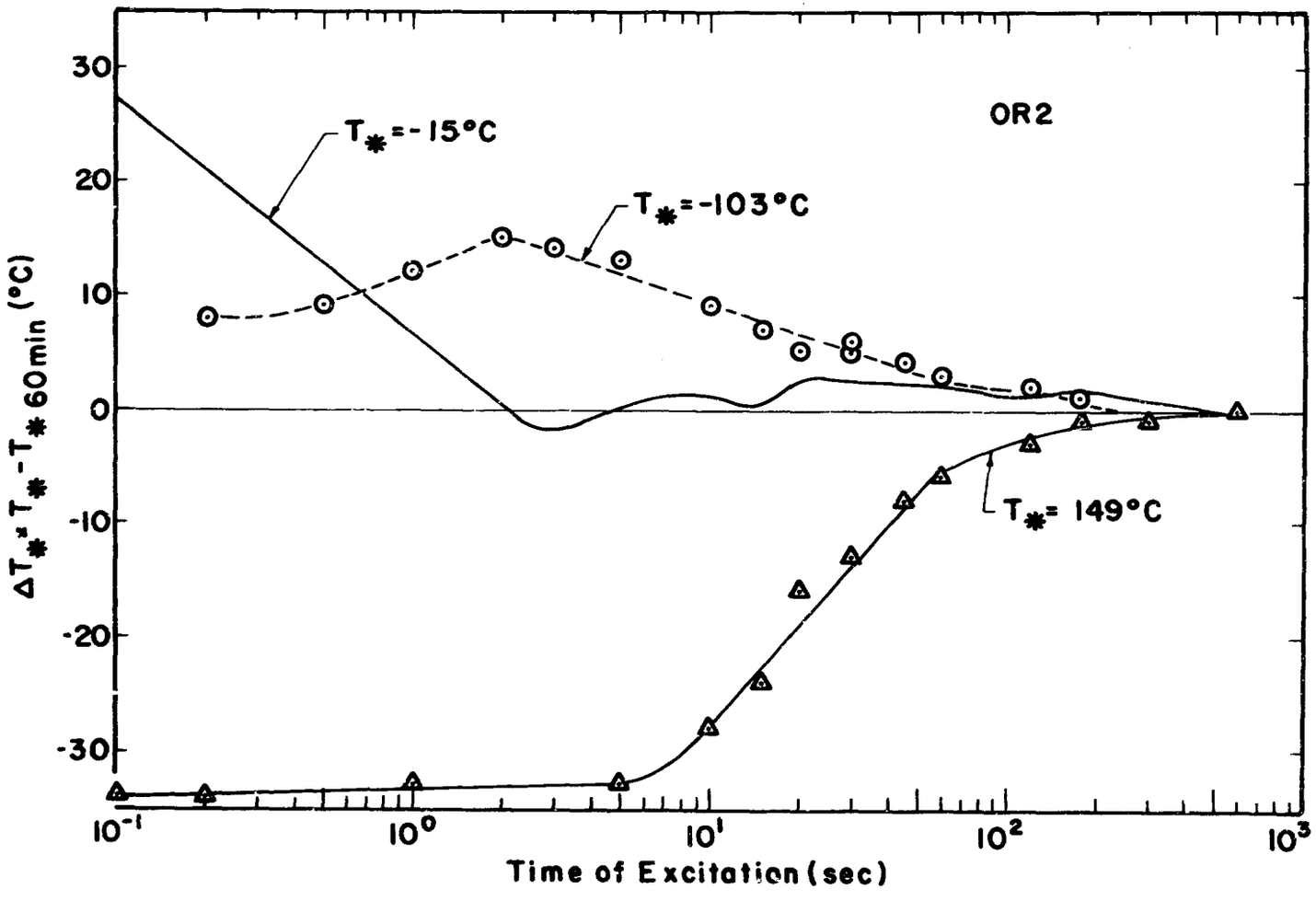

Figure 10. Shift of peak temperature as a function of dose for ThO_2: OR2

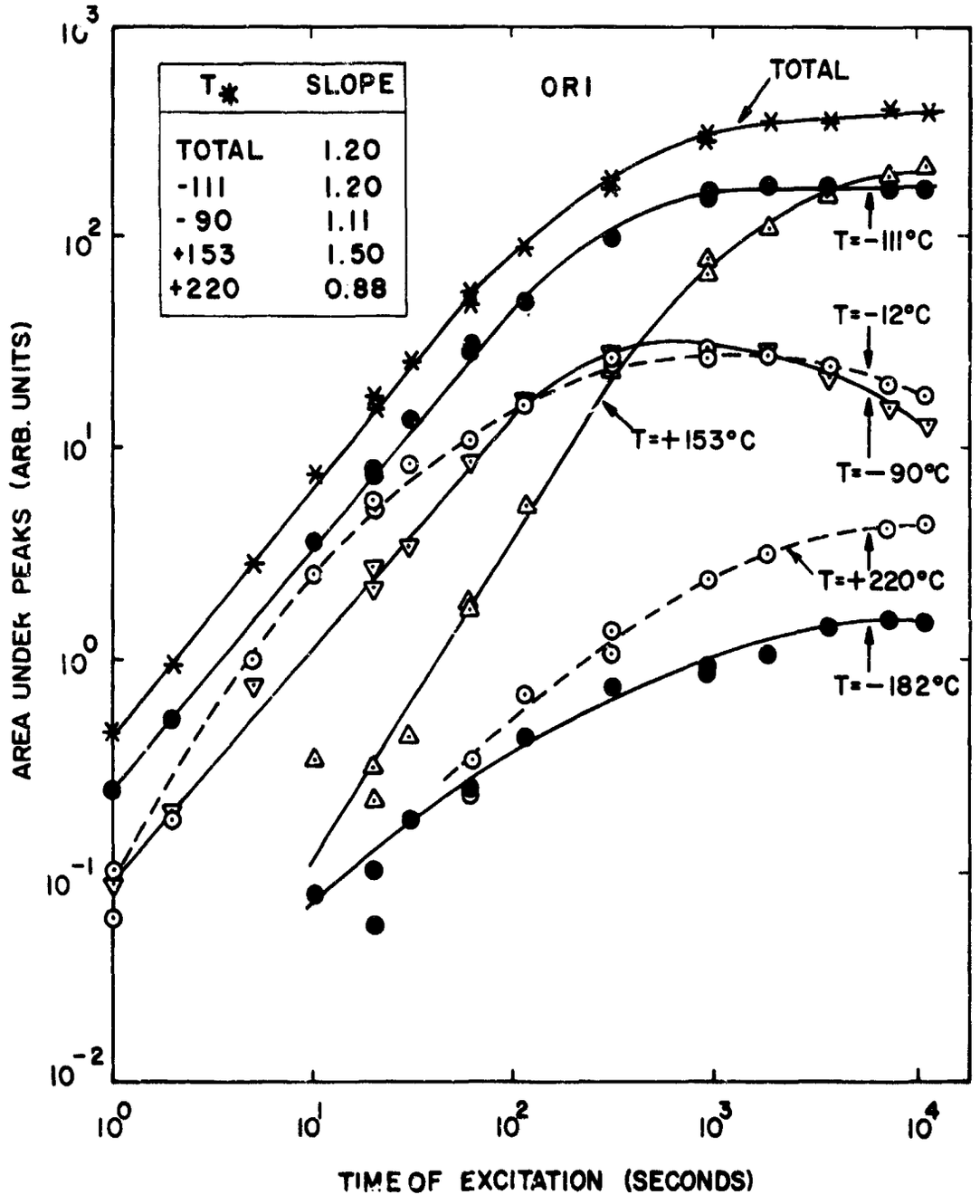

Figure 11. Dosage curves for ThO_2: OR1

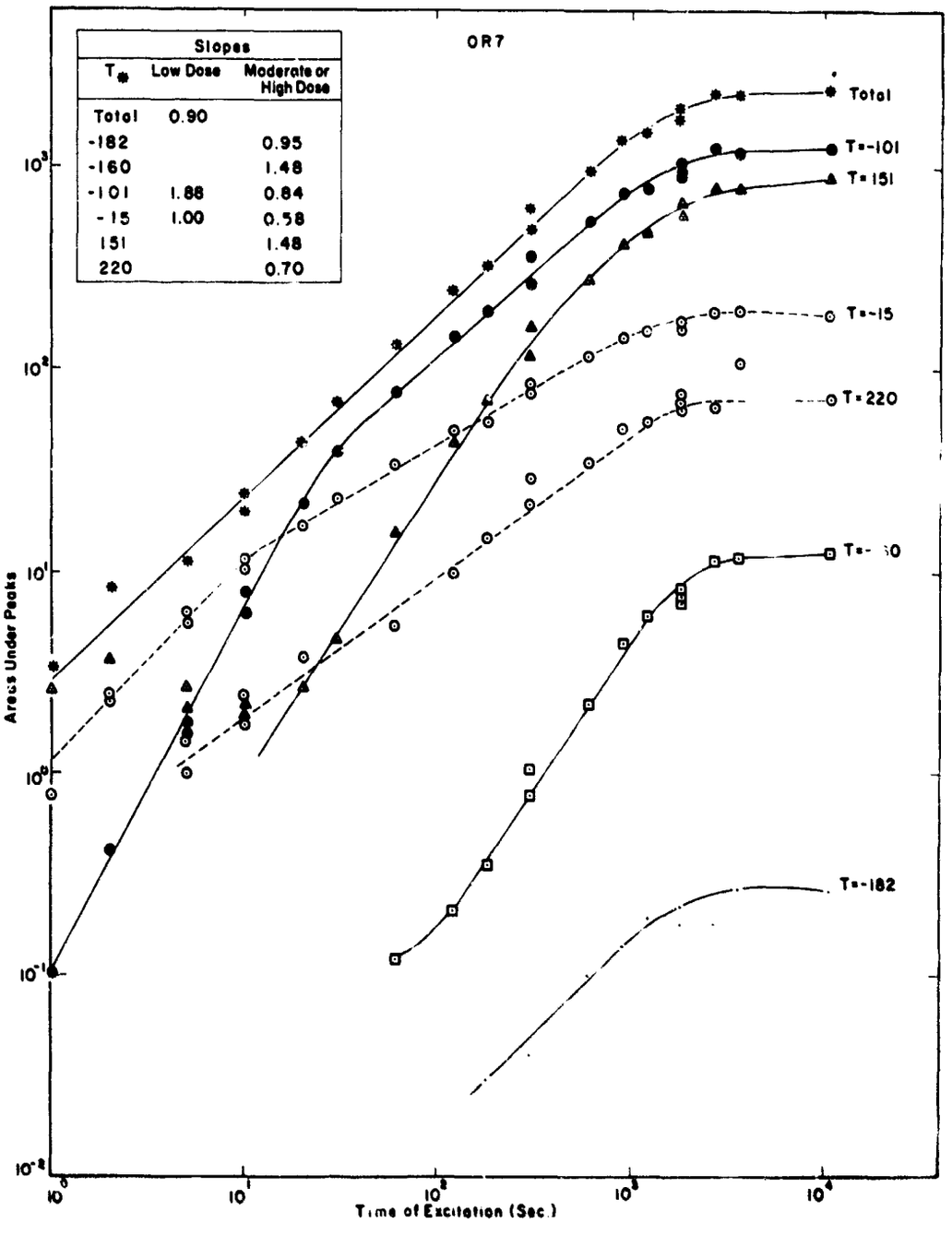

Figure 12. Dosage curves for ThO_2: OR7

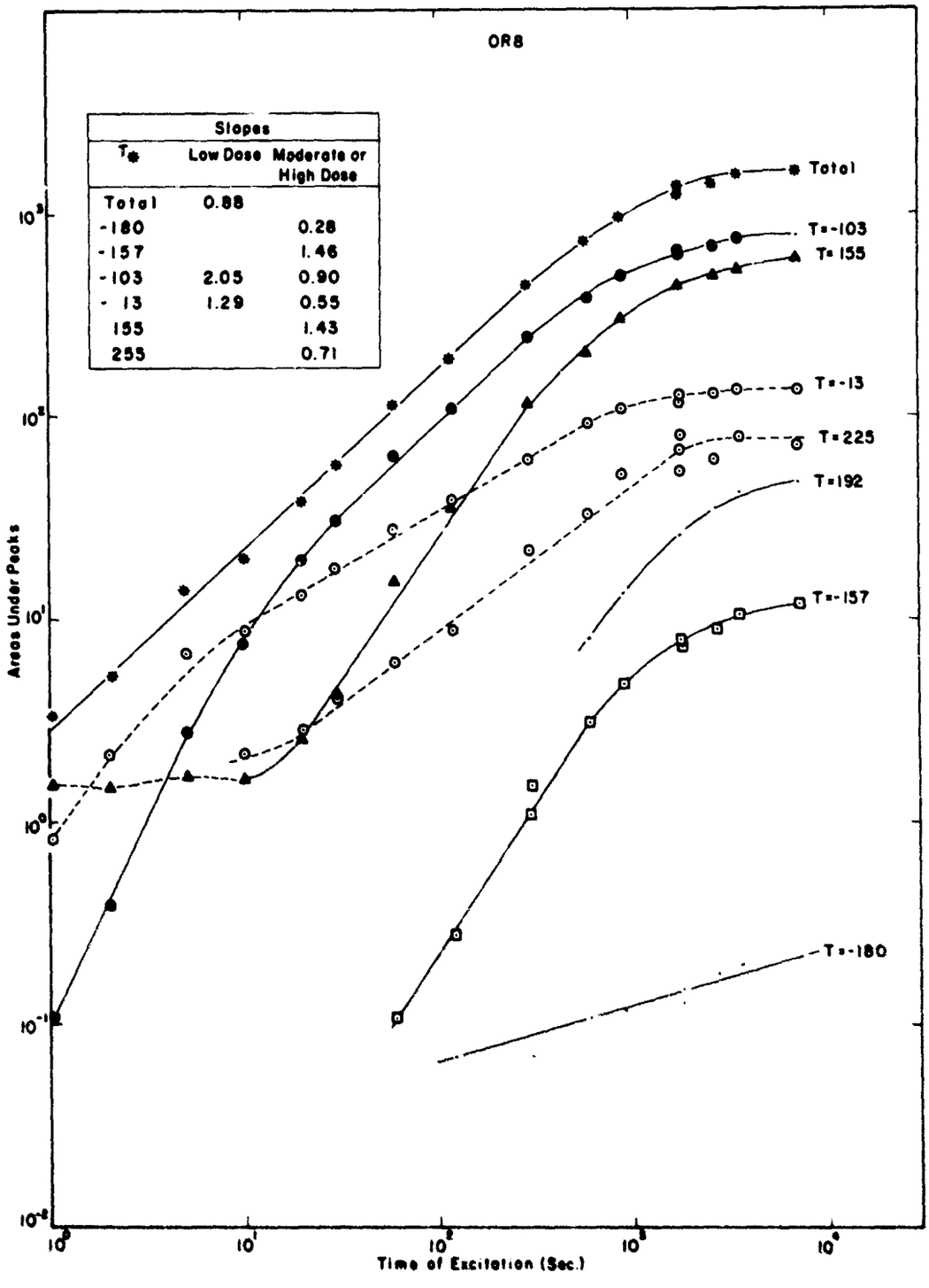

Figure 13. Dosage curves for ThO_2: ORS

similar to OR2 than to OR1. Crystals OR7 and OR8 were analyzed for impurities by Battelle. Figures 12 and 13 were generated after excitation with the full deuterium source, so they are the equivalent of Figure 8.

Inspection of the three figures (9,12,13) indicates that there are no gross differences between them. The shapes, magnitudes, and relative intensities of the individual growth curves compare favorably with each other. It is seen that the slopes of the growth curves for the three crystals are 0.92, 0.90, and 0.88. The -101°C peak in each crystal has a growth curve that is nearly identical to the curves in the other two crystals. The growth curves for the other peaks common to all three crystals are also very similar although there are a few exceptions. It is obvious that the homogeneity among the samples in the batch was very good.

Dosage curves for the OR4 crystal are shown in Figure 14. This crystal is from the second batch obtained from Oak Ridge. During growth it was attempted to incorporate a significant amount of Ca into the crystals but this was not successful since the impurity analysis showed no more Ca in these crystals than in others. However, there were a number of drastic differences in the optical properties of the batch. The thermoluminescence was very weak: the total glow was about two orders of magnitude less than the other crystals and there was less variation in total glow between very low dose and very high dose. Also, the relative strengths of the various peaks were more nearly equal, i.e., principal peaks that were several orders of magnitude larger than the other peaks were not observed. The glow curve shown in Figure 5 indicates that the principal peak at -103°C was split into two peaks. The initial slope of the growth curve for the total glow was equal to 1.0. It is evident that one of the conditions of growth of this batch acted as a "poison" for the thermoluminescence, perhaps by the exclusion of recombination centers or by provision of a method of competing nonradiative transitions. Note that the peaks above room temperature are not present. A very small peak at 205°C was noted but is not shown in the figures. It is shown later that for OR2 the traps associated with the largest of the high temperature peaks, 149°C, are occupied when charge is released from the traps giving rise to the peaks at -103°C and -15°C. This is probably true for other thoria crystals and is consistent with the fact that the -103°C and 150°C peaks are missing from OR4. For very low dose they were missing from OR2 also, and there were peaks near -120°C and -93°C, as there are for OR4.

For the OR4 crystal, the total glow and the dosage curves for the individual peaks had slopes of about 1.0 between 10 and 20 sec. The -14°C and -53°C peaks were rather anomalous. The behavior of these two peaks will be noted again when discussing the excitation spectra. Note that for the OR1 crystal in Figure 11, the -12°C peak showed a reduction in intensity at high excitation levels and, in both OR1 and OR2, this peak did not show simple growth behavior.

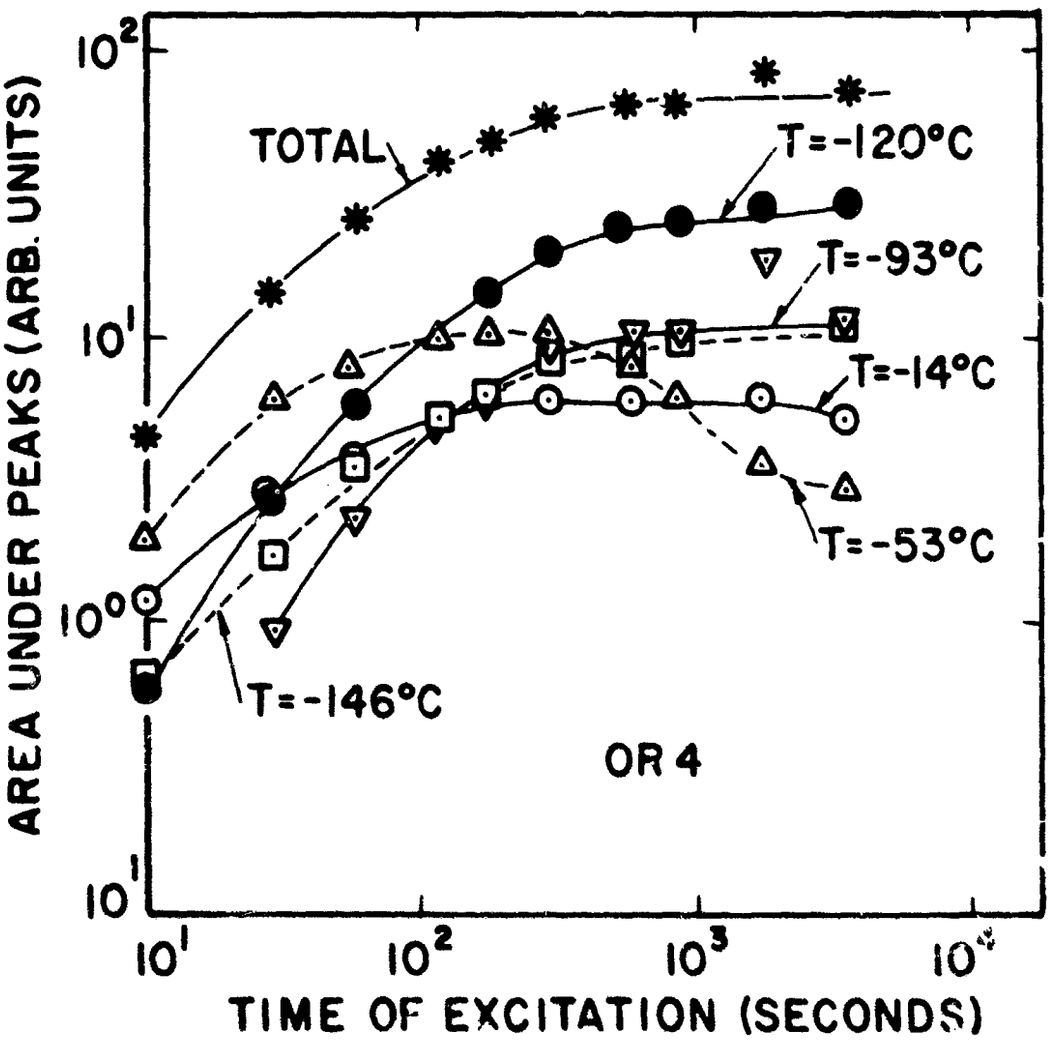

Figure 14. Dosage curves for ThO_2: OR·

4. Dosage Curves for N 1 (Self-Excitation)

The dosage curves for the Norton crystal N 1 are shown in Figure 15. Observe that again the principal peaks occur at -119°C, -13°C, and 166°C, as was the case for the previous crystals. For times of excitation between 1 sec and 100 sec the curves are quite straight. The slopes for the total glow and the -119°C peak equal 1.0 and for the -13°C peak the slope is slightly greater than one. The growth behavior for the -146°C peak is sublinear (slope = 0.87) and for the 166°C it is superlinear (slope = 1.35). Saturation was attained but not at the same time for all peaks. The total glow was large and equivalent to the OR2. Only slight shifts of the peak temperatures with dose were observed and there was no apparent bleaching. Note that the -103°C and 150°C peaks are significantly shifted and the high temperature peak is relatively weak, as was true for OR4.

The interesting feature of this dosage study is the flattening of the curves at low dose levels. We observed that simply cooling the sample to liquid nitrogen temperature and immediately warming produced a glow curve that was similar in nature with respect to peak temperature and relative strength to the glow curves seen after ultraviolet excitation. The growth of the self-excitation can be seen in the lower right-hand corner of Figure 15. In this case, the "time of excitation" means the time that the sample was left at liquid nitrogen temperature in the dark. As can be seen, the total glow after two hours is only 10 units compared to over 3,000 units after 2 hours of ultraviolet excitation. However, the glow after 2 minutes is about 1 unit, which is the apparent equivalent to 0.01 sec of ultraviolet excitation. The minimum time required during a normal run to turn the sample around to face the photomultiplier, etc. is about 2 minutes, so it is felt that the glow seen at low dose levels is primarily due to the self-excitation. An extrapolation of the dosage curves supports this observation.

The self-excitation is considered to be a result of the natural decay of thorium, which gives off 3.98 MeV alpha particles and 0.055 MeV gamma rays with a half-life of about 10^{10} years. Linares[28] has reported that the alpha radiation produces no noticeable degradation of the luminescing ions in rare earth doped thoria but that 0.055 MeV x-rays at room temperature produced sharp thermoluminescence which annealed out at a rate dependent on the dopant. Finch et al[30] also observed self-excited thermoluminescence in thoria crystals grown by them. Linear growth of the self-excitated thermoluminescence was observed by them for periods up to 30 days

5. Conclusions

It is seen that considerable information can be obtained about a sample from a study of the dosage curves. The principal trapping states and their relative strengths can be determined: the three principal trapping states are characterized by peaks at -120 to -90°C, -14°C, and 147°C. An

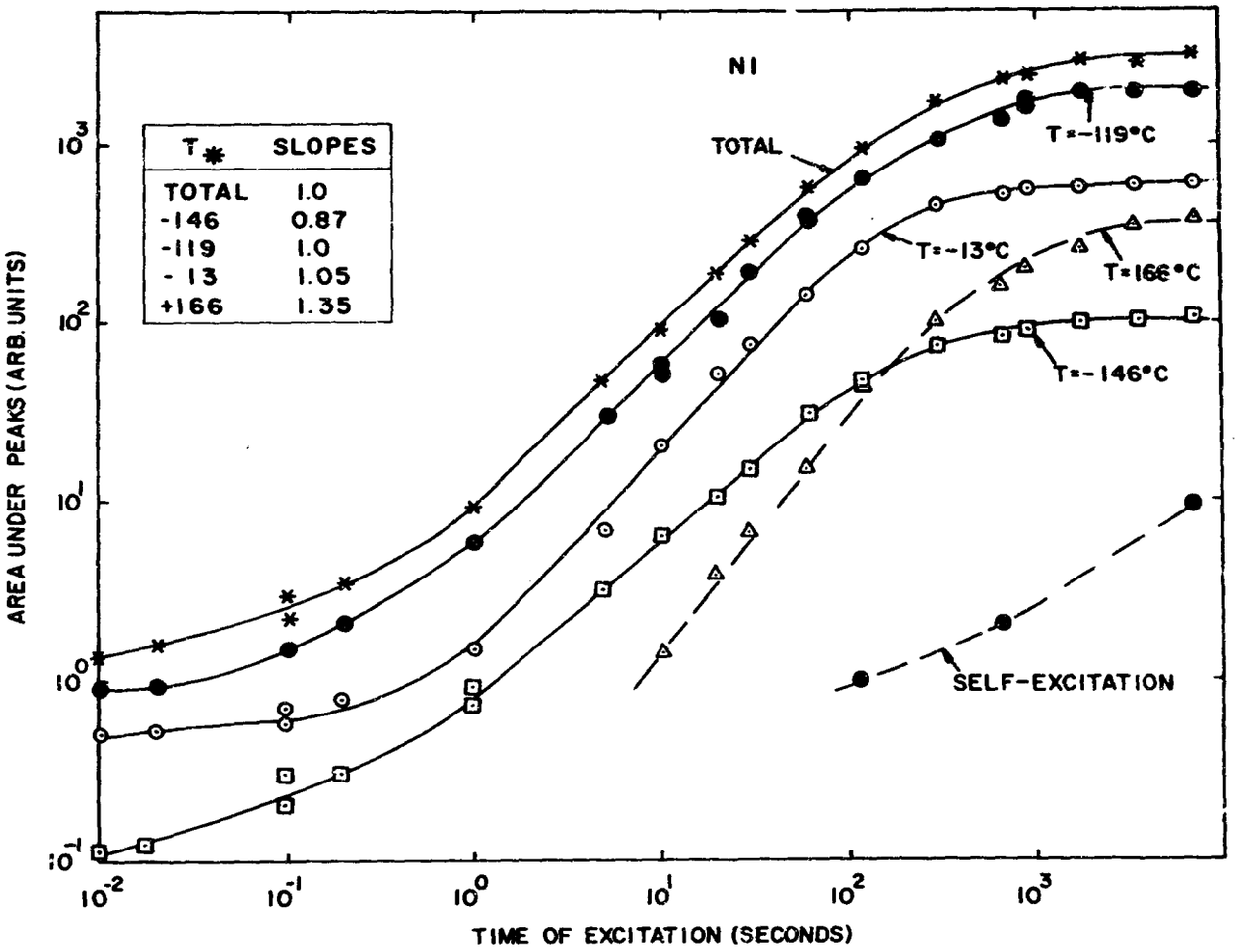

Figure 15. Dosage curves for ThO_2: N 1

examination at low dose levels only would have yielded entirely different conclusions. The growth rates of the total glow and of the individual peaks yield information about the excitation process and the trapping probabilities of the traps. The initial growth rates and magnitudes of the saturation values are probably of the most importance. Information about the basic processes was noted by the shift of peak temperature with dose. It is also apparent that the most consistent data with regard to peak temperature, peak height, and relative magnitude are obtained under saturation conditions which are established by dosage studies. The dosage levels attained during excitation spectra studies can sometimes be selected to occur in a region where dosage effects are minimized, i.e., where the growth curves are relatively parallel and preferably linear.

C. THERMAL ACTIVATION ENERGIES

The thermal activation energies and frequency factors for the principal traps in six crystals were calculated. Data were obtained by the methods of initial rise, inflection points, and halfwidths; calculations were performed with a computer according to monomolecular and bimolecular models. With the occurrence of complex peaks and multiple processes, each method of analysis has certain limitations and also possibilities for conflicting results. Each method analyzes a particular set of data point pairs and they may or may not agree. It is believed that self-consistent data obtained by initial rise is more likely to yield an accurate value for the energy of a trap than any other method. In the event of a multiple peak, the initial rise analysis may yield the energy of one of the peaks quite accurately or it may yield too high an energy, depending on the relative strengths of the components.

1. Initial Rise Results

The results of the initial rise calculations on OR2 are shown in Figure 16. As discussed in a previous section, each rise had from 4 to 12 data point pairs (temperature and intensity) and the energy and frequency factors were calculated between each consecutive pair of points and between the first point and all other points. A large number of rises were recorded and the average values of the calculated energies for a monomolecular model were plotted as a function of the average temperatury of the rise. The approximate scatter in the data is also shown. The thermoluminescence peak temperatures of the traps involved are shown as vertical marks along the abscissa. As each initial rise depletes a certain portion of the trapped charge, the peak temperature may shift, as illustrated by the -103°C peak which shifts upward as the peak is decayed. This shift is believed to occur because the peak is complex, and successive rises simply decay the lower components. The shift could also be due to strong retrapping, as discussed in a previous section. Retrapping is considered to be the principal reason for the shift of peak temperature (not shown) of the -15°C peak.

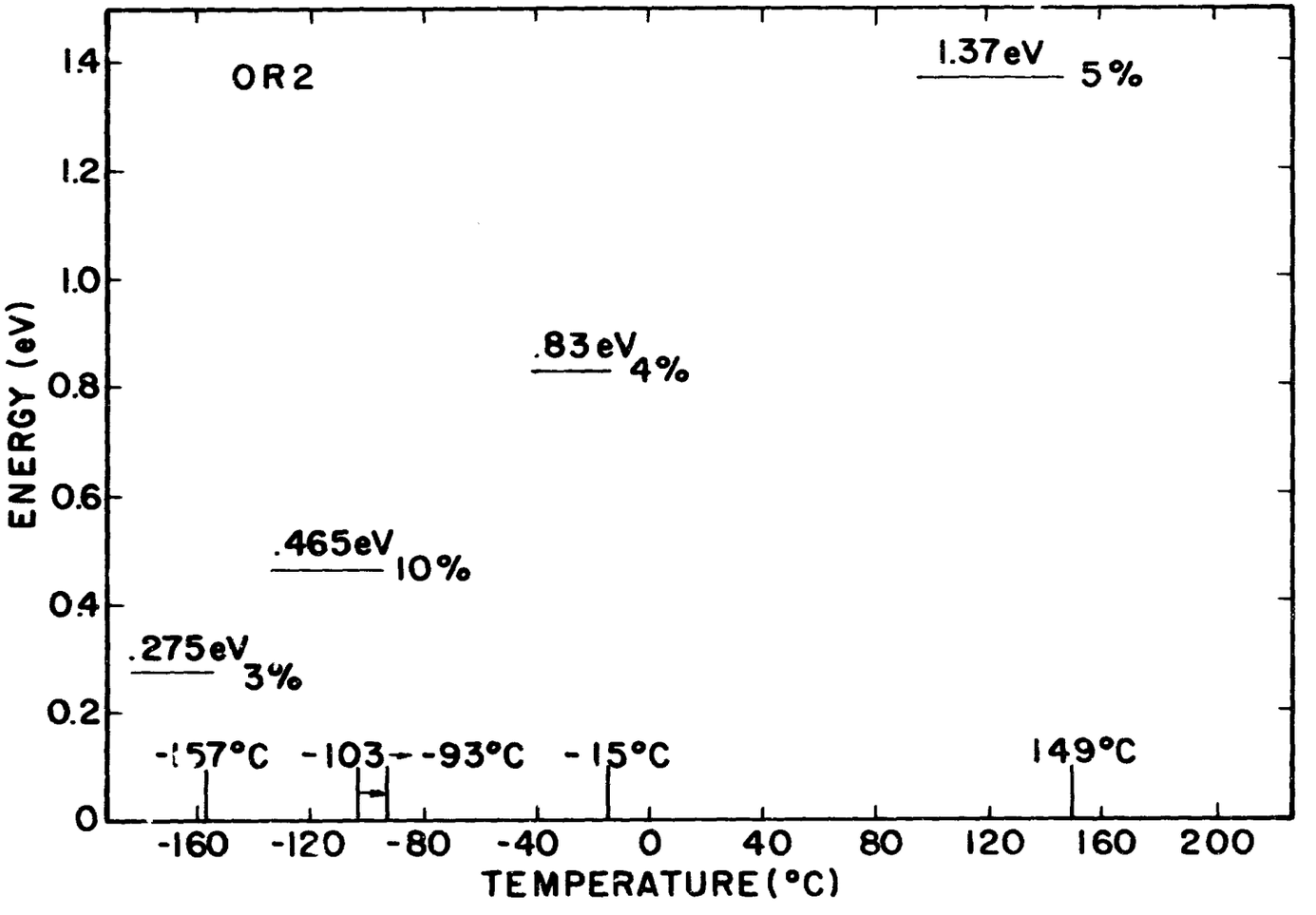

Figure 16. Thermal activation energies of traps from initial rise data ThO_2: OR2 (average values, monomolecular form)

2. Comparison with Results from Inflection Point Method

Table IV was prepared to compare the results of the energy calculations on all six crystals by the three different methods. The data are organized according to peak temperature. The composite glow curves in Figures 5, 6, and 7 showed that a number of peaks are common to all crystals, so the energy calculations on a particular peak can be compared between crystals. The values of E and $\log \phi$ obtained by the method of initial rise are for the monomolecular model only. Calculations were performed using the inflection points of both the rise and fall of the glow peaks, i.e., the low and high temperature sides. The results of these calculations according to monomolecular and bimolecular models are shown in Table IV. Halfwidth calculations are shown for the monomolecular model (EM) and bimolecular model (EB). In all cases, the exponents of ϕ were rounded off to integers.

It is immediately obvious that the values of E and ϕ as calculated by the inflection point method were somewhat different from the initial rise calculations and also showed more scatter. For example, for OR2 the average values of E as calculated by the inflection point method, according to the monomolecular model, were 0.24, 0.24, 0.59, and 2.25 eV for the four peaks shown in Figure 16, in order of increasing peak temperature. The differences are seen to vary from a few hundredths of an electron volt to a factor of two.

There are several possible reasons for these differences. The calculations are based on specific and rather simple models. It is possible that the thermoluminescence does not obey simple analytical forms. A more likely situation is that the peaks are not analytical because of peak multiplicity and retrapping. Consider the -103°C peak: the energy calculated by the inflection point method is about half the value calculated by the initial rise. The peak may in reality be a multiple peak the components of which are very close to each other in energy, peak temperature, growth habits, and emission. The overlap of the peaks could result in too high an energy value as computed from initial rise data and too low a value by inflection points. Another possibility would be the occurrence of strong retrapping, which may have the effect of broadening a peak and giving too low an energy value by the inflection point technique. This could also cause the shift of peak temperature from -103°C to -93°C with decay of the peak. One means of studying such peaks is to decay the peak more extensively and observe the changes in the shape and peak temperature. If a peak is a superposition of two monomolecular peaks, further cleaning could result in a convergence of the initial rise and inflection point energies as a function of cleaning. Similar arguments can be made for the other peaks.

Further evidence of the complexity of the situation is noted by the large spread in values between the rise and fall inflection points and between the calculations based on the two

Table IV

Thermal activation energies and frequency factors for thermoluminescence peaks from six ThO_2 single crystals according to initial rise, inflection points, and halfwidths

		Initial Rise monomolecular		Inflection Points monomolecular rise		Inflection Points monomolecular fall		Inflection Points bimolecular rise		Inflection Points bimolecular fall		Halfwidths monomolecular		Halfwidths bimolecular	
T_*	Sample	E	log ϕ	E	log ϕ	E	log ϕ	E	log ϕ	E	log ϕ	EM	log ϕ	EB	log ϕ
-157	OR2	0.275	11	0.232	9	0.260	10	0.297	12	0.415	17	---	---	----	---
-157	OR7	---	---	0.265	11	0.229	9	0.303	12	0.397	17	0.25	10	0.30	12
-156	OR8	---	---	0.263	10	0.251	10	0.301	12	0.391	16	0.28	11	0.32	13
-148	OR4	---	---	0.355	13	0.254	9	0.392	15	0.461	18	---	---	---	---
-103	OR2	0.465	13	0.264	6	0.216	5	0.325	8	0.358	9	---	---	---	---
-111	OR1	0.45	13	0.278	7	0.213	5	0.324	9	0.394	11	0.27	7	0.30	8
-101	OR7	0.48	13	0.287	7	0.217	5	0.342	9	0.360	9	0.28	7	0.33	9
-100	OR8	0.48	13	0.281	7	0.216	5	0.341	9	0.359	9	0.27	7	0.31	8
-122	N 1	0.40	10	0.249	7	0.160	4	0.300	9	0.272	8	0.24	7	0.28	8
-122	OR4	---	---	0.457	14	0.405	12	0.513	16	0.729	23	---	---	---	---
-15	OR2	0.83	15	0.609	10	0.568	10	0.664	12	1.01	18	---	---	---	---
-09	OR1	0.86	15	0.624	11	0.579	10	0.738	13	0.980	18	0.68	12	0.79	14
-14	OR7	0.85	15	0.646	11	0.572	10	0.77	14	0.949	17	0.73	13	0.79	15
-13	OR8	0.85	15	0.577	11	0.565	10	0.741	13	0.939	17	0.66	11	0.76	14
-13	N 1	0.75	12	0.428	7	0.296	4	0.530	9	0.506	8	0.46	8	0.53	9
-17	OR4	---	---	0.797	14	0.607	10	0.960	18	1.03	19	---	---	---	---
+146	OR2	1.37	15	1.63	18	2.93	34	2.07	23	4.87	57	---	---	---	---
162	OR1	1.39	15	1.31	14	1.43	15	1.60	17	2.38	26	1.44	15	1.67	18
150	OR7	1.37	15	1.62	18	1.54	17	1.90	21	---	---	1.62	18	1.89	21
153	OR8	1.32	15	1.38	15	1.95	22	1.74	19	3.22	36	1.53	17	1.78	20
166	N 1	1.25	13	1.13	11	0.970	9	1.38	14	1.72	18	1.22	13	1.42	15

different models. An extreme example of this is the 149°C peak for OR2. For this peak, all inflection point calculations appear to give too high an en gy value. Even the lowest value for the exponents of ϕ (18) is higher than can be reasonably expected. The large differences between the values calculated from the rise and fall inflection points for both the monomolecular and bimolecular models show that simple analytical forms do not apply.

3. Analysis of Major Peaks Common to all Crystals by Three Methods

The ~157°C peak is apparently monomolecular. The energy data obtained by all three methods are fairly consistent in monomolecular form. The average monomolecular inflection point energy is slightly less than the monomolecular initial rise energy while the average bimolecular energy is slightly higher. The differences between the energy values calculated from the rise and fall inflection points are about 10% for the monomolecular model and 30% for the bimolecular model. A frequency factor exponent of 11 is quite reasonable whereas a frequency factor exponent as large as 17 as obtained from bimolecular calculations appears to be too high. The numbers obtained for OR4 are consistently higher than for the other samples, as expected for a higher peak temperature. This peak did not have sufficient intensity for initial rise analysis for crystals other than OR2.

The situation of the ~103°C peak is somewhat unclear. The large differences of E as calculated by initial rise and inflection points for OR2 were discussed in an example above and are seen to be quite consistent in the other crystals. The values of E as determined by initial rise for the Oak Ridge crystals agree within 5% between crystals. The inflection point calculations yield results that are rather different from the initial rise. Possible reasons for these differences were discussed above. For crystals OR1, OR2, OR7, and OR8, the inflection point calculations (monomolecular and bimolecular, rise and fall) agree within 5% between samples (not between methods). For the monomolecular model, E for the rise is 20% or more higher than E for the fall. For the bimolecular model, E_{fall} is about 15% larger than E_{rise}. The differences between the average monomolecular results and the average bimolecular results are as high as 30%. The table indicates that a value of 6 would be a reasonable average for the exponent of the frequency factor according to the monomolecular model while a value of 9 would be appropriate for the bimolecular model. There is no a priori reason for ruling out either of these values even if a value of 9 appears more reasonable when compared with other peaks. Hence it is obvious that the ~103°C peak is quite complex. This is in part due to the multiplicity of the peak. In several crystals (OR1 and OR2) this peak has been observed to be split into at least two components at low dose conditions (see dosage curves for OR2 in Figures 8 and 9). This peak was also observed to be multiple from the emission spectra of OR1 (Figures 20,21). The possibility of self-retrapping was discussed above. The EPR study[32] or OR1 and OR2 indicates that some of

the charges released from the ~103°C and ~14°C peaks are retrapped by two similar but not identical traps associated with the 149°C glow peak and do not participate in the glow until the 149°C glow peak is emptied. Only a small fraction of the charge available for recombination do so rradiatively. The ~103°C peak is thus the result of competition between many processes and does not yield to simple analysis

For the ~15°C peak, the initial rise results for E and ϕ were very consistent for four of the Oak Ridge crystals. OR4 did not have sufficient intensity for analysis and N 1 gave results that showed marked deviation. The Norton crystal showed considerable deviation from the Oak Ridge crystals for nearly every peak. The inflection point data are reasonably consistent between samples with a deviation of about 5%. The differences between the rise and fall calculations are about 10% for the monomolecular calculations and about 30% for the bimolecular calculations. However, the average (midway between the rise and fall) agrees fairly well with the initial rise determination. The high temperature inflection point according to the bimolecular model yields a frequency factor that is higher than can be reasonably expected. It is believed that the strong self-retrapping associated with the shift of T_* with dose (Figure 10) and the retrapping of the charge from this trap by the 149°C peak (EPR study) contribute to the complexity of the process.

The peak at 149°C also does not appear to fit a simple model. The initial rise analysis yields energy values that are very consistent between crystals (except for N 1) and appear to be quite reasonable. The inflection point calculations show tremendous variations and scatter. In all cases, the energy and frequency factor, based on the high temperature inflection point are considerably higher than those based on the low temperature inflection point. For example, for OR2 the monomolecular model yields energy values of 1.6 and 2.9 eV to give an average of 2.25 eV. The frequency factors obtained are much too high to be reasonably considered. Examination of the glow peak reveals that the peak is abnormally narrow (18°C) for such a high temperature peak and the high temperature side of the peak appears to be truncated. The sharp cutoff is reflected in the high energy value. It is quite likely that the cutoff of this peak is caused by the depletion of available recombination centers which would be most likely to occur for the highest temperature peak of a glow curve. Such a case has been disucssed by Halperin[6] and Land.[8,9] This would result in a peak temperature that is too low, which would cause the value of E as calculated by initial rise to be too low. Examination of the EPR data[32] on OR1 and OR2 reveals that the resonance line associated with the 174°C peak is the strongest line in the spectra. The 174°C glow peak is quite weak compared with the other glow peaks. This indicates that the ratio of nonradiative to radiative recombinations drastically increases in the region of 150°C, possibly as a result of the depletion of optical recombination centers.

The calculations based on the halfwidth were generally in approximate agreement with the inflection point calculations rather than the initial rise.

D. EMISSION SPECTRA (THERMOLUMINESCENCE AND FLUORESCENCE)

The thermoluminescence emission spectra for several of the thoria crystals were measured, primarily with the filter wheel. The excitation was with the full deuterium source for a sufficiently long time to insure saturation. Saturation conditions were used to provide maximum intensity and also because at saturation conditions the peak temperatures and the relative magnitudes of the peaks and their multiple components were constant. Some check runs were made with the monochromator as the excitation source.

1. Thermoluminescence and Fluorescence of OR2

The most interesting thermoluminescence spectrum was from the crystal OR2. Only one filter on the filter wheel gave a response to the emission, so the monochromator was placed between the sample and the photomultiplier and manually scanned while the sample was warming. We observed that the emission consisted of a single line at 545 nm with an estimated width of less than 2 nm and was the same for all glow peaks. The emission was rechecked using the filter wheel and the EMI-9558Q photomultiplier. This photomultiplier had more sensitivity and more red response than the RCA-1P28 used previously. The spectra obtained are shown in Figure 17. Careful examination revealed additional structure and subtle differences between peaks. Again the 533 filter showed the largest response: after corrections for the response of this photomultiplier were made, the peak transmission of this filter was shifted to 549 nm, so in Figure 17 the spectra are all normalized to 549 nm. Note that the 174°C peak is more "blue" than the low temperature peaks and that the 155°C peak has the strongest red response. The emission group at 680 nm was quite weak but was not detected by the other methods of measurement. The structure and differences between peaks were seen with the filter wheel because of the lower resolution and greater optical speed as compared to the monochromator. There is also a certain amount of spectral overlap between the filters.

The fluorescence of OR2 was measured in an attempt to identify the thermoluminescent emission spectra and is shown in Figure 18. No additional lines were observed in the region from 3000 Å to 8000 Å. The data are not corrected for photomultiplier response, which is shown on the graph; also, there were no corrections for the transmission of the spectrometer which should peak at 5000 Å according to the blaze angle of the grating. The fluorescence was quite weak so the slits had to be opened quite wide resulting in considerable dispersion. Observation of the fluorescence with the EMI tube failed to reveal additional lines or structure.

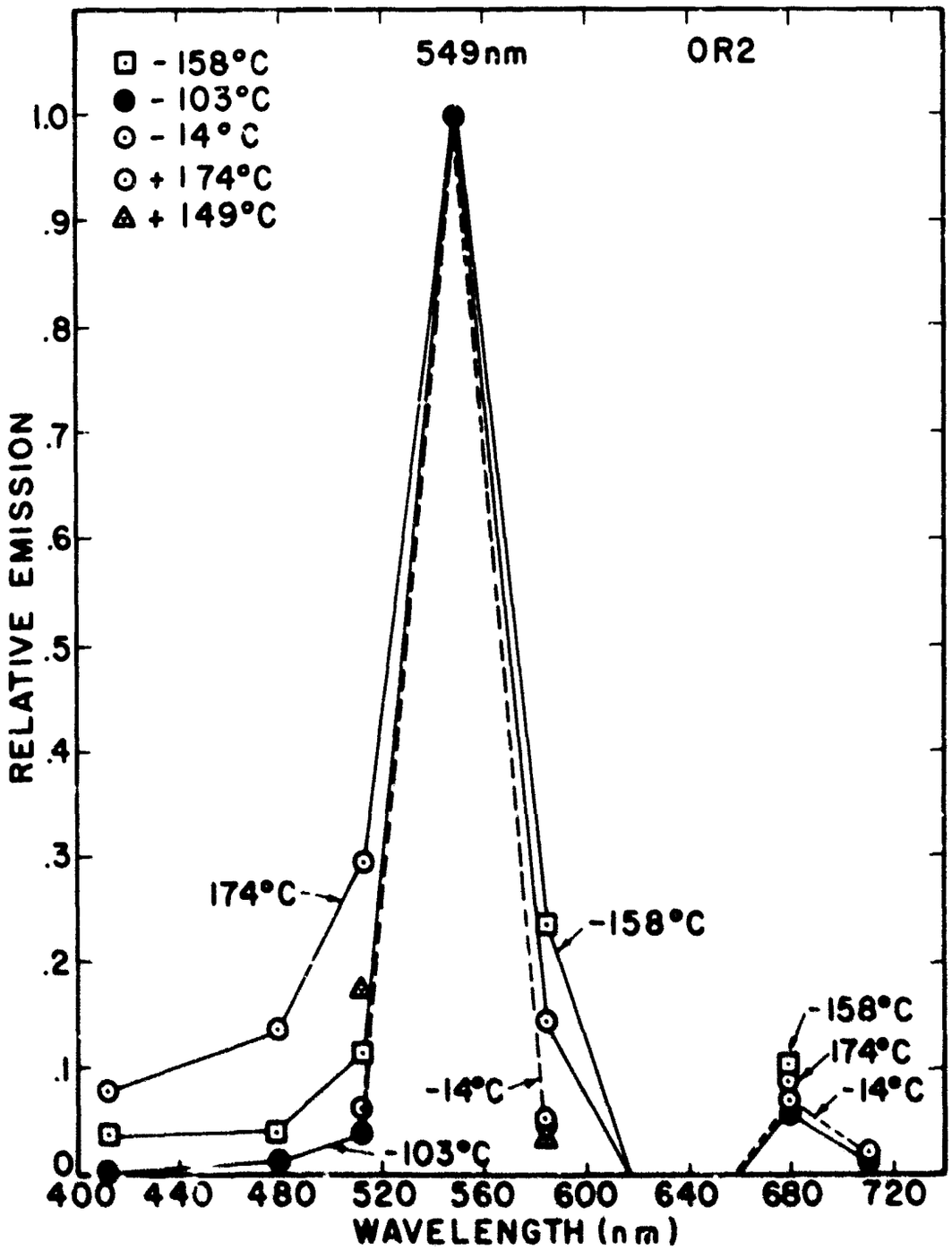

Figure 17. Emission spectra using filter wheel for ThO_2: OR2

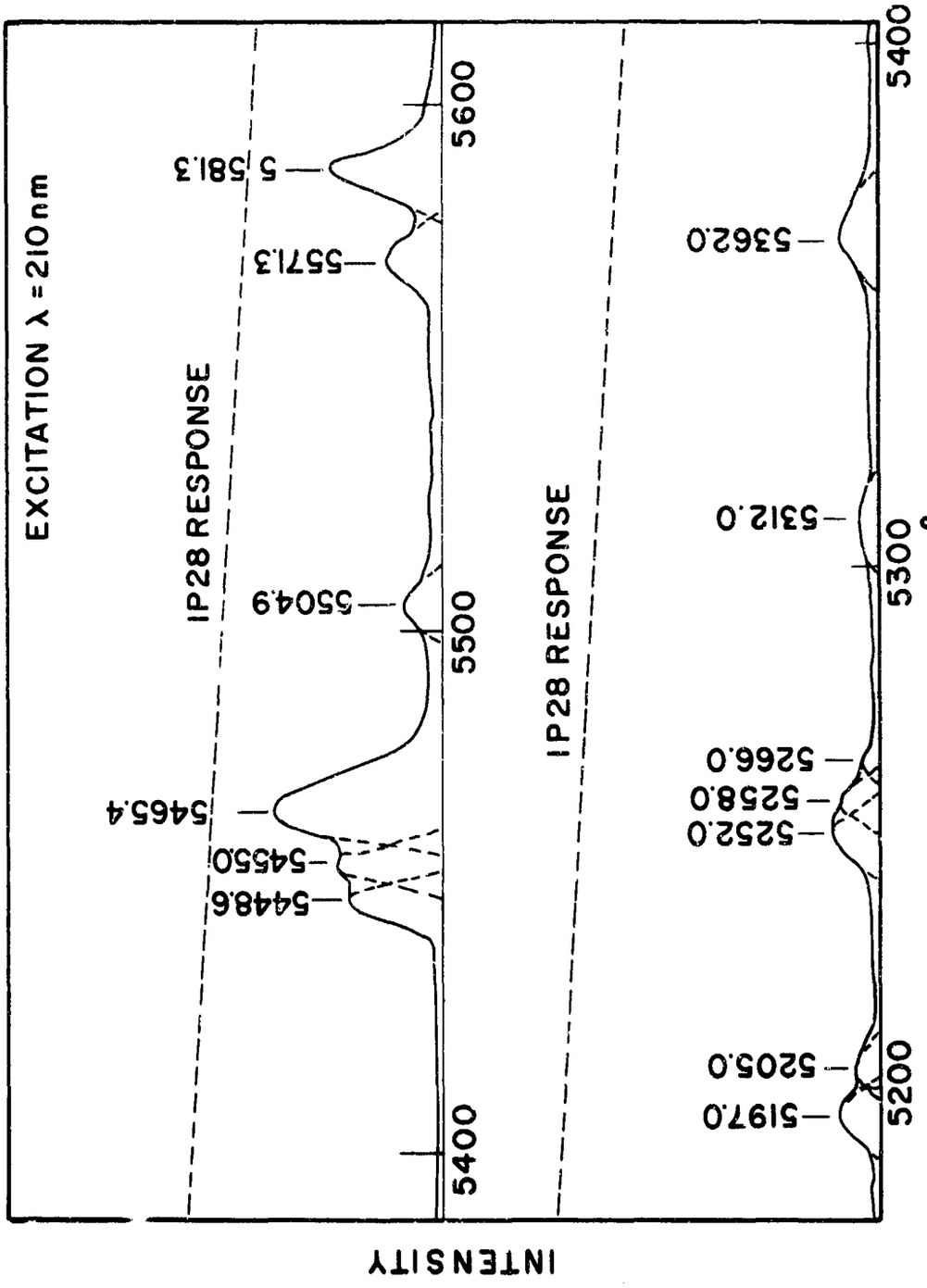

Figure 18. Fluorescence emission spectrum for ThO_2: OR2

The thermoluminescence emission was checked again by simply holding the sample in front of the entrance slit to the spectrometer as it warmed and quickly scanning selected regions of the spectrum. We determined that the thermoluminescence emission was identical to the fluorescence in Figure 18, i.e., it was multiline, and the single line previously observed at 5450 Å was split into three components and the other lines were also observed. It was determined that the spectrum seen from OR2 was due to Er^{3+} ions by comparison with the fluorescence of a thoria sample doped with Er and by comparison with the work of Trofimov.[31]

2. Thermoluminescence and Fluorescence of Rare Earth Doped Crystals

The thermoluminescence emission spectra of some rare earth doped thoria crystals are shown in Figure 19. The spectra are shown as measured with the highest resolution, not the highest sensitivity. For example, the spectrum shown for OR2 was measured with the monochromator; Figure 17 showed that using the filter wheel and the EMI photomultiplier revealed additional structure and broadening due to the higher sensitivity and lower resolution of the system. Hence some of the other spectra shown in Figure 19 may have additional structure. The spectra of Figure 19 show only relative intensities within each spectrum. The magnitude of each spectrum has been normalized for convenient presentation.

In Figure 19 one can see that each rare earth dopant produces a unique emission spectrum. The glow curves from these crystals, shown in Figures 5, 6, and 7, were nearly identical. Therefore, it must be concluded that the thermoluminescent emission of at least the Oak Ridge crystals is primarily a rare earth process and that the trapping states are nearly independent of the rare earths. The emission spectra of the crystals doped with Tb, Nd(Gd), and Pr are not shown because the intensity of the glow was insufficient for meaningful measurements. The thermoluminescence emission spectra in Figure 19 agree with the fluorescence lines as reported by Trofimov.[31]

The fluorescence spectra of a number of rare earth doped thoria crystals were measured. The spectra in several cases were very bright and in all cases consisted of many sharp, narrow lines. The spectra turned out to be rather complex. Some lines had a strong temperature dependence; some lines were excited by one narrow band of excitation light while others were excited by several bands. The detailed results of that study will be published separately.[43] In general, there was good agreement between the fluorescence data of this investigation and the spectra reported by Trofimov and Linares. The fluorescence spectra appeared to agree with the thermoluminescence spectra in Figure 19, although some additional fluorescence lines were seen.

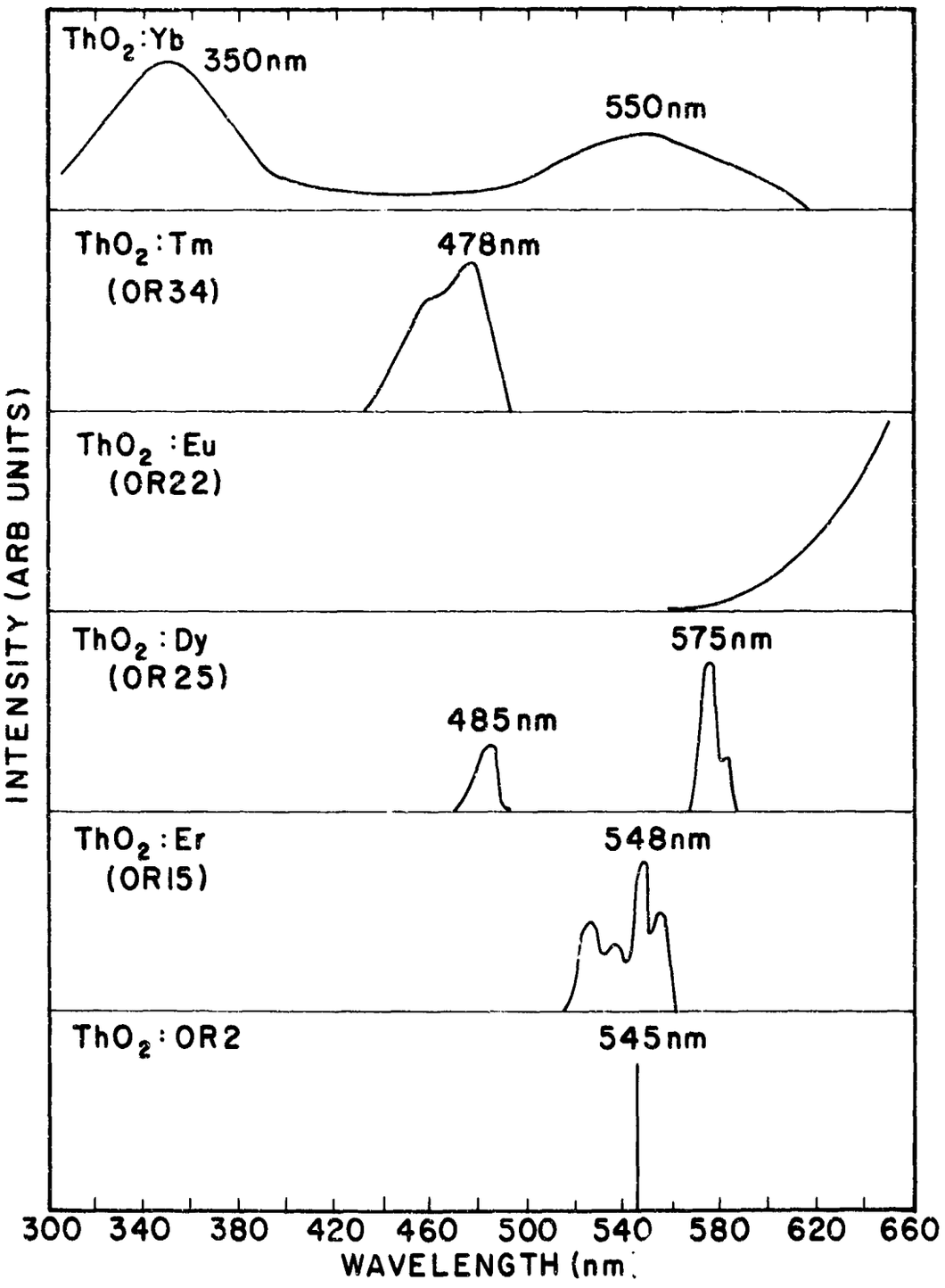

Figure 19. Thermoluminescence emission spectra for rare earth doped ThO_2 crystals

3. Emission from OR1, OR4

The emission spectra of the crystal OR1, which was from the same batch as the OR2, were also measured. The spectra as measured with the filter wheel were not nearly as sharp, with a halfwidth of around 40 nm, although the peak emission was the same as for the OR2. An interesting feature of the emission of the OR1 crystal, which also serves to illustrate the usefulness of using the filter wheel to analyze the emission, is that the -95°C shoulder to the -110°C peak is seen to be clearly separated from the main peak by examining the emission. Figure 20 shows the uncorrected filter response curves for six filters for the -110°C peak. It is obvious that the main peak at -114°C and the shoulder at -95°C are spectrally different and that the apparent peak at -110°C is a result of the overlapping shoulder. Thus the anamolous behavior of this peak in the dosage studies may be attributed to peak multiplicity.

Figure 21 shows the resultant emission spectra after the proper correction factors for the filter transmission and photomultiplier response have been applied and the data have been normalized to unit amplitude at 548 nm. It can be seen that the -110°C peak and the -95°C shoulder are emitting further into the red than is possible to detect with the 1P28 photomultiplier which cuts off just above 600 nm. Of principal interest, however, is that the peak at 548 nm is nearly equal to the sharp emission seen from the OR2 crystal. Note that again it is the low temperature peaks that have the most "red" emission.

The emission from the OR4 crystal was examined but was too weak for meaningful analysis. Indications were that the emission tended towards the red.

4. Emission from FI 1, FI 2, N 1, and PE 2

The emission spectra of the crystals obtained from the Franklin Institute were measured and are shown in Figures 22 and 23. The spectra from the two samples are quite different. The spectrum of the FI 1 crystal has a peak at 447 nm but the principal emission is evidently in the red as seen by the rapid rise of emission with increasing wavelength. It should be recalled that this crystal has a reddish-brown coloration. The data for the three peaks were normalized at 447 nm for illustration purposes. The emission for the FI 2 crystal also has a maximum of 447 nm for all peaks and is quite red but does not show the rapidly increasing red emission seen in FI 1. The emission is apparently made up of several components, indicating a rather complicated emission process. It is of interest to note that the strength of the red emission increases with the peak temperature, i.e., the -19°C peak is more red than the -71°C peak which is more red than the -115°C, etc.

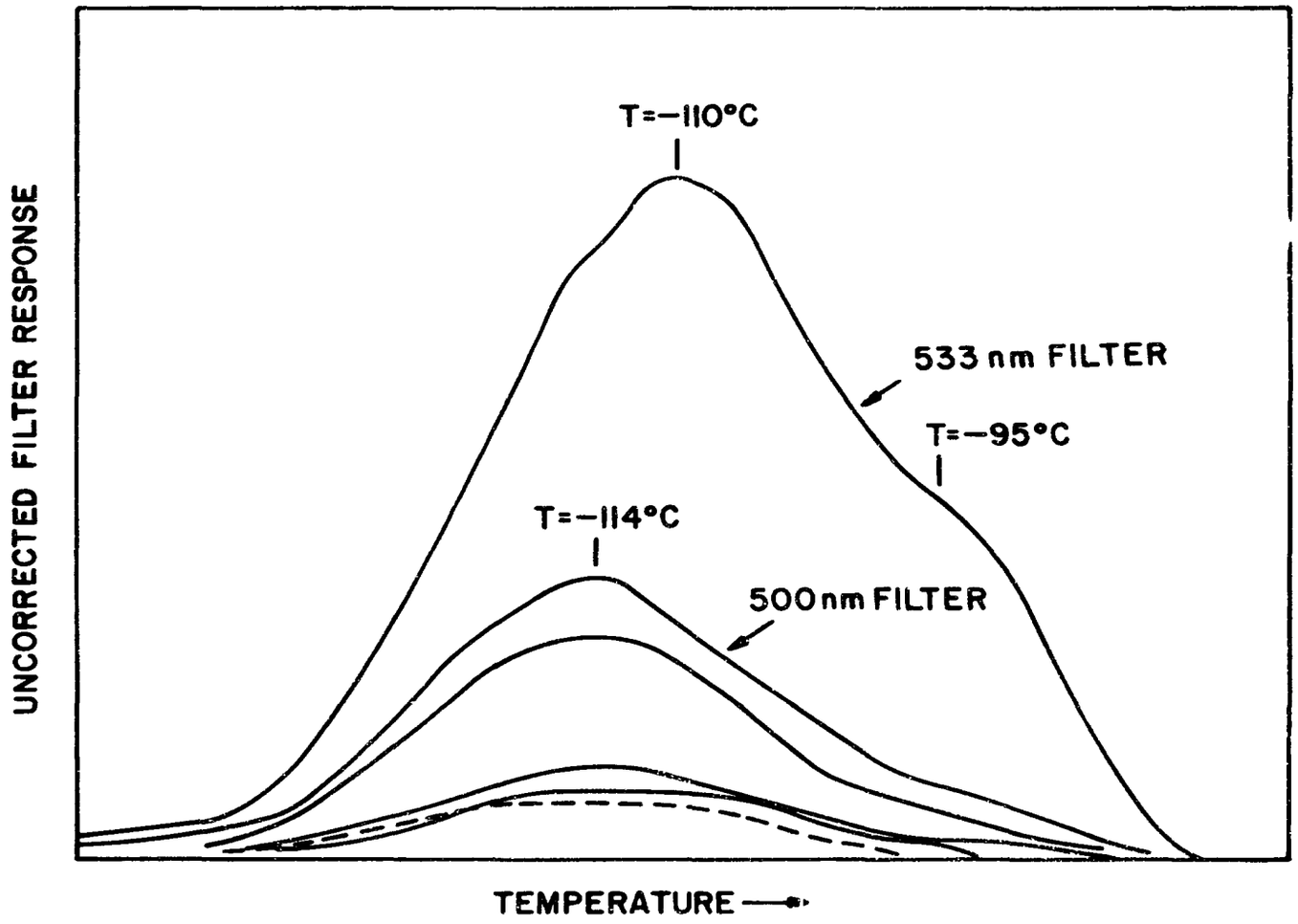

Figure 20. Uncorrected filter response vs. temperature for emission of-110°C peak, ThO_2: OR1

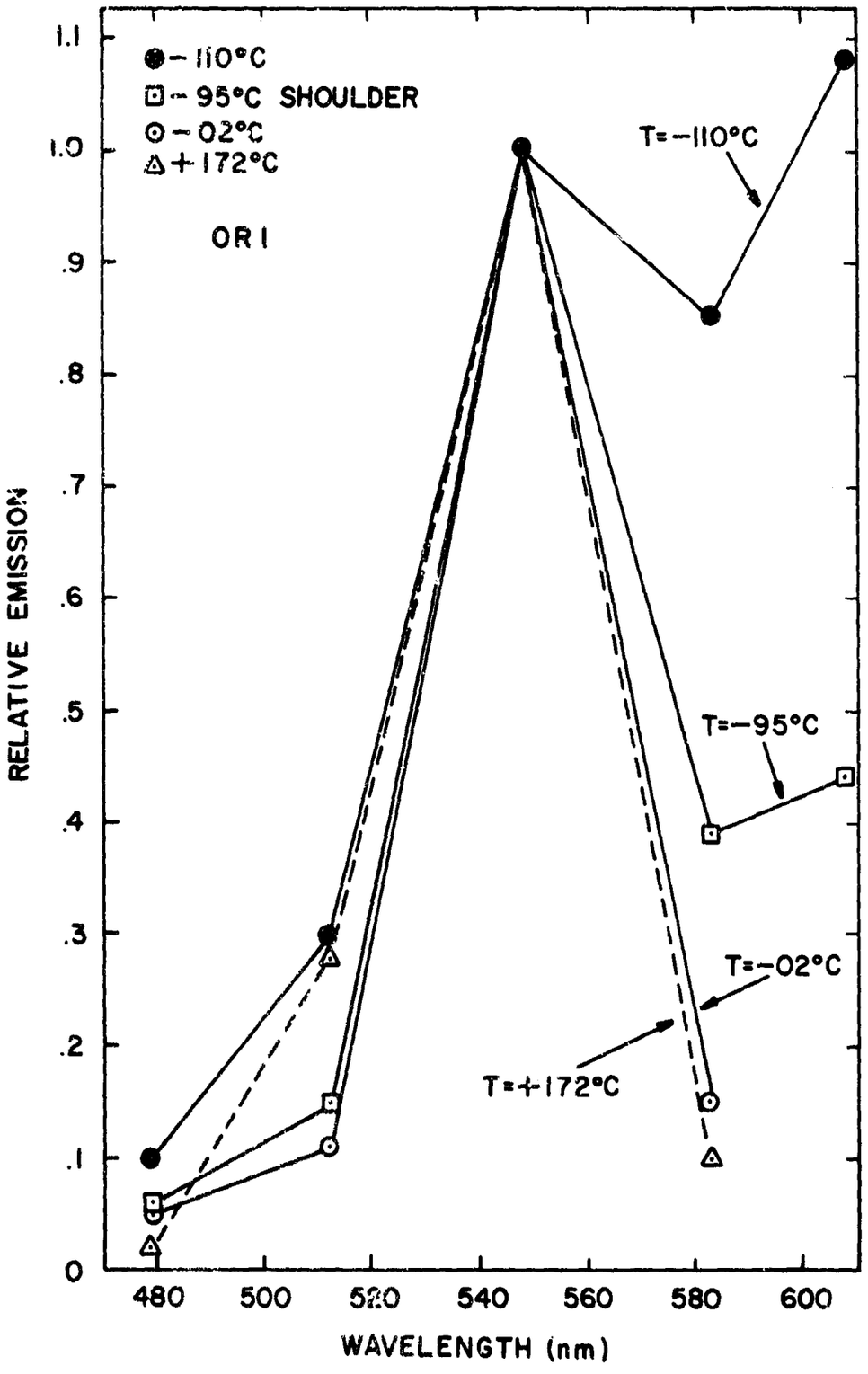

Figure 21. Emission spectra of ThO_2: OR1, data normalized 548 nm

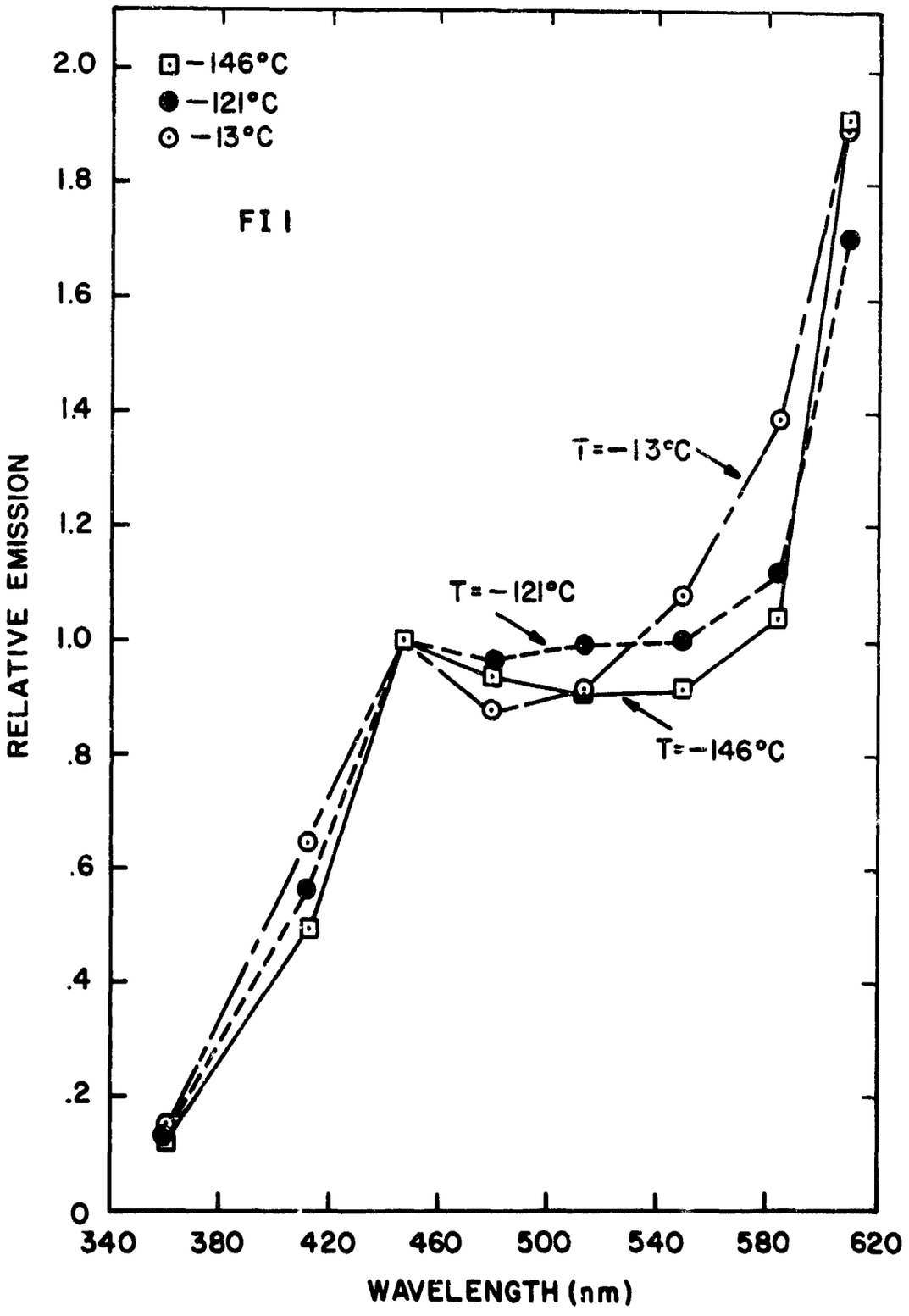

Figure 22. Emission spectra of ThO_2: FI 1, data normalized 447 nm

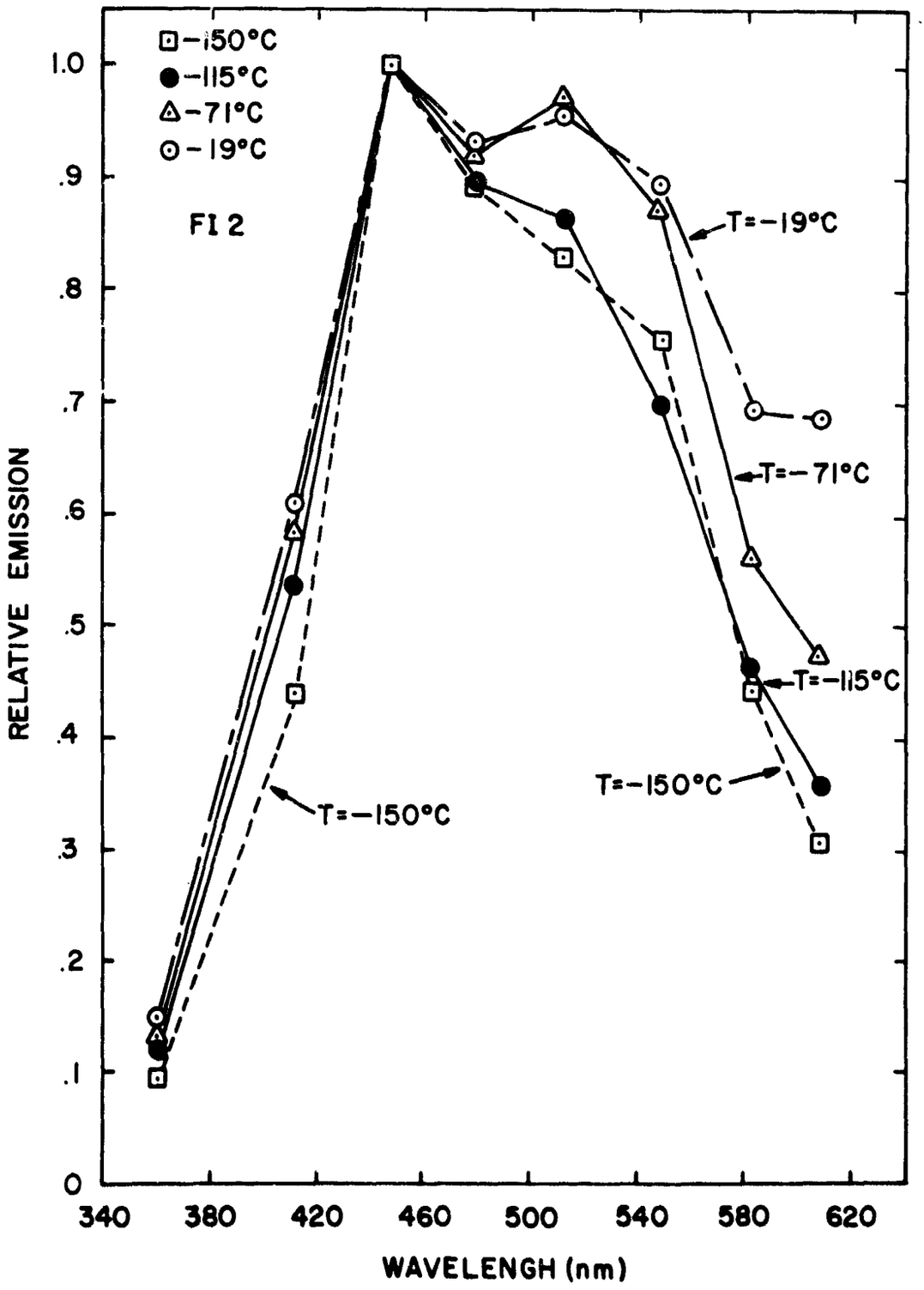

Figure 23. Emission spectra of ThO_2: FI 2, data normalized 447 nm

The emission spectra of the Franklin Institute crystals are seen to be very different from the Oak Ridge crystals and also very different from each other. The emission is apparently quite broad with several emission bands spread out over a large portion of the visible spectrum. The glow curves of the Franklin Institute crystals were very similar to the glow curves from the other crystals except that the -160°C and -80°C peaks were much stronger than in the other crystals. The glow from FI 1 was much weaker than the glow from FI 2. Also, the Franklin Institute crystals did not show appreciable glow above room temperature, a significant factor. It will be shown below that the large high temperature peak in the Oak Ridge crystals is due to retrapping from the low temperature peaks. Apparently, some of the trapping states are common to all batches, their relative strengths being different while unique trapping states as well as unique recombination mechanisms are available in each.

The emission spectra of the Norton crystal N 1, shown in Figure 24, are remarkable because of the wide variation of spectral content as a function of temperature. There were three main peaks in the glow curve: -119°C, -13°C, and 166°C. The emission of the -119° C peak has a maximum at 447 nm with very strong emission in the red. The -166°C peak has very little blue emission and has a strong maximum at 583 nm. The -13°C peak shows a distinct transition from a peak with strong blue to a peak that is predominantly red. This can be seen in Figure 24 from the spectra shown for the low temperature side (which has a lot of blue) and for the high temperature side (which is predominantly red). This is also shown in Figure 25, which shows the uncorrected filter response vs. temperature for the -13°C peak. The blue filters peak at -16°C while the red filters peak at -9°C. This is strongly indicative of at least two recombination processes taking place for this peak. The orderly shift of emission from blue to red as a function of temperature as seen in this sample and other samples may also denote a change of the recombination probabilities. That is, certain transitions may be allowed only in restricted temperature regions.

The emission spectrum of the PE 2 crystal was also measured but the emission was quite weak, so a meaningful spectrum could be obtained only for the -144°C peak. The spectrum is shown in Figure 26. It is very broad with two overlapping peaks which have maxima at 447 nm and at 512 nm. To an extent, the spectrum is similar to the spectra obtained from the Franklin Institute crystals.

E. EXCITATION SPECTRA AND OPTICAL ABSORPTION

The excitation spectra were measured for four of the Oak Ridge crystals: OR1, OR2, OR4, and OR7. The monochromator was used so the dosage levels were quite low compared to saturation. The same number of photons were incident on the sample for each excitation; hence,

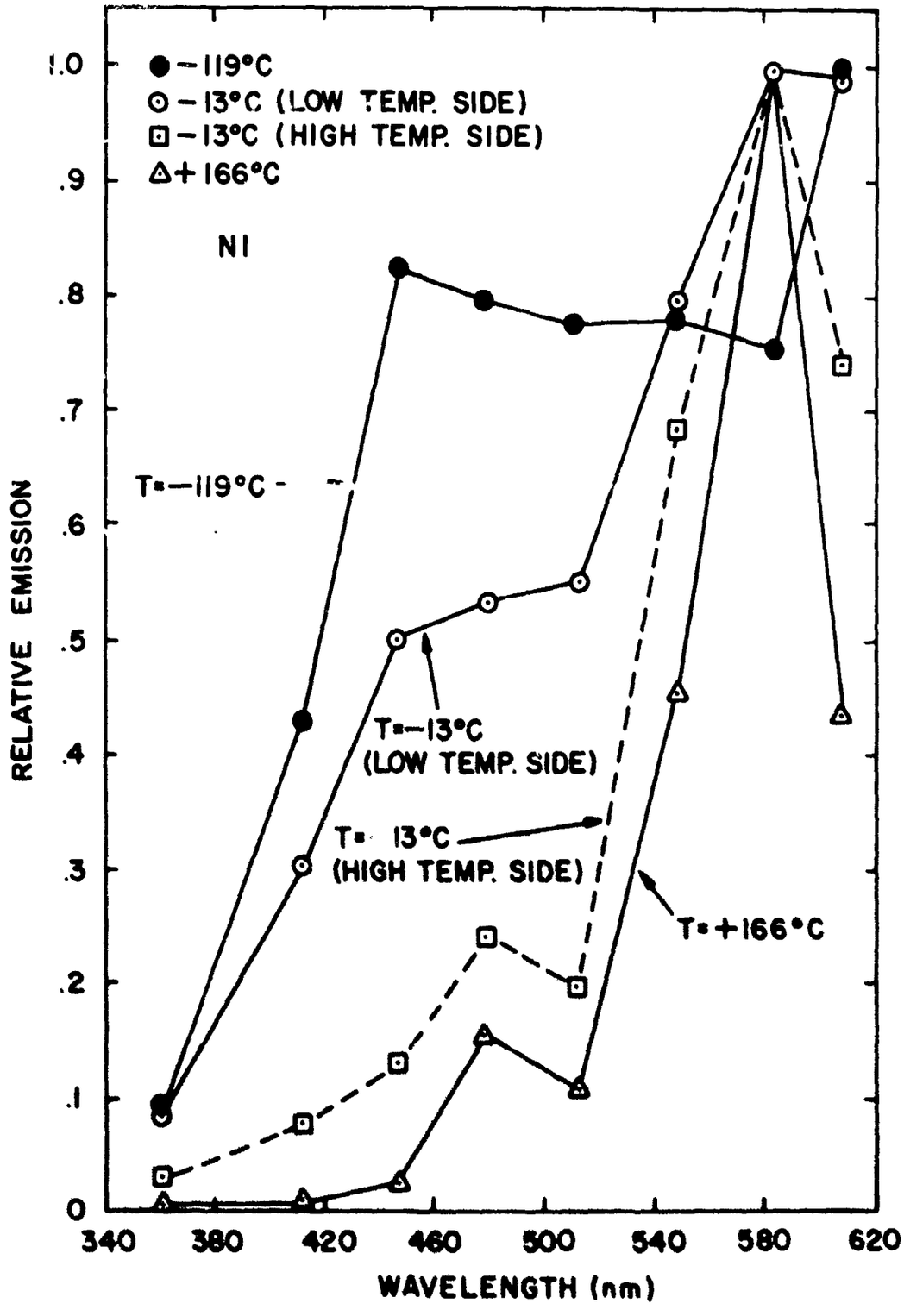

Figure 24. Emission spectra of ThO_2: N 1, data normalized at maximum response

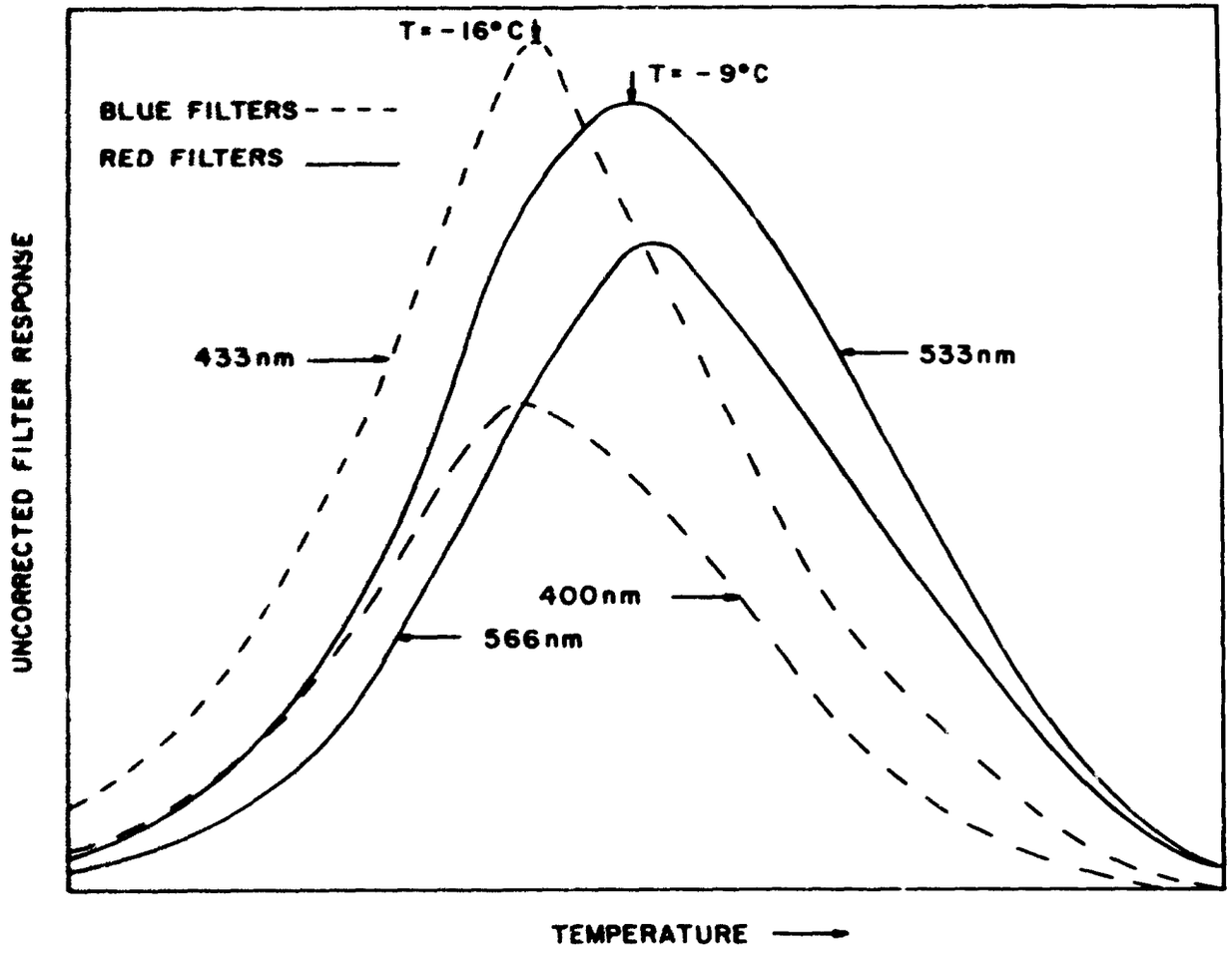

Figure 25. Uncorrected filter response vs. temperature for emission of -13°C peak, ThO_2: N 1

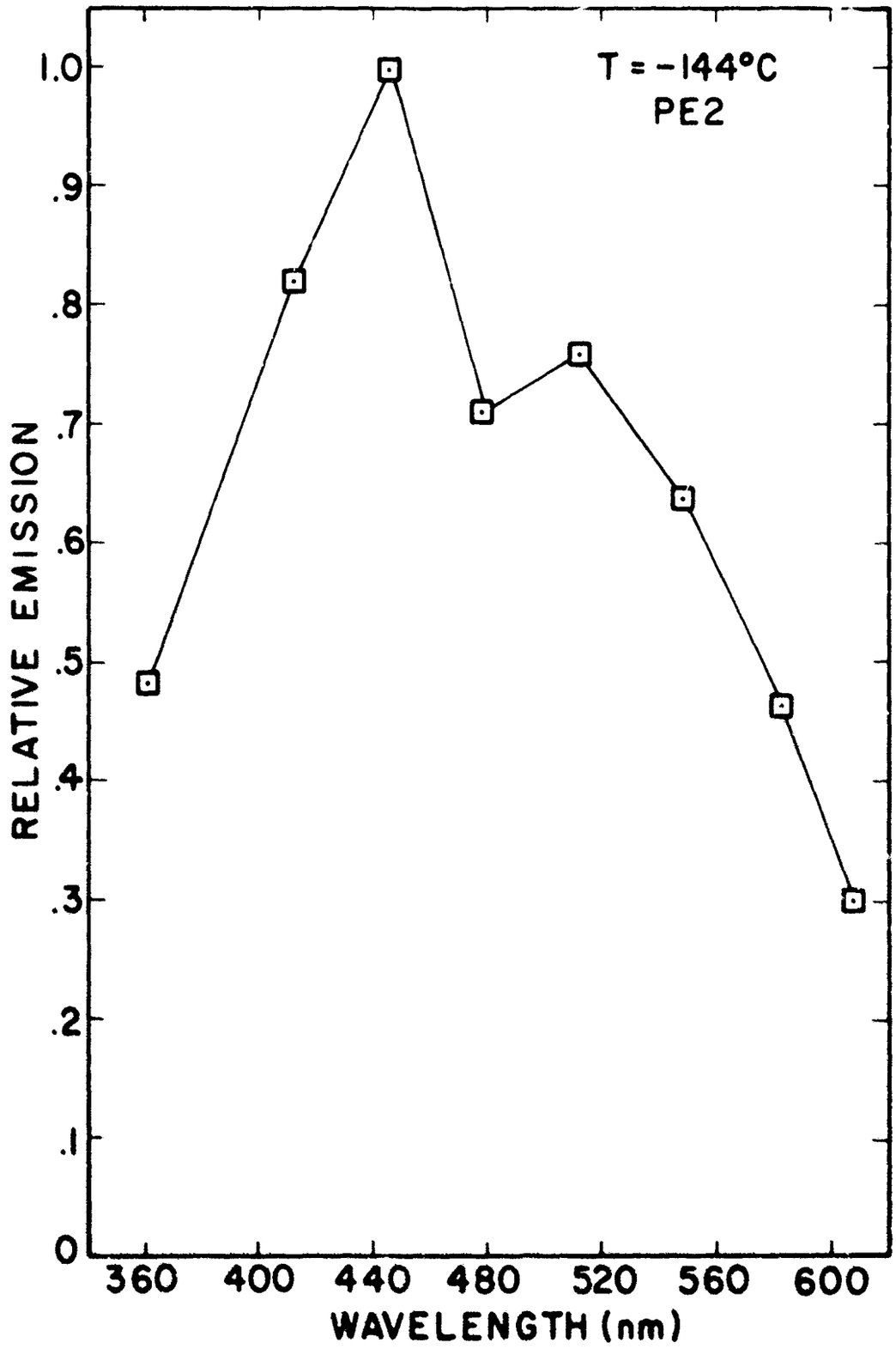

Figure 26. Emission spectrum of -144°C peak, ThO_2: PE2

the dosage levels were different for each wavelength. The dosage curves above showed that at low dose levels the relative strengths of the peaks can change rapidly as a function of dose; hence the effects of dose and wavelength are difficult to separate. An alternative is to excite the sample to a particular dose level for all wavelengths in order to determine the occurrence of preferential filling of the nearly empty traps.

The excitation spectra plotted show the areas under the glow peaks as a function of excitation wavelength. Each unit of area represents one square centimeter on the data chart, normalized to a signal on the 10^{-7} ampere scale of the electrometer. The areas under the peaks are directly comparable between samples and between dosage and excitation spectra. Recall, however, that the dosage curves were in nearly all cases generated using the full deuterium source for excitation and the excitation spectra were generated by using the monochromator. Also, there are undoubtedly variations of experimental conditions between experiments such as variation of light output of the lamps, filming of the windows, etc. such that exact comparisons should not be made.

1. Spectra for OR2, OR1, and OR7

The excitation spectra for OR2 are shown in Figure 27. The total glow for the 210 nm excitation is approximately equal to the total glow for a 5-second dose with the full source (Figure 8). The relative peak amplitudes are, however, more like that for a 1-second dose. There was a misunderstanding at the time these data were taken and it happened that the excitation conditions were near to those which would yield a constant total glow. The actual areas are shown by the unconnected symbols and these areas were corrected to correspond to a constant number of photons assuming that the growth with dose was linear. (No corrections were necessary for the data at 230 nm so only one set of points is shown.) It is clear that for nearly equal total glow for 210 nm and a 230 nm excitation the relative areas of the -18°C and -105°C peaks are inverted. It appears that the -18°C peak is preferentially excited at 210 nm in comparison to longer wavelengths, and it is seen that the excitation of all peaks is most efficient in the range 210 to 220 nm.

The excitation spectra for the OR1 crystal are shown in Figure 28. The spectra are somewhat broader than for OR2 and also have a more asymmetrical shape. The maxima are at about 220 nm as was the cause for OR2. The emission spectra for OR1 were considerably broader than for OR2, so it is quite likely that there are some additional processes taking place in OR1. The total glow at 210 nm is approximately equal to a 10-second dose with the full source (Figure 11) while that for all other wavelengths was smaller. The relative amplitudes of the individual peaks are in the same order as in the low dose region. One can see, in analogy to the

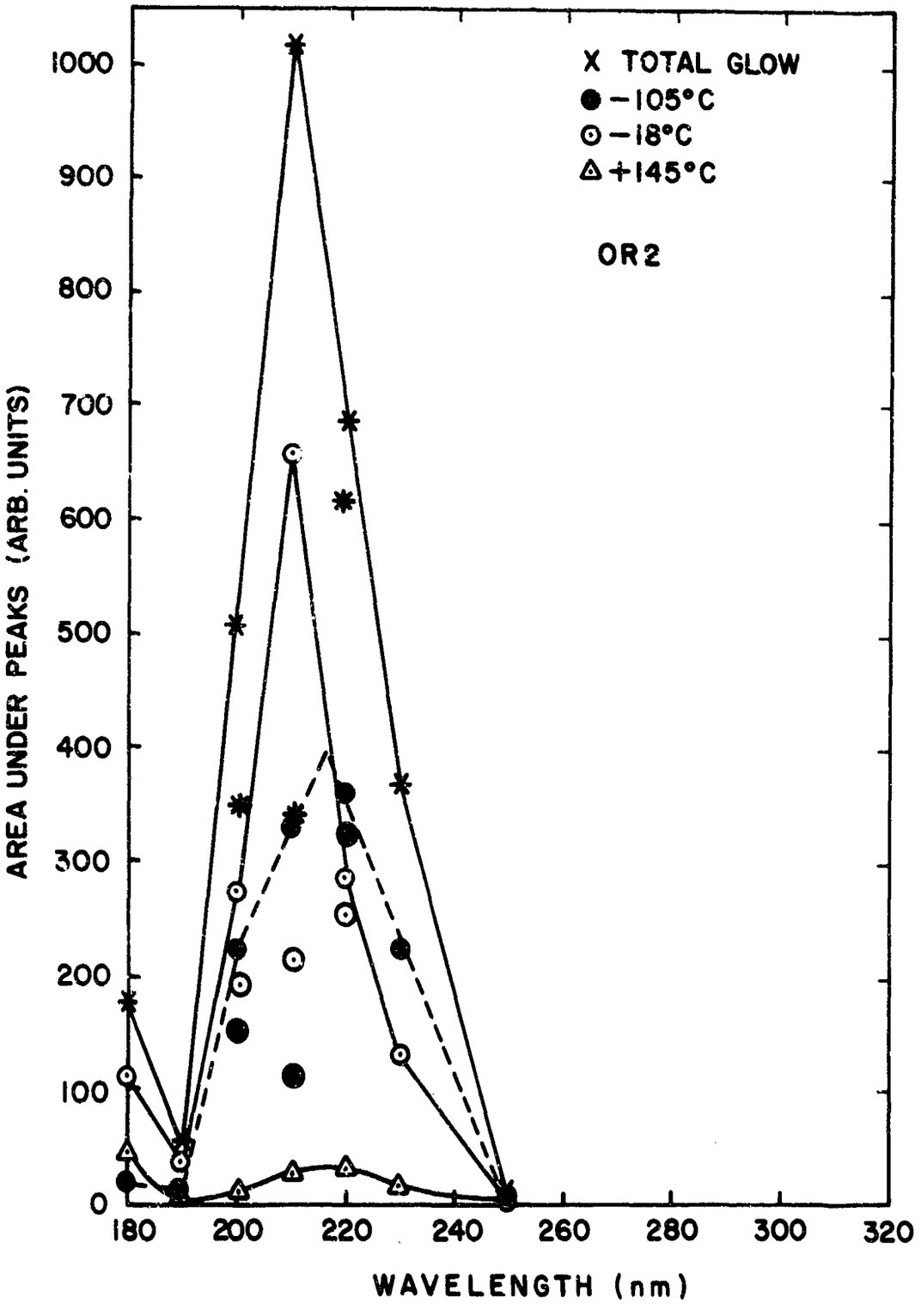

Figure 7. Excitation spectra for ThO_2: OR2

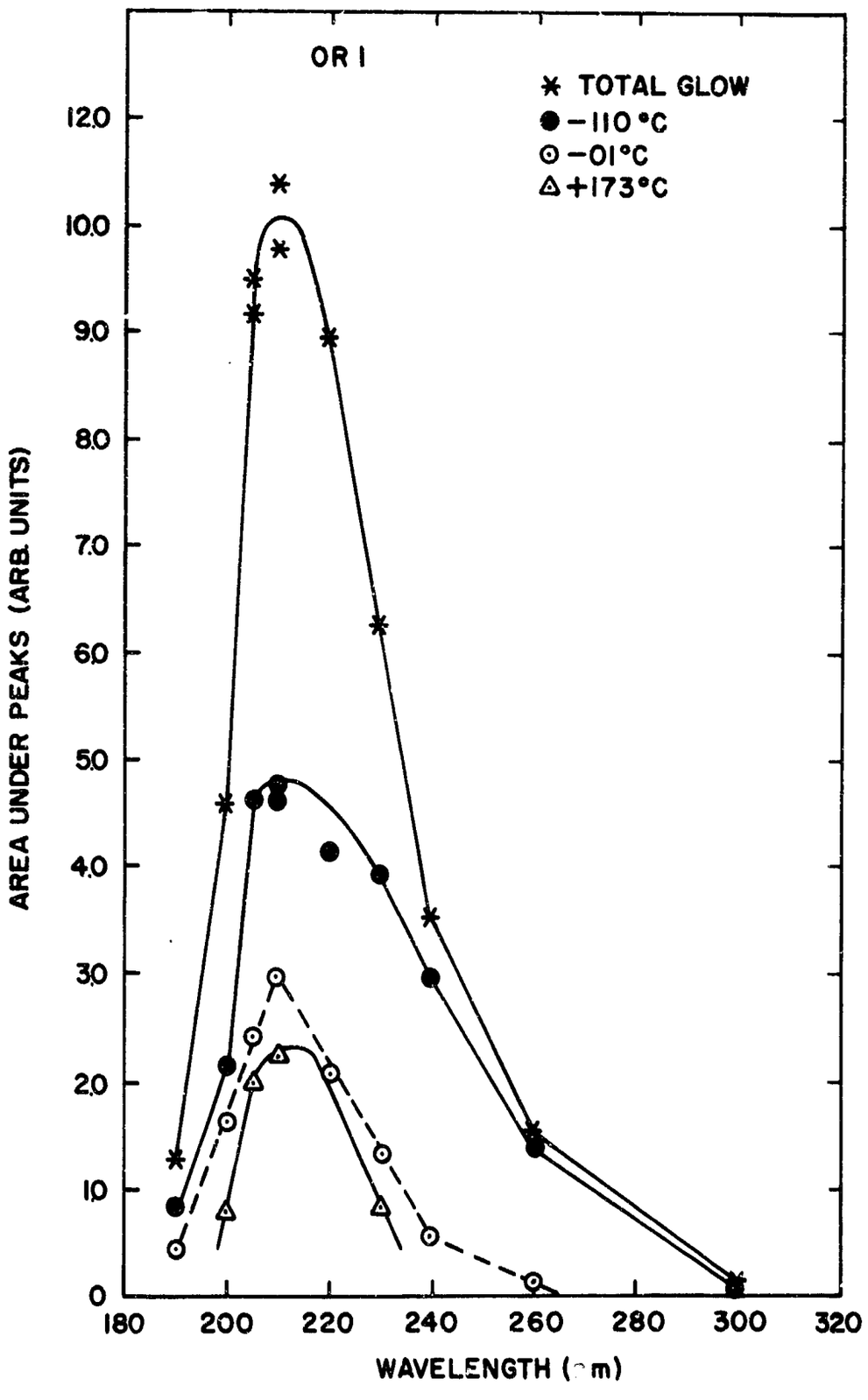

Figure 28. Excitation spectra for ThO_2: OR1

case of OR2 as well as for OR7 to follow, that the ratio of glow peak areas for the -110°C peak to the -1°C peak tends to be larger for wavelengths greater than 210 nm. The peak at -1°C is consistent with dosage curves which shifted from -13°C at large dose to the neighborhood of -1°C at small dose.

The excitation spectra for the crystal OR7 are shown in Figure 29. This crystal was from the same batch as OR1 and OR2; the glow curves and emission spectra were more similar to OR2 than to OR1. The excitation spectra for OR7 are quite narrow and have maxima at 210 nm, as was the case for OR1 and OR2. The narrowness of the peaks make the spectra more similar to OR2 than to OR1 as would be expected. The total glow for OR7 at 210 nm is approximately equal to that for 50 seconds of full source excitation and the peak at about 165°C has the largest area. For the individual peaks, the excitation at 210 nm yields areas equivalent to full source doses of one and ten seconds for the -105°C and -3°C peaks respectively. In the dosage data and in all other cases where excitation was with the full source the 165°C peak was not observed. At high dose with the full source there is a major peak at 150°C, while at low dose there are peaks near 130°C and 220°C. In some cases smaller peaks were observed between 180 and 190°C, but the areas under these peaks at high dose levels were less than ten units. The reason for the relatively large response at 165°C for monochromatic excitation of OR7 is not understood. There are no cases of analogous behavior.

2. Spectra for OR4 (Including Relative Excitation)

The excitation spectra for the crystal OR4 are shown in Figures 30 and 31. This crystal was intended to be doped with Ca but impurity analysis showed no more Ca in the crystal than in other batches. Figure 30 shows the excitation spectra for the individual peaks. The general shapes of the curves (except for the 182°C peak) are similar to that of the total glow. There is considerable scatter in the data and the curves cross each other frequently. The total glow at 210 nm, shown in Figure 31(a), is approximately equal to that for 30 seconds of full source excitation. The relative areas of the individual peaks are approximately consistent with those for full source excitation in this dosage range. The spectra are asymmetrical towards the long wavelength side in a manner similar to OR1.

Figure 31(b) is a plot of the relative intensities of the peaks. Shown are the percentages of glow area under each peak with respect to the total glow as a function of wavelength. The data presented are from a partial check series of runs. The total glow in this plot would be a straight line at 100%; the method of plotting emphasizes the shoulders of the excitation peaks. Note that at 220 nm the -14°C and -52°C peaks show a minimum while the -148°C, -121°C, and -95°C peaks have maxima. Thus it is seen that the relative maxima for OR4 do not agree with those for

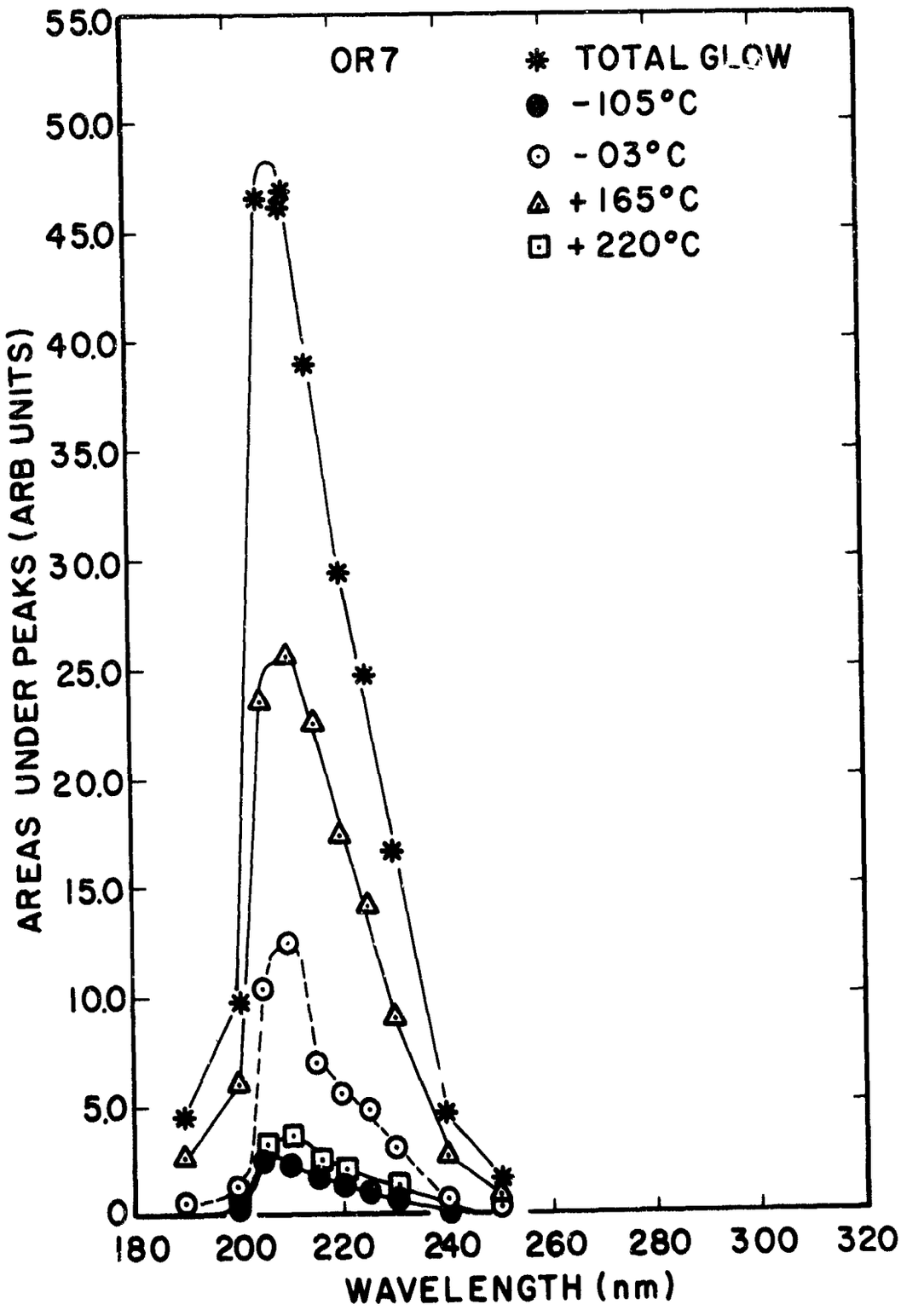

Figure 29. Excitation spectra for ThO_2: OR7

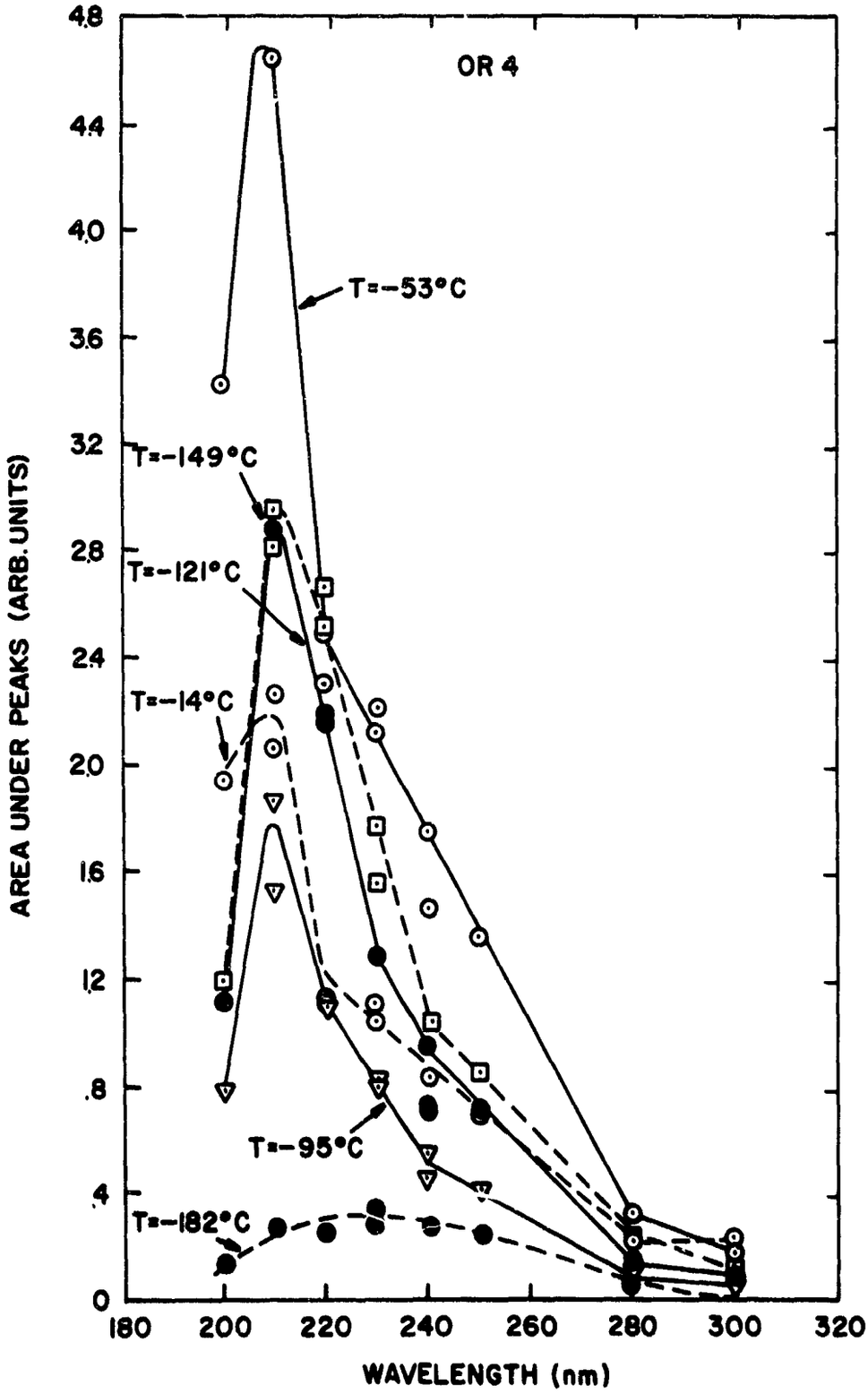

Figure 30. Excitation spectra for ThO_2: OR4

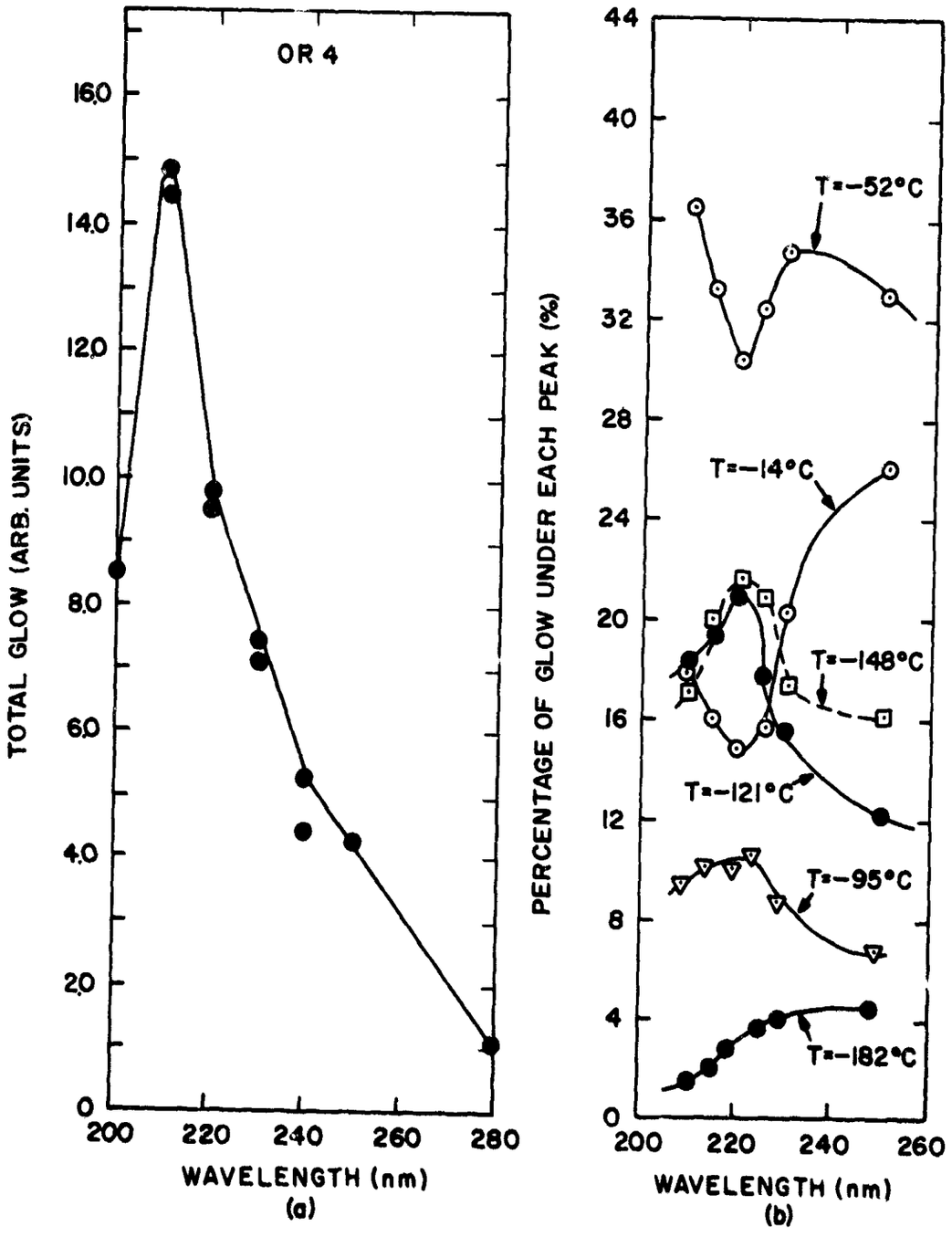

Figure 31. Excitation spectra for ThO_2: OR4

(a) totai glow vs. λ

(b) relative excitation vs. λ

OR1, OR2, and OR7. The data for these crystals indicate that the peaks at -1°C, -18°C, and -3°C have a larger relative response at excitation wavelengths of 210 nm and below when compared with the peak at -105°C or -110°C.

The dosage curves (Figure 14) showed that the -53°C peak rapidly reaches saturation and then diminishes with increasing dose. The -14°C peak reaches saturation at about the same time as the -53°C peak. The lack of a linear growth region and the rapid saturation are additional unique characteristics for these peaks in this sample. It was observed that for this sample there was a fairly strong background after excitation, from liquid nitrogen temperature to about -75°C. The background gave a signal of about 0.5×10^{-8} amperes between liquid nitrogen temperature and -75°C where it dropped to about 0.2×10^{-8} amperes, the usual level for most samples. The low temperature background did not drop as a function of time nor could it be thermally cleaned by heating to some temperature below -75°C. It could be cleaned only by heating through -75°C; hence it was a form of thermoluminescence the nature of which is not understood.

3. Optical Absorption

The optical transmission of OR2 was measured from 1800 nm to 200 nm; very little structure or change of the absorption was observed until the onset of the ultraviolet cutoff below 240 nm. At 215 nm the absorption became too strong to follow. An ultraviolet cutoff at 215 nm corresponds to a band gap of 5.75 eV, which is a higher energy band gap than previously observed.[22,26,27]

4. Conclusions

The maxima of the excitation spectra for all four crystals are at 210 nm. The spectra are of different widths for the different crystals and are asymmetric towards the long wavelength sides of the spectra. The maxima coincide fairly well with the ultraviolet cutoff as determined by the optical transmission of OR2. Therefore, the data indicates that the thermoluminescence excitation is a direct transition across the band gap.

The emission of these samples (with the possible exception of OR4) is primarily a sharp line rare earth process. Hence it is reasonable to look for a rare earth assisted excitation. Several of the rare earths (Gd and Ce) show strong absorption in the ultraviolet. The EPR study[32] indicated a Gd spectra at 77°K that bleached upon ultraviolet irradiation. As the Gd spectra was bleached, new lines that could be associated with the traps appeared. These lines will be discussed below. The wavelength dependence of the bleaching was not determined, so it is not know if the Gd bleaching is accomplished by the 210 nm band gap or by light $E < E_{band\ gap}$. In any case, impurity analyses of crystals from this batch showed a very small Gd concentration so only a few ions are participating.

Band gap excitation is usually considered to be a single process, i.e., a single photon is absorbed for each transition. It is possible, however, for the ground state of an impurity ion such as a rare earth to be well below the valence band edge with an excited state such that a two-step process is possible. In this case two photons would be absorbed for each excited charge. It is not unreasonable to look for such models since the dosage curves for these crystals showed that the growth behavior of several of the peaks were quadratic, which could indicate double photon absorption.

F. OPTICAL BLEACHING

Extensive optical bleaching studies were conducted on the OR1 and OR7 crystals. The results were quite similar for the two crystals so complete data are shown only for the OR1 with partial data for OR7.

1. Bleaching of OR1

Figure 32 shows the bleaching of OR1 as a function of bleaching time. For each run the sample was first excited to saturation conditions with ultraviolet light in the usual manner and then irradiated with the full tungsten source. The tungsten source was a 108 watt tungsten bulb that was a part of the Bausch & Lomb high intensity monochromator. In this case the light source was used without the monochromator and was focused on the sample with a lens. The areas under the glow peaks at saturation conditions with no bleaching are taken as the norms in this experiment. The effectiveness of bleaching is measured by the change of area as a function of bleaching. Hence in Figure 32 the percentage of the saturated glow remaining is plotted as a function of bleaching time.

Figure 32 shows that the low temperature peaks are bleached more rapidly and more completely than the high temperature peaks. The peaks appear in Figure 32, from bottom to top in order of increasing peak temperature.

The same information was plotted on a log-log plot of area vs. time which emphasizes the short time bleaching. The plot was quite similar to a dosage curve with reversed axes, and some of the slopes corresponded to the slopes of the growth curves. The analogous behavior is not unexpected but the two experiments measure different parameters. The dosage curves are dependent upon the cross section of the sources while bleaching involves the cross sections of the charges in the traps.

The information that is of the most interest is the spectral dependence of the bleaching. Figure 33 shows the percentage of glow remaining after bleaching as a function of bleaching

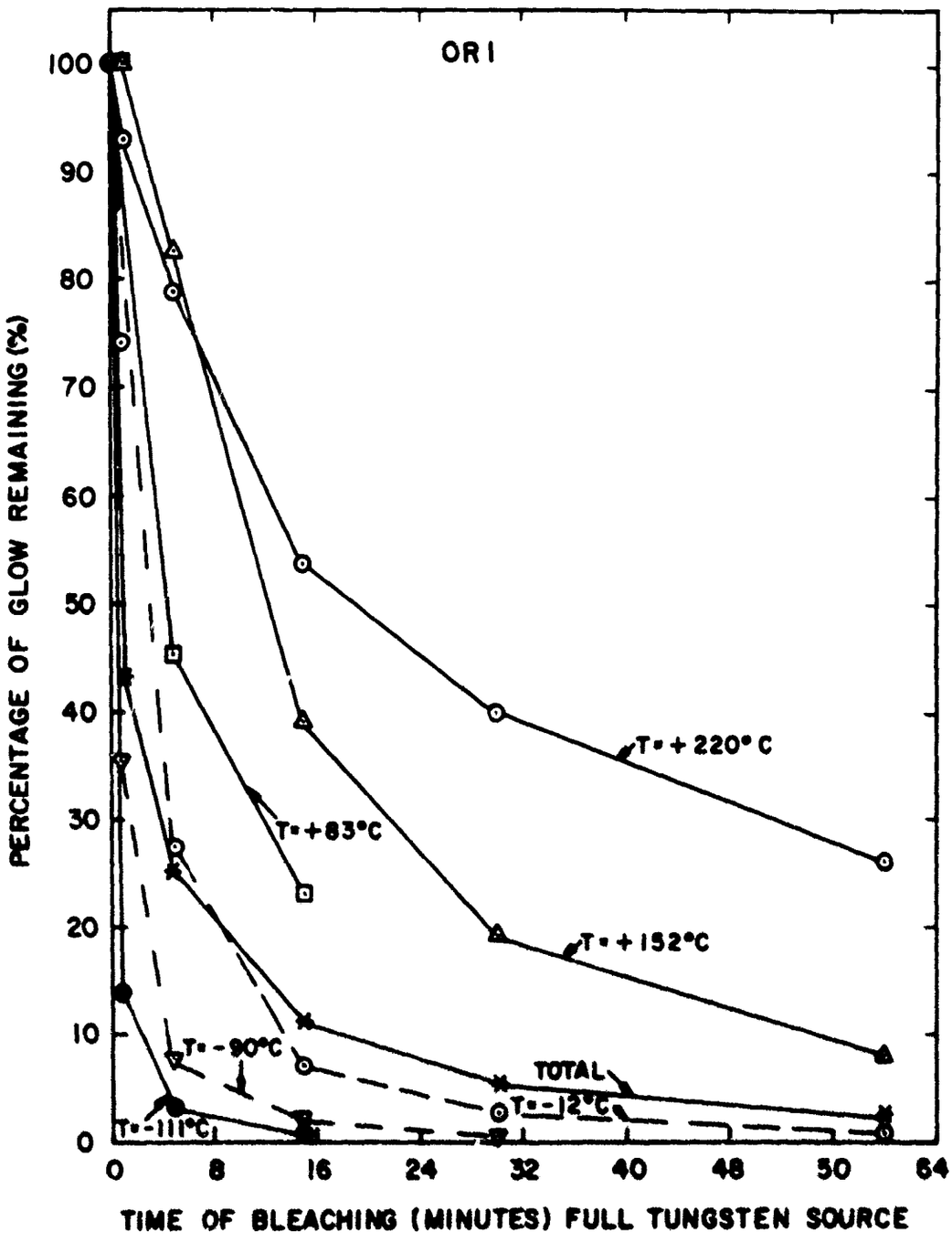

Figure 32. Bleaching with full tungsten source for ThO_2: OR1

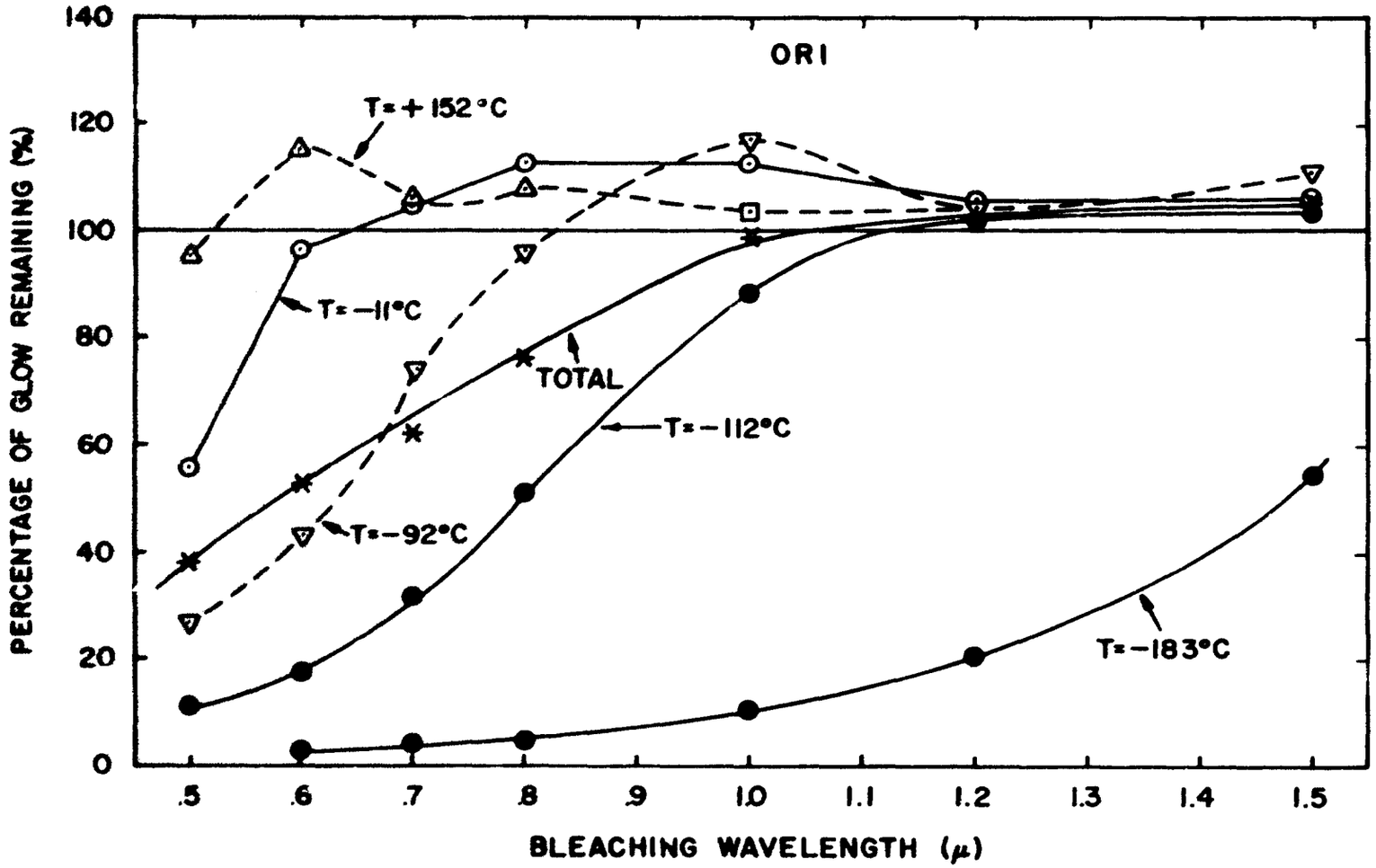

Figure 33. Bleaching as a function of wavelength for ThO_2: OR1 (100% corresponds to saturation excitation without bleaching)

wavelength. The sample was bleached by the same number of photons at each wavelength in a manner similar to the technique for the excitation spectra. The sample was excited to saturation with ultraviolet before each bleach. There is no sharp bleaching cutoff but, rather, a broad spectrum. The peaks are again bleached in order of peak temperature. At the dose levels used for this experiment (much lower than for the bleaching vs. time experiment) some of the higher temperature peaks show enhancement. This is because charge liberated during the low temperature peaks is being retrapped by the deeper traps rather than going to the recombination centers. This will be elaborated in the section on spin resonance.

It is clear that retrapping effects, the effects of dosage, etc. are not easily separated from the spectral dependence of the bleaching. In Figure 33, the bleaching at 0.5 μ is much more effective (62% of total) than at 1.0 μ (2% of total). For the data in Figure 33, the sample was bleached for 85 minutes at 0.5 μ and for 4 minutes at 1.0 μ. Figures 34 and 35 show the bleaching vs. time at 0.5 μ and 1.0 μ respectively. The times of bleaching for the data in Figure 33 (85 minutes and 4 minutes) are marked in Figures 34 and 35. In Figure 35 it is clear that 1.0 μ light effectively bleaches the sample when sufficient bleaching time is provided. Actually, the amount of bleaching with 1.0 μ light for 85 minutes is very similar (although not identical) to the bleaching with 0.5 μ light for 85 minutes. Hence it is very difficult to separate the effects of dosage from the spectral dependence of the bleaching.

2. Optical Activation Energies of OR1

One objective of a bleaching study is to determine an optical activation energy for each trap and relate this to the thermal activation energy. For several peaks, comparison was not possible, i.e., the -92°C peak was not separated sufficiently from the -112°C peak for analysis of a unique thermal energy. Calculations of an optical activation energy for these traps are of dubious value without a well defined cutoff. However, for a rough idea of the magnitudes involved, consider the wavelengths at which each peak has been bleached to 50% of its unbleached strength in Figure 33. The results of these calculations are shown in Table V.

The optical energies are about three times the thermal energies. The optical energies calculated here may be higher than justified but are felt to be fairly reasonable. The optical energies are expected to be higher than the thermal energies since by the Frank-Condon principle the optical transitions occur without a change in the position of the ions. Curie[12] discusses cases where the optical energy may be equal to or less than the thermal energy because of the displacement and shapes of the potential energy curves of the ground and excited states of the traps on a configuration coordinate diagram. Nahum and Halperin[44] found a sharp bleaching cutoff in diamond and calculated optical

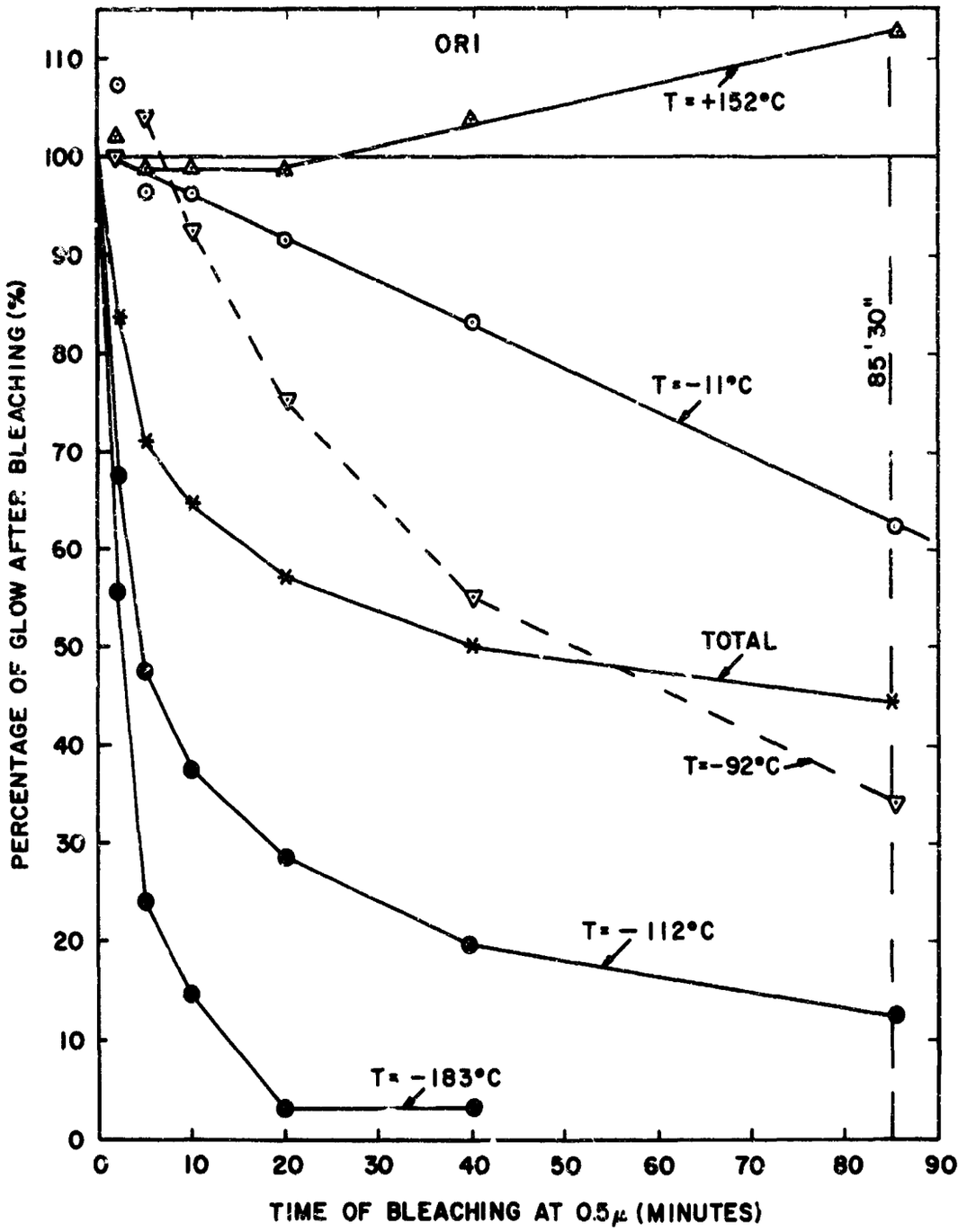

Figure 34. Bleaching at 0.5 μ vs. time, ThO_2: OR1

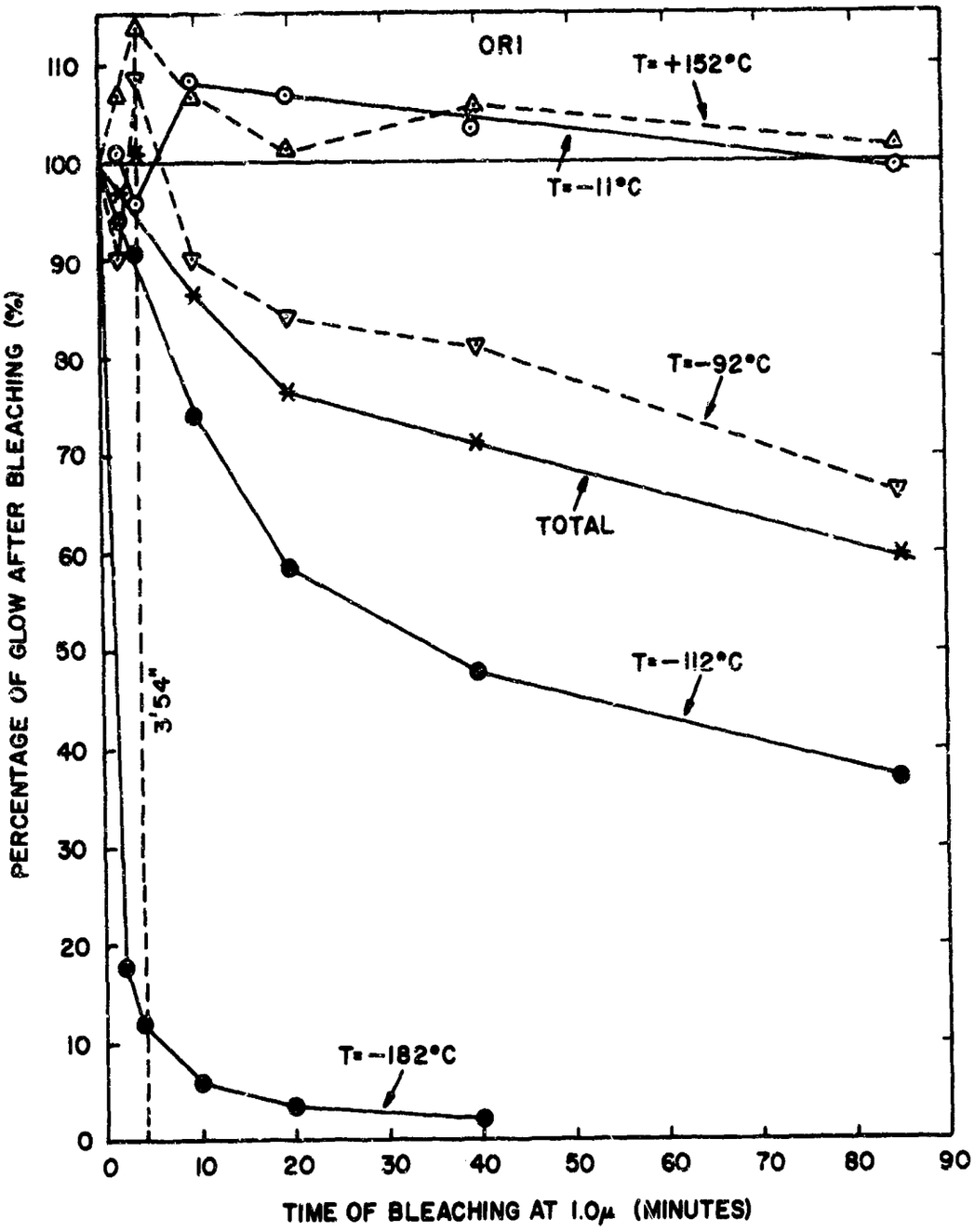

Figure 35. Bleaching at 1.0 μ vs. time, ThO_2: OR1

Table V

Comparison of optical and thermal activation energies

Peak Temp	λ (50%)	E_{opt}	$E_{thermal}$
-183°C	1.48 μ	0.84 eV	0.25 eV
-112°C	0.80	1.55	0.45
-92°C	0.63	1.96	----
-11°C	0.50	2.48	0.86

energies from the long wavelength break in the curves. If the calculations in Table V had been made at the wavelengths where the curves first dip below 100%, the resulting energies for the higher temperature peaks would have been nearer 1 eV. Indication of smaller energies still would be expected to result if bleaching studies were conducted on each individual peak by exciting to saturation at a temperature just below the onset of glow and then irradiating with the bleaching light. Thus one could assume that the initial population of traps giving rise to the peak under study would be normal and that the dominant process during the initial bleach would be optical excitation of the charge of the trap in question and possibly significant self-retrapping. This would obviously involve much more work.

3. Bleaching of OR7

The bleaching vs. time curves for OR7 are shown in Figure 36. The curves are quite similar to the curves for OR1 in Figure 32, but the bleaching is not as effective for OR7 as for OR1. A region of enhancement of the 150°C peak is again observed. The bleaching vs. wavelength curves are shown in Figure 37. Comparison with Figure 33 shows that again the bleaching efficiency for OR7 is considerably less than for OR1 but the general shapes for the curves are very similar.

Finch et al[30] also saw extensive broad bleaching of ultraviolet excited thoria samples. The shape of the bleaching vs. wavelength curve was quite similar to the curves shown for the total glow in Figures 33 and 37.

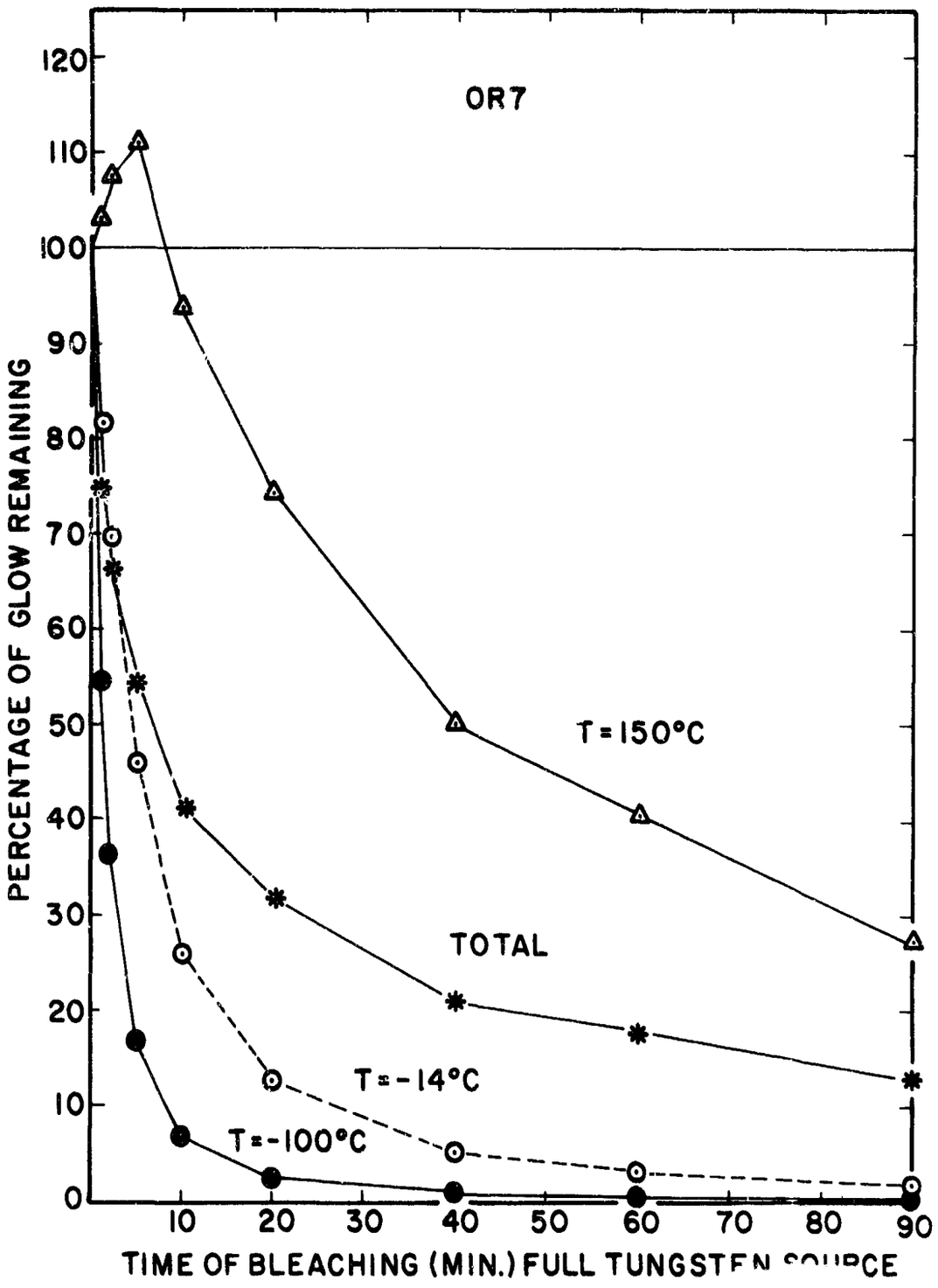

Figure 36. Bleaching with full tungsten source of ThO_2: OR7

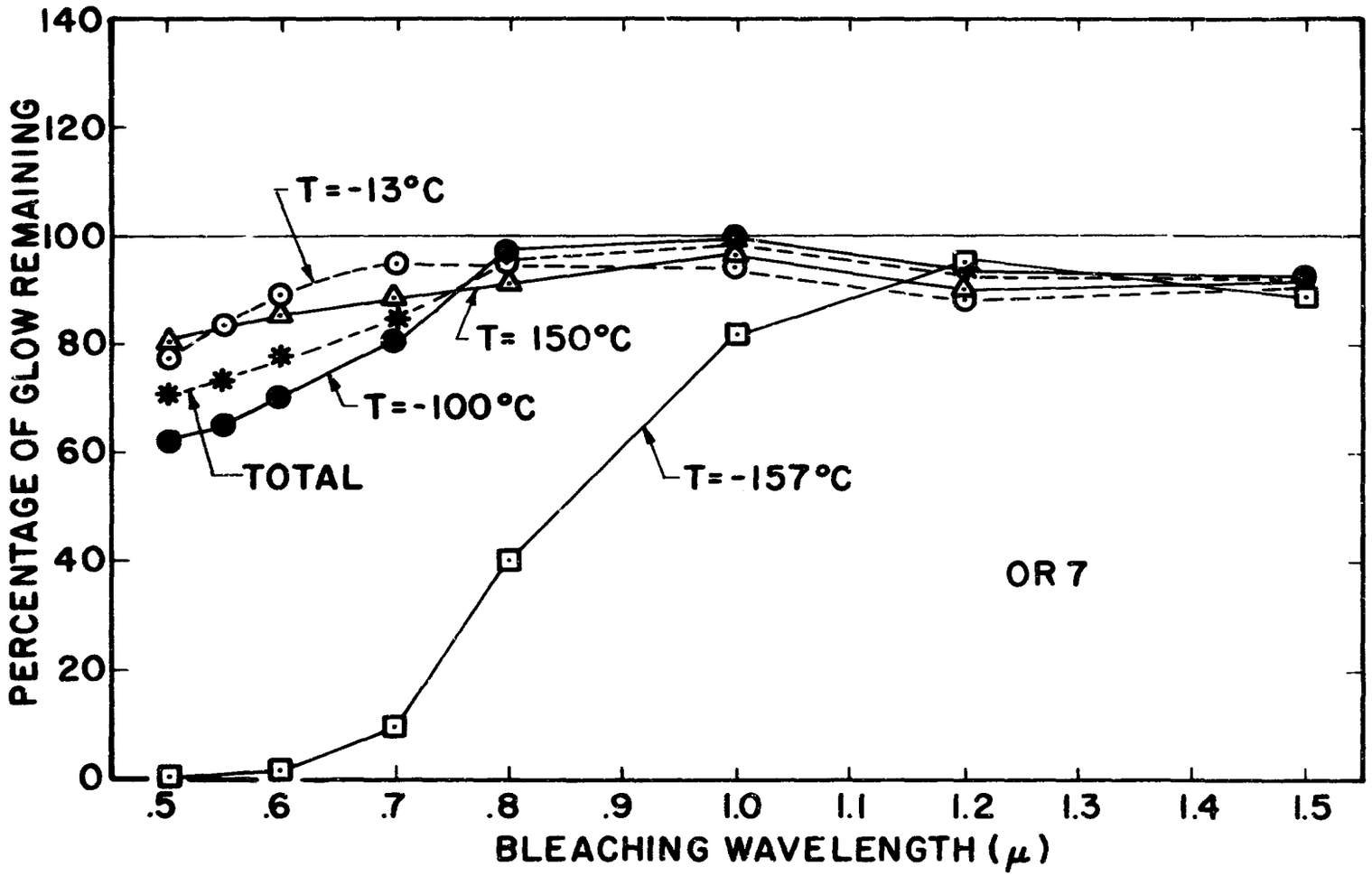

Figure 37. Bleaching as a function of wavelength for ThO_2: OR7
(100% corresponds to saturation excitation without bleaching)

Section VI

SPIN RESONANCE

Several of the crystals studied for thermoluminescence in this laboratory were loaned to Dr. A. Neaves and G.S. Tint of the Franklin Institute Research Laboratories, Philadelphia, Pennsylvania, for the purpose of conducting EPR studies in their laboratory. The most extensive work was performed on OR2, a crystal which had been carefully studied for thermoluminescence by the author and which was discussed in the preceding sections. The detailed results of the EPR study†, with appropriate theoretical development and description of the experimental facilities have been published by Neaves and Tint.[32] The EPR work on thoria has also been described and discussed by Tint[45] in a doctoral dissertation.

A. MEASUREMENT AND ANALYSIS OF EPR SPECTRA

The study of thoria was made with the intention of correlating the results of optical property and magnetic resonance studies. An attempt was made to make the experimental conditions of irradiation and heating as similar as possible. The correlation of the EPR and thermoluminescence measurements was very good and they complement each other in various ways. Therefore, the EPR measurements will be discussed in considerable detail and typical drawings taken directly from the Franklin Institute report[32] will be used to illustrate the data.

The resonance measurements were performed with a Varian V-4500 EPR spectrometer. The sample was mounted in a specially designed optical cavity such that the temperature could be varied from -188°C to 300°C. The sample holder was a "Suprasil" quartz rod. The temperature was varied by a stream of gas that was directed over the sample after passing over a resistance heater. The temperature was controlled by a thermocouple and an electronic bridge network. A thermocouple was also mounted on the quartz rod in contact with the sample to measure the actual sample temperature. The sample was irradiated with a Bausch & Lomb high pressure deuterium lamp identical to the unit used in this laboratory for thermoluminescence excitation. The focusing system and the distance of the lamp from the sample were different so an intensity of 22mW/cm^2 was attained, while in this laboratory an intensity of 13mW/cm^2 was generally used.

Prior to an EPR run, the sample was annealed at 175°C (about the peak temperature of the last glow peak) to empty all of the thermoluminescence traps. The sample was then cooled to

† The report is available to the interested reader from the Clearinghouse, U.S. Dept. of Commerce, Springfiled, Virginia, 22151

-188°C and the spectrum was run by scanning the magnetic field between 600 gauss and 8600 gauss. Only resonance lines due to Gd^{3+} were observed, which is an indication of high sample purity. After irradiation, the EPR spectrum was again scanned and five new resonance lines were observed. Warming the sample to room temperature and recooling resulted in the disappearance of three of the lines and the appearance of two additional new lines. Hence there were a total of seven radiation induced resonance lines observed.

Three basic experiments were performed on each resonance line: (1) the angular variation where the magnetic field was rotated with respect to the crystal axes to determine the symmetry of the site, the g value, and sign of the charge; (2) dosage curves that were run in the same manner as the thermoluminescence dosage runs and with the same motivation; (3) annealing curves which are similar to the thermoluminescence glow curves. The two lines that appeared only after warming to room temperature were found to bleach under ultraviolet light at -188°C so bleaching curves were run instead of dosage curves.

As an example of EPR dosage curves, Figure 38 shows the dosage curve for the V_F lines on a log-log scale. The legend makes the curves self-explanatory. The data for the thermoluminescence dosage curve in this figure are the same as for Figure 8. However, here the time scale is shifted to accomodate the different light intensities utilized in the two laboratories and the data were normalized. The time span for the EPR work was not as large as for the thermoluminescence so the initial quadratic growth behavior was not observed. The EPR lines did not broaden as a function of dose. The growth rates and saturation doses for the two curves are identical. The correlation is not as clear-cut as it appears from the dosage data, as will be seen from the annealing curves for the V_F lines.

Figure 39 shows a typical annealing curve, in this case for the -158°C line. To obtain such a curve, the sample was irradiated (to saturation) for 30 minutes at -188°C and then warmed to a temperature T at a rate of 20°C/min and then immediately cooled. The strength of the resonance line was measured again at -188°C and the sample was warmed to $T + \Delta T$ and again cooled and scanned with the spectrometer. This was repeated until the line was completely annealed as shown by the S vs. T curve in Figure 39. The EPR intensity S is proportional to N, the number of charges remaining in the traps. If N_0 is the number of charges in the traps at saturation, and n is the number of traps emptied with a particular warming cycle, then

$$S \propto N = N_0 - n$$

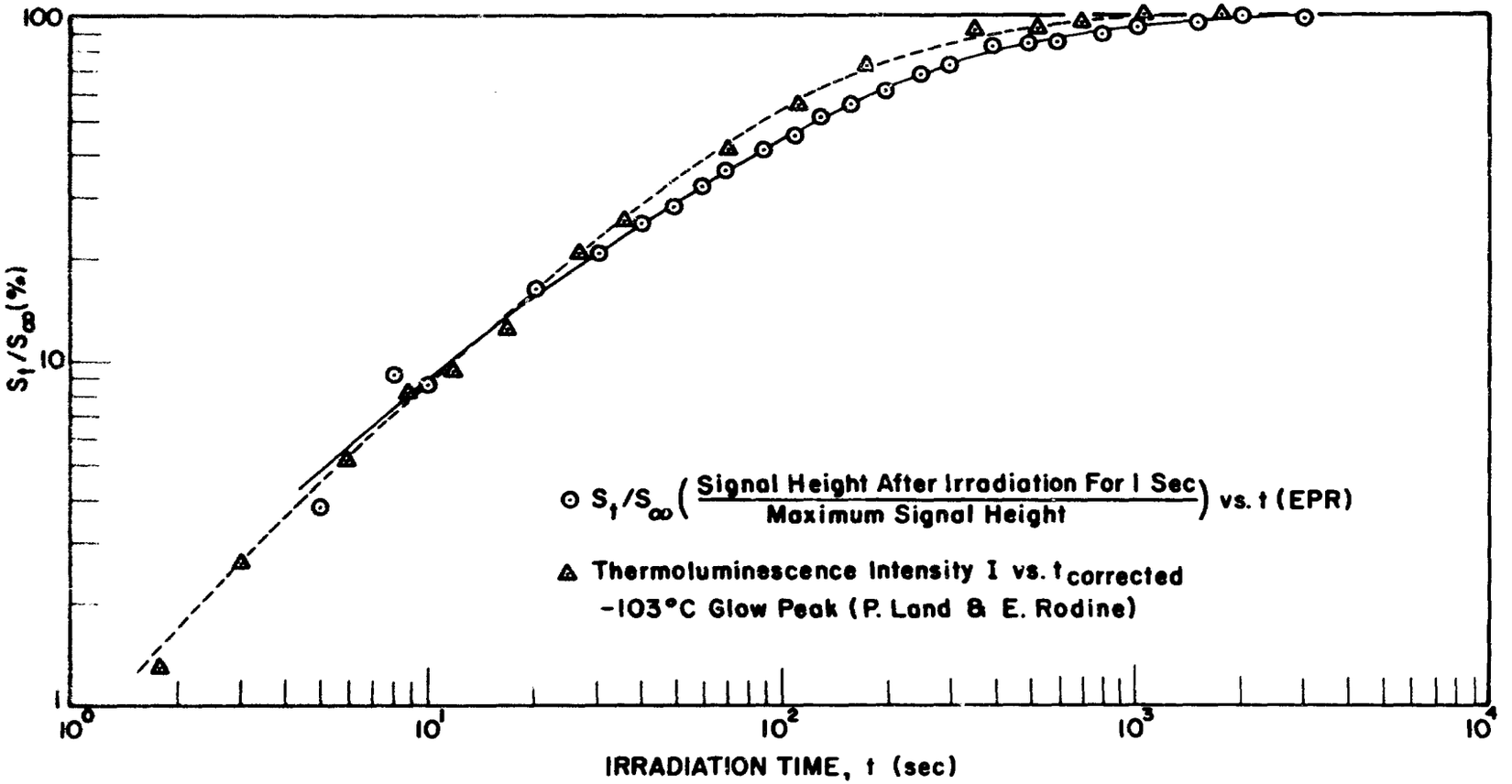

Figure 38. Comparison of dosage curves of EPR and thermoluminescence for V_F center (Figure 23, reference 32)

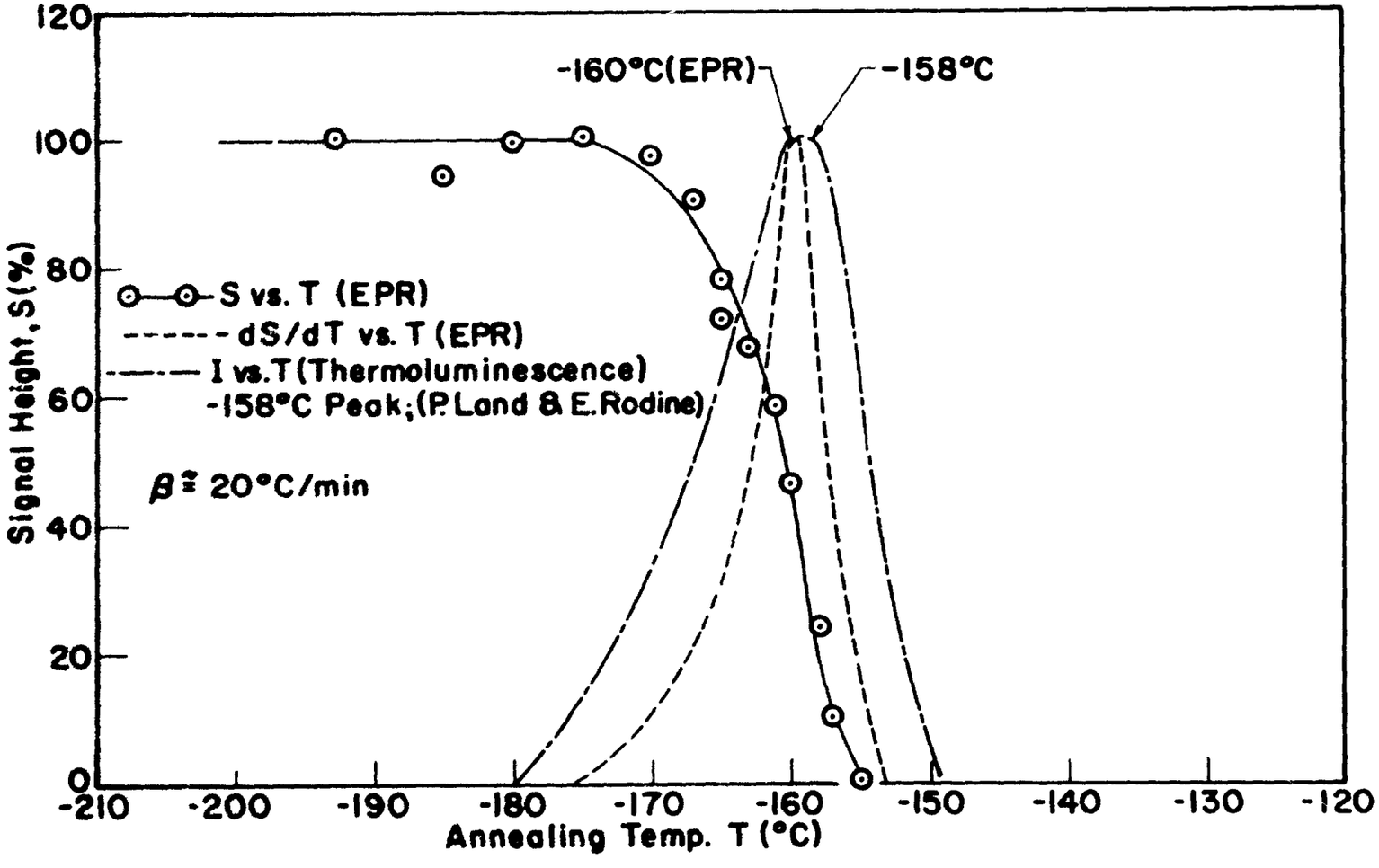

Figure 39. Annealing curve for -158°C trap, ThO_2: OR2, % signal height and dS/dT vs. annealing temperature T (Figure 19, reference 32)

and

$$\frac{dS}{dT} \propto \frac{dN}{dT} = \frac{-dn}{dT} \propto I$$

so

$$\frac{dS}{dT} \propto I$$

where I is the thermoluminescent intensity.

A plot of -dS/dT vs. T can be compared with the thermoluminescent glow curves, which is done in Figure 39. In all cases the EPR annealing curves were narrower than the thermoluminescent glow curves. The EPR curves were generated by a stepwise anneal, however, and the foregoing equations were used as though the anneal were continuous. This approximation tends to narrow the EPR anneal curves but probably not to the extent observed. Neaves and Tint modified the usual annealing procedure for one or two cases by reirradiating to saturation between heating cycles, and they indicated that the EPR anneal curve was not substantially modified. It would be desirable to analyze the stepwise anneal in a manner which permits a more detailed comparison with the thermoluminescent glow. Currently, questions about some details such as curve complexity cannot be resolved, nor can assumptions about the invariance of parameters throughout the glow curves be tested. The approximate correlation is, however, very significant and both kinds of measurement provide guidance or restrictions on the interpretation of the other.

B. RESULTS AND CORRELATION WITH THERMOLUMINESCENCE

The seven radiation induced EPR lines are shown in Figure 40(a). This figure was taken directly from the report by Neaves and Tint[32] and was Figure 17 in that report. The identifying names for most of the lines refer to their correlation to the thermoluminescence. Figure 40(b) is a summary of the pertinent EPR data. Shown are the symmetries (where determined) of the sites, the g values, EPR annealing temperatures, the association with thermoluminescence glow peaks, and the sign of the charge.

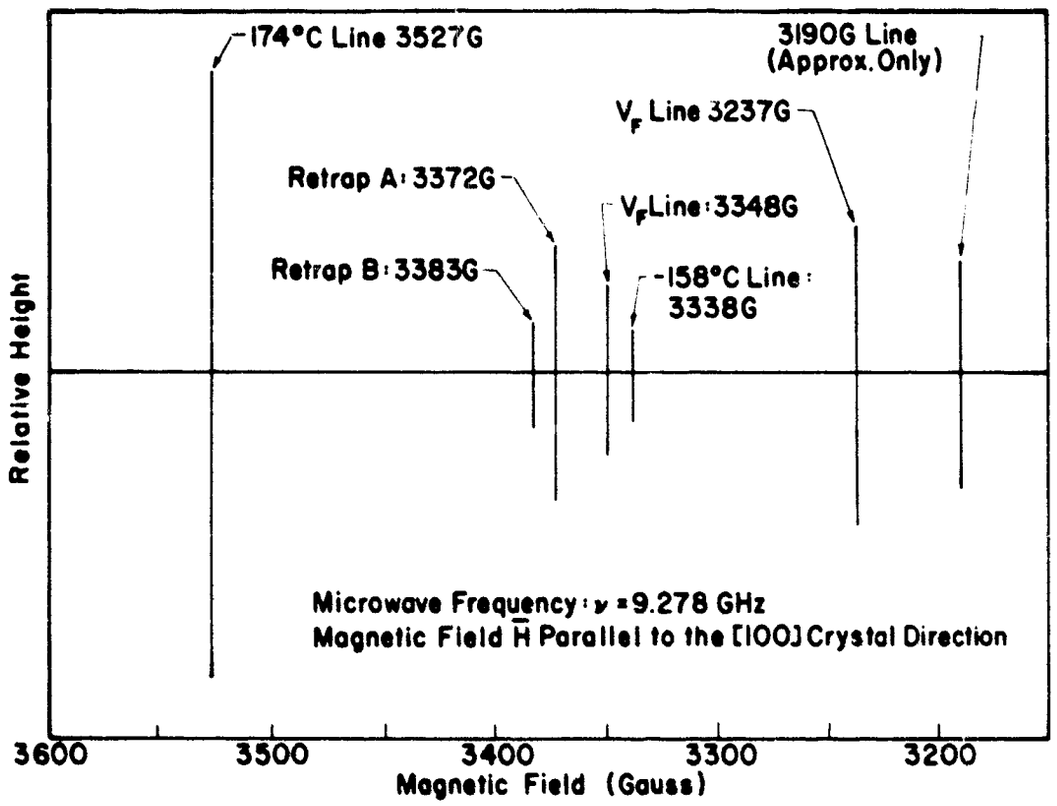

(A) Approximate Relative Heights of the EPR Lines Seen After Irradiation of Thoria Crystal OR2

Line	Symmetry	g_{xx}	g_{yy}	g_{zz}	T	T_Φ	Charge
-158	isotropic	1.9867 =	1.9867 =	1.9867	-160°C	-158°C	e^-
Retrap A	axial<111>	1.9619 =	1.9619	1.9742	148°C	-103,-14,149°C	e^-
Retrap B	axial<111>	1.9547 =	1.9547	1.9682	148°C	-103,-14,149°C	e^-
174	axial<111>	1.8887 =	1.8887	1.8633	159°C	174°C	e^-
V_F		2.054	2.043	1.980	-127°C	—	e^+
31906		>2	>2	>2	151°C	—	e^+

(B) Summary of Pertinent EPR Data

Figure 40. Spin resonance data for: ThO_2: OR2
(a) Approximate relative heights of the radiation induced EPR lines (Figure 17, reference 32)
(b) summary of pertinent EPR data

The -158°C line was found to be isotropic with a spin of 1/2. The dosage curves by EPR and thermoluminescence were of the same general shape but the slope of the EPR growth was 1.1 and the slope of the thermoluminescence growth was 1.28. The resonance characteristics indicate a trapped electron but may simply imply an odd number of trapped electrons. Tint[45] has proposed a triply charged oxygen vacancy which has yet to be tested.

The dosage curves for the "V" lines, shown in Figure 38 agree very well with the thermoluminescence dosage curves for the -103°C peak but the annealing temperatures do not agree. Neaves and Tint[32] interpreted these lines as being due to a trapped hole between two nearest neighbor oxygen atoms next to a cation vacancy. There is no thermoluminescence evidence of hole retrapping and the -103°C peak appears to be an electron recombination, so these lines cannot be cimply correlated with the glow peaks.

The lines labelled Retrap A and B, representing trapped electrons, were not seen at 77°K before or after irradiation; they do not appear until the irradiated sample has been warmed above 100°C. Recooling and further irradiation reveals that the lines are bleached at 77°K at different rates.

There are two types of annealing curves for the retrap lines: one for how they fill and one for how they empty. The filling curves were generated in the same manner as the annealing curves in Figure 39 except that in this case the signal grew with each successive increase of sample temperature until a saturation value. The derivative of the signal intensity vs. temperature curve was plotted vs. temperature to yield the "annealing curve." Figure 41 shows the growth of the signals from the retrap lines and also the signal derivative curve. Thus it is quite clear that the EPR lines are associated with states which retrap charge released during the glow period at -103°C. As the temperature is cycled higher, the retrapping states begin to grow again as the -14°C glow peak is emptied. The maximum of the derivative curve was at 24°C. This difference was not considered serious since the growth of signal during the emptying of this peak was only 15% of the total signal and experimental errors could have caused such a difference. It was also observed that the A and B lines grew at slightly different rates as the -14°C peak was emptied. The 15% growth of the lines during the emptying of the -14°C peak correlates with the area under the -14°C glow peak in that its area is about 15% of that under the -103°C glow peak. These retrap lines were annealed in the manner described previously. The dS/dT curve for the A site had a maximum at 147°C and for the B site at 150°C. Both derivative curves had the same shape and nearly the same peak temperature as the 149°C thermoluminescent glow peak. The differences between the A and B sites probably reflect local variations due to impurities, etc.

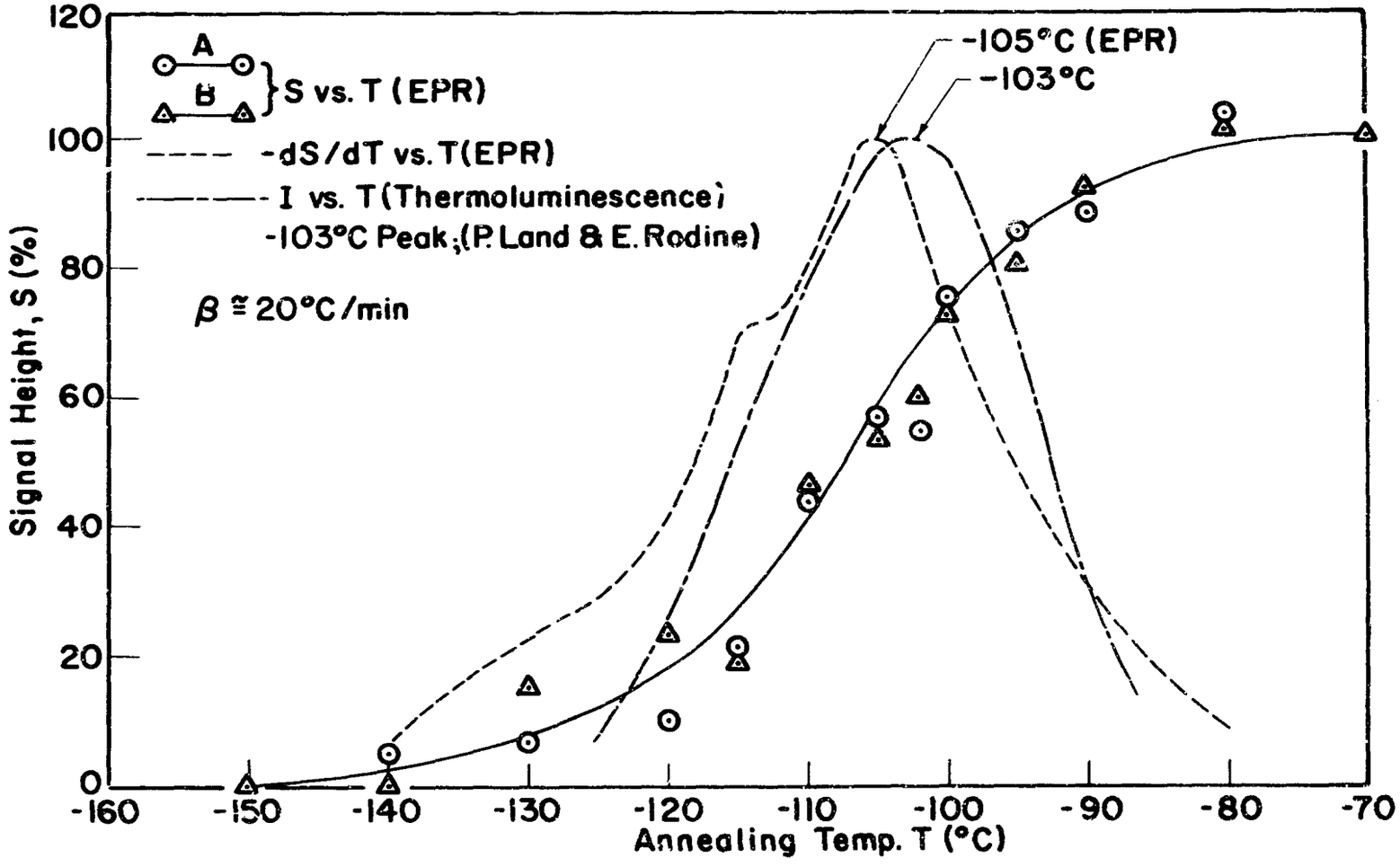

Figure 41. Filling of retrap centers A and B in the vicinity of the -103°C glow peak (Figure 29, reference 32)

The EPR line labelled 174°C can most likely be associated with the 174°C glow peak. The shapes of the dosage curve and the annealing curve agree quite well with the dosage and glow curves of the thermoluminescence but the annealing temperature is somewhat different. The sum of the intensities of the two retrap lines associated with the 149°C glow peak is about equal to the intensity of the 174°C line. However, the area under the 149°C glow peak is about 25 times larger than the area under the 174°C glow peak so one might estimate that only 3 or 4% of the charge released from the trap with a T_* of 174°C participates in the luminescence. It was postulated above that the truncated form and the inconsistent energy analysis of the 149°C glow peak were due to a depletion of available recombination centers prohibiting further radiative recombination. It is also possible that the ratio of radiative to nonradiative recombination changes rapidly in the neighborhood of 150°C.

The data on the final EPR line (3190G) were somewhat incomplete. It appears to be due to a trapped hole. The dosage curve showed growth until a peak after about 8 minutes of excitation, a sharp decrease and finally an equilibrium condition. This behavior has been observed for a V_K center in CaF_2.[46] However, this line is stable at much higher temperatures than the V_K centers in the fluorides. The annealing curve was very broad and peaked at 151°C.

Some EPR measurements were also performed on the crystal OR1. This crystal was from the same batch as OR2 and had thermoluminescence properties similar but not identical to OR2. The EPR spectra of OR1 were essentially the same as for OR2.

Before irradiation, a Gd^{3+} spectrum was observed in both crystals at 77°K. Irradiation with ultraviolet light at 77°K bleached the Gd spectrum, and the dose required for complete bleaching was about the same as that required to saturate the traps. Heating the crystal resulted in the restoration of the Gd spectrum in two broad temperature regions centered at -100°C and +100°C.

Most of the radiation induced EPR lines are related to the thermoluminescence traps, and the observations reinforce the conclusion that the rare earths do not participate in trapping and that the most probable trapping defects are intrinsic.

The 80°C glow peak was never associated with an EPR line which may be because the trapping state is nonparamagnetic, as is apparently the case for the -14°C and -103°C peaks which also were not observed directly by EPR. More information about the trapping states and the recombination centers might be obtained if the investigation were extended to liquid helium temperature which permits the observation of EPR states with short lifetimes.

Section VII

DISCUSSION

Thermoluminescence can be considered to be composed of three parts: excitation, trapping, and recombination. Obviously, the parts are not independent of each other, and none of the experiments described above can be said to measure one of the processes to the exclusion of the others. Each of the experiments does depend on one of the parameters more than the others so each experiment contributes information needed to either build a model of the defect structure or to restrict the number of applicable models for consideration. This investigation has identified a number of the basic processes taking place and the results can be used to identify important features of each of the three main categories mentioned above.

A. ESTIMATED NUMBER OF DEFECTS

The defect concentrations necessary for the thermoluminescence are very low. The number of photons that are detected from a glow peak can be calculated in the following manner. The recorder charts of the glow curves are plots of current (as measured by the electrometer) vs. time. The dosage curves, excitation spectra, etc. were all plotted as the areas under the peaks in square centimeters normalized to the 10^{-7} ampere scale with a common chart speed of one inch per minute vs. time of excitation or wavelength of excitation. Each square centimeter of area under a glow peak, when measured on the 10^{-7} ampere scale of the electrometer, corresponds to 0.189×10^{-6} amp-sec. The emission from many of the samples was centered near 550 nm, so the calculations will be carried out for that wavelength. At 550 nm the sensitivity of the RCA-1P28 photomultiplier used was, according to an RCA brochure:

$$\text{sensitivity} = 1.85 \times 10^{4} \ \frac{\text{microamp}}{\text{microwatt}}$$

Photons with a wavelength of 550 nm have an energy of 2.25 eV. Also,

$$1 \text{ microwatt (at 550 nm)} = 2.78 \times 10^{12} \text{ photons/sec}$$

Therefore,

$$\text{sensitivity} = 1.85\times10^{4}\ \frac{\text{microamp}}{\text{microwatt}} \times \frac{1}{2.78\times10^{12}}\ \frac{\text{microwatt}}{\text{photons/sec}}$$

$$= 0.666\times10^{-8}\ \frac{\text{microamp - sec}}{\text{photon}}$$

Therefore, the number of photons per unit area on the chart paper is:

$$\frac{0.189\ \text{microamp - sec}}{0.666\times10^{-8}\ \frac{\text{microamp - sec}}{\text{photon}}} = 2.83\times10^{7}\ \frac{\text{photons}}{\text{unit area}}$$

According to the geometry of the setup and the size of the photocathode, only 0.33% of the isotropically emitted photons hit the photocathode so the number of photons being emitted from the sample for each square centimeter of chart area is:

$$\frac{2.83\times10^{7}}{3.3\times10^{-3}} = 8.5\times10^{9}\ \text{photons/cm}^2\ \text{of chart paper}$$

Glow peaks of area equal to one square centimeter are commonly observed, so it can be said that roughly 10^{10} transitions are necessary for detection with the equipment used. In Section V, Tables II and III gave the areas under the glow curves in cm^2 on the 10^{-7} scale. These numbers, and all the numbers shown along the ordinates of the figures for the dosage curves, excitation spectra, etc. can be multiplied by 10^{10} to obtain the number of optical transitions during the course of a glow curve or glow peak, assuming monochromatic emission at 550 nm. The EPR data measures the number of paramagnetic spin states created by the optical excitation and hence should measure the number of trapped charge. Tint[45] estimates that the total number of spin states created by irradiation in OR2 is about 10^{15} so it can be inferred that the thermoluminescence process is considerably less than 100% efficient. An efficiency of a few percent would be fairly reasonable.

This discussion can be extended by use of the impurity analyses which will be discussed in the next section. It was shown above for many of the crystals, especially the crystals doped with rare earths, that the emission is primarily from particular rare earth ions. The crystal doped with Er was reported to have 10 ppm Er. The crystal had a volume of about $10^{-3}cm^3$ so there were 10^{15} Er atoms in the crystal. The total area under the glow curve at saturation was $1.34x10^4$ cm^2 which implies $1.3x10^{14}$ photons were emitted from the sample. Therefore,

$$\text{efficiency of Er emission} = \frac{1.3x10^{14} \text{ photons}}{10^{15} \text{ atoms}} = 13\%$$

Similar calculations indicated 3.4% efficiency from Eu doped OR21 and 2% efficiency from Dy doped OR26.

These calculations are very rough for several reasons. The number of photons coming out of the sample was calculated as if the emission were monochromatic at 550 nm. This is not correct. The impurity analyses could easily be off by a multiplicative factor of 3 or more. The calculations assume that each rare earth ion is used just once which is questionable when no charge conversion of the rare earth was observed. The calculations are of interest because of their agreement with previous estimates.

B. IMPURITY ANALYSES

Impurity analyses listing elements in moderate or high concentrations for 12 thoria crystals are shown in Table VI. The crystals to be analyzed were selected to be representative of each batch of crystals by making a number of thermoluminescence runs on them before they were sent in for analysis. The crystals OR7 and OR8 are from the original undoped batch of thoria crystals received from Oak Ridge. Their thermoluminescence characteristics were very similar to OR2. The crystal OR6 is from the same batch as OR4 and was intended to be doped with Ca. The origin of the other crystals is self-explanatory. Comments about the methods of analysis were made in Section IV. It should be noted that the expected accuracy of the analyses is such that the actual impurity levels are within a factor of 3 of the stated levels with perhaps more uncertainty for the smallest concentration levels. Also, many of the smallest concentration levels indicate the limits of detectability for the method of analysis. Some of the samples had a volume of less than 10^{-3} cm^3 so analysis was very difficult. Table VI shows that the crystals are very pure. There are only a few impurity elements that are present in more than one sample in appreciable quantities (a few ppm or more) and there are very few elements that are present in large concentrations in all samples. The only impurities that are present in appreciable quantities

Table VI

Impurity analyses of some ThO_2 single crystals

Element	OR7	OR8	OR6	PE	PE2	N2	OR12 Er	OR29 Nd(Gd)	OR21 Eu	OR26 Dy	OR31 Yb	FI2
Li	0.10	0.1	0.2	n.d.	0.005	<0.003	0.6	0.1	high	high	high	0.6
B	0.04	0.1	0.1	500.	3.	0.02	<3. a	<1. a	<0.02	<0.02	<0.02	1.
C (b)	150.	<300.	<100.	<300.	<30.	<15.	(c)	(c)	1500.	700.	700.	1000.
N (b)	5.	<150.	< 20.	< 30.	< 50.	< 4.	<5.	< 3.	< 100.	<100.	3000.	20.
F	0.2	0.5	<0.2	100.	100.	0.2	<0.2	<0.2	20.	60.	40.	10.
Na	<1.	6.	6.	30.	10.	0.3	10.	5.	6.	600.	200.	6.
Mg	1.	3.	1.	<1.	3.	1.	< 2.	<2.	2.	20.	10.	1.
Al	0.03	3.	1.	2.	1.	3.	4.	1.	2.	60.	10.	10.
Si	10.	100.	1500.	3.	40.	2.	40.	40.	60.	400.	6000.	30.
P	0.03	0.1	0.1	0.2	0.1	0.01	1.	1.	0.6	20.	2.	0.6
S	5.	15.	2.	150.	3.	3.	2.	2.	20.	40.	20.	10.
Cl	5.	5.	2.	1.	15.	0.5	20.	3.	high	high	300.	2.
K	0.5	2.	0.7	0.4	1.	0.2	15.	2.	1.	150.	30.	1.
Ca	2.	2.	4.	1.	1.	30.	3.	3.	1.	40.	40.	10.
Ti	0.6	0.6	0.2	<1.	6.	2.	0.2	0.5	< 0.4	4.	< 0.4	2.
V	<0.02	<0.05	<0.01	< 0.03	<0.02	<0.02	<0.04	<0.04	10.	1.	0.4	0.1
Cr	0.06	0.2	<0.04	0.3	<0.06	<0.02	<0.04	<0.04	< 0.1	4.	< 0.4	0.1
Mn	0.01	0.2	0.1	0.02	<0.07	<0.02	0.2	0.3	< 0.04	4.	0.04	1.
Fe	0.2	0.5	2.	0.5	0.5	0.7	2.	2.	1.	100.	10.	2.
Co	0.02	<0.04	<0.1	< 0.03	<0.1	<0.02	<0.04	2.	0.2	1.	< 0.4	0.1
Cu	1.	0.5	0.5	0.2	0.3	0.05	0.1	1.	0.2	60.	2.	0.2
Zn	0.05	1.	0.4	<1.	1.	0.1	0.2	0.2	< 0.5	< 0.5	<0.5	0.2
Ge	<0.1	<0.3	<2.	< 0.5	10.	<0.3	<0.2	<0.2	< 0.2	< 0.2	< 0.2	<0.2
As	<0.03	<0.2	<0.2	<0.2	1.	<0.1	<0.06	<0.06	< 0.7	≤ 2.	< 0.3	<0.06
Se	<0.1	<0.2	<0.2	<0.1	<2.	<0.1	<0.1	<0.1	< 0.4	< 0.4	< 0.4	<0.04
Sr	<0.03	<0.1	<0.1	<0.2	<0.1	0.1	<0.03	<0.03	<0.07	<0.07	<0.07	1.
Y	<0.03	<0.2	<0.2	<0.2	<0.2	400.	0.2	0.6	< 0.2	2.	1.	0.4
Zr	<0.02	<0.2	0.4	<0.03	<0.2	10.	<0.2	<0.2	< 1.	<1.	< 0.3	<0.2
Nb	<0.01	<0.3	<0.1	<0.02	<0.1	<0.04	<0.02	<0.02	< 2.	(i)	(i)	<0.1
Mo	<0.04	<0.4	<0.4	< 0.2	<1.	<0.2	<0.3	< 0.3	< 0.2	10.	< 2.	<0.2
Rh	<0.01	<1.	<0.6	< 3.	<0.1	<0.4	<0.1	<0.1	< 0.2	0.4	1.	<0.2
Pd	<0.04	<1.	<1.	<0.1	<0.4	<0.4	3.	1.	< 0.4	< 0.4	<0.4	<0.1
Ag	<0.2	(d)	(d)	<0.4	(d)	(d)	60.	6.	< 0.2	< 0.2	<0.2	<0.2
In	<0.05	<0.1	<0.2	< 0.02	<0.4	<0.04	<0.03	<0.03	< 0.2	< 1.	<2.	0.04
Sn	<0.05	<0.4	<0.4	<0.07	<1.	<0.2	<0.1	<0.3	< 0.3	< 1.	<0.3	<0.2
Sb	<0.03	1.	6.	<0.04	<3.	<0.3	<0.2	<0.2	< 0.2	< 0.2	<0.2	<0.06
Cs	<0.02	<0.1	<1.	<0.1	<0.2	<0.05	<0.03	<0.03	< 0.1	< 0.1	<0.1	<0.1
Ba	<0.02	<0.2	3.	<0.1	<0.2	<0.1	<0.05	<0.05	< 0.1	< 0.3	<0.1	<0.1
La	<0.02	<0.2	<0.1	< 0.03	<0.1	5.	<0.03	<0.03	< 0.4	< 0.4	<0.1	4.
Ce	<0.02	< 0.2	20.	20.	50.	10.	0.1	10.	20.	5.	5.	6.
Pr	<0.02	<0.05	<0.1	<0.03	<0.2	1.	<0.04	<0.04	< 0.4	< 0.4	<0.4	0.4
Nd	<0.06	<0.2	<0.4	200.	500.	6.	<0.4	80. e	< 0.4	< 0.4	<0.4	2.
Sm	<0.06	<0.2	<0.1	<0.1	<1.	2.	<0.06	<0.06	< 0.5	< 0.5	<0.5	<0.2
Eu	<0.04	<0.1	<0.6	<0.06	<0.4	<0.1	<0.06	<0.06	600.f	< 0.2	<0.2	<0.1
Gd	<0.06	<0.2	<0.4	<0.6	<0.7	0.5	<0.1	5.	< 0.2	< 0.2	<0.2	<0.6
Tb	<0.02	<0.1	<0.04	<0.3	<0.4	0.6	<0.06	<0.04	< 0.04	< 0.1	<0.1	<0.04
Dy	<0.07	<0.2	<0.6	<0.4	<1.	4.	<0.1	<0.1	< 0.4	30.g	<0.4	<0.1
Ho	<0.02	<0.1	<0.1	<0.3	<0.3	1.	<0.04	<0.04	< 0.1	< 0.1	<0.1	<0.04
Er	<0.07	<0.3	<0.2	<0.1	<0.5	2.	10.	<0.4	< 0.4	< 0.4	<0.4	<0.1
Tm	<0.02	<0.04	<0.04	<0.03	<0.1	<0.1	<0.04	<0.04	< 0.1	< 0.1	<0.1	<0.04
Yb	<0.07	<0.3	<0.1	< 0.1	<0.2	1.	<0.1	<0.1	< 0.4	< 0.4	20.	<0.1
Ta	<1.	<3.	<2.	<3.h	<1.	<0.2	<0.1	<0.1	≤ 4.	< 4.	< 2.	<4.
W	1.	10.	4.	< 0.1	<0.2	<0.2	6.	1.	400.	~3%	~1%	1.
Re	<0.04	<0.2	<0.1	< 0.05	<0.1	<0.1	<0.1	<0.06	< 0.2	1.	<0.6	<0.1
Pt	<0.1	<1.	<0.6	0.1	<0.6	<0.3	<0.1	<0.1	< 0.2	< 2.	<0.6	<0.4
Hg	<0.3	<1.	<0.2	<0.1	<0.5	<0.3	<0.1	<0.1	< 0.4	< 4.	< 1.	<0.4
Pb	<0.2	<0.5	<1.	≤100.	600.	<0.2	<0.1	<0.1	< 0.1	< 1.	< 1.	<0.4
Bi	<0.1	<1.	<0.6	1.	20.	<0.1	<0.2	<0.2	< 2.	< 2.	< 2.	<0.6
U	<0.1	<0.1	<0.2	<0.3	<0.1	0.3	<2.	<2.	< 0.2	< 0.6	< 0.2	<0.2

(a) mortar contamination
(b) samples not baked
(c) briquetting material
(d) not determined/ silver epoxy
(e) enriched in $^{144}_{153}Nd$
(f) enriched in ^{153}Eu
(g) enriched in ^{164}Dy
(h) contamination from Ta electrode holders
(i) precluded by W^{6n} ions

in all samples are C, Na, Si, S, C1, and Ce. Most of these elements appear in the highest concentrations in the samples that have weak to moderate thermoluminescence so there is no indication that these elements participate in the trapping. It was not possible to associate high concentrations of particular impurities, or the absence of particular impurities except for the rare earths, with the thermoluminescence of the samples. It was not possible to establish conclusively that the samples with a high total impurity content had more or less optical activity than the relatively clean samples. However, it may be the wrong approach to try to associate large concentrations of an impurity with the thermoluminescence. The calculations above indicated that very few transitions were necessary for detection, and the EPR study indicated a very small number of spin states associated with the thermoluminescence traps. It was indicated that only sub-parts per million of a particular species were necessary for the thermoluminescence observed. Therefore, any of a very large number of impurities listed in Table VI could be responsible for the trapping states. Furthermore, it is quite apparent that the visible thermoluminescent recombination is through the rare earth ions and that the number of rare earth ions in these crystals is quite limited. There was evidence from one of the crystals (OR2) that the recombination centers were filled before all of the traps were emptied, so it would appear that the total glow depends more on the number of rare earth ions than on the total number of traps.

It cannot be established that impurities other than the rare earths significantly affect the thermoluminescence of these thoria samples. A large number of samples, with a good sampling of commonly occurring impurities in varying concentrations were investigated. Hence it is believed that impurities play a very minor role in the thermoluminescence. It is entirely possible that the trapping states are due to stoichiometric defects. Oxidation or reduction of the crystals has not been attempted, partially because of the lack of suitable quenching apparatus for a careful and thorough study.

C. RARE EARTH SUBSTITUTION AND CHARGE COMPENSATION

It was established in the preceding sections that in many cases the thermoluminescence emission is the characteristic sharp line spectra of small concentrations of tripositive rare earth ions. This is a very important factor in the construction of a model of the defect structure. Abraham et al[33,34,35], Linares,[28] Neeley et al,[39] and Marshall[37] have shown that rare earth ions are incorporated into the thoria lattice by substitution for Th atoms. The rare earths are able to substitute for the Th atoms and retain the normal cubic symmetry of the sites. If the required charge compensation for the 3+ ion in a 4+ site is in the immediate neighborhood of the rare earth, the cubic symmetry is destroyed. Abraham et al[33] reported the presence of tetragonal symmetry about the (100) axis and trigonal symmetry about the (111) axis due to charge compensation at nearest neighbor and next nearest neighbor sites respectively. They

reported that charge compensation by an oxygen vacancy in a nearest neighbor position will result in trigonal symmetry about the (111) axis. Charge compensation in the immediate vicinity of the 3+ ion will cause more distortion of the lattice than compensation at a distance[47,48] and a higher resultant energy state of the crystal. The demands of charge neutrality are commonly relaxed to permit compensation at a distance. Compensation can be accomplished by means of foreign impurities or stoichiometric defects. Finch et al[30] found that in their thoria samples that were rather heavily doped with Dy^{3+} or Eu^{3+} the ratio of rare earth ions to W^{6+} impurities was 6:1 enabling them to attribute the charge compensation of the rare earths to interstitial tungsten. Linares[49] discussed the various types of rare earth compensation and measured the flourescence of some thoria crystals doped with rare earths and compensator ions. He showed that many of the characteristic Eu lines in the neighborhood of the 5902 Å line were suppressed while the 5902 Å was enhanced by the addition of Ta^{5+} or F^{1-} to Eu doped crystals. A highly probable means of charge compensation in thoria is by oxygen vacancies. Two tripositive rare earth ions would be compensated by one oxygen vacancy.

The rare earths that have been observed to yield thermoluminescence emission cannot be reduced to a 2+ state at these temperatures; hence they do not participate in the trapping.[30,36] The emission spectra are characteristic of the 3+ states of the rare earths and the EPR data indicate the excited charge to be electrons instead of holes so the energy must be transferred to the rare earth without the transfer of charge. Numerous examples of resonance or tunneling energy transfer have been reported in the literature.

The optical activity shown by one rare earth can be enhanced or suppressed by the addition of another rare earth or some other compensating ion. The work of Linares[49] was cited above as an example. Wanmaker et al[50] investigated the luminescence of Tb^{3+} in alkaline earth phosphates. An excitation band with a peak at 220 nm and the characteristic Tb^{3+} emission were observed. The Tb luminescence was enhanced by the addition of Sn^{2+} and Cu^{1-}. Garrett and Kaiser[51] enhanced the luminescence of Tb in CaF_2 with the addition of Ce. This is of particular interest to this study since CaF_2 is somewhat similar to ThO_2, the emission of OR2 is very similar to Tb, and Ce is present in mostof our samples. Wanmaker et al[52] also enhanced the Tb emission in some alkali-earth borates by the addition of Gd. There are numerous other examples in the literature, usually connected with the search for efficient laser materials. Recall, however, that very few trapping states or recombination centers are required for thermoluminescence or are present in our samples, so detailed analysis is very difficult.

It is apparent that the traps and the sources are not due to the rare earths. Further evidence is seen from the fact that the rare earth states that are responsible for the thermoluminescent emission also show fluorescence that is, if not identical, very similar to the thermoluminescence.

No degradation of the fluorescence as a function or irradiation time was observed, further indicating that the rare earths do not participate in the trapping. The most efficient excitation wavelengths of the thermoluminescence and fluorescence were not always the same, indicating that the rare earths do not participate in the excitation. The fluorescence excitation in most cases was characteristic of the rare earth while the thermoluminescent excitation indicated a band-to-band transition.

D. OXYGEN VACANCIES IN THORIA

Previous investigations have shown that oxygen vacancies play an important role in the optical properties of thoria. These investigations will be discussed and important connections between the literature and the present investigation will be established. It will be shown that phenomena previously attributed to oxygen vacancies are observed in the crystals used here and, with the aid of some simple calculations, it will be shown that it is reasonable to consider oxygen vacancies as key defects giving rise to thermoluminescence.

Weinreich and Danforth[26] and Danforth[22] studied the optical properties of arc grown thoria crystals and their dependence on the oxygen content. They found an absorption peak at around 400 nm after heating to 1800°C in vacuum. The peak was eliminated by heating in air. Weight change measurements indicated that approximately 10^{18} oxygen atoms per cm^3 were removed during heating in vacuum and replaced when heating in air. Bates[27] also studied changes of the absorption spectra as a function of oxygen content and found the production of oxygen vacancies to be quite easy.

The presence of oxygen vacancies in a crystal gives rise to speculation about their suitability as trapping sites and the creation of defects analogous to F centers in the alkali halides. Danforth[22] and Weinreich and Danforth[26] noted a red coloration of their oxygen deficient samples. Linares[28] observed color centers of two types in thoria single crystals. The addition of Ca^{2+} ions shifted the ultraviolet cutoff to longer wavelengths and produced an orange color that was of a permanent nature and not bleachable. Crystals grown from a lead flux were clear until ultraviolet light colored them. These color centers could be bleached by heating to 300°C or storing them in the dark for several days. Linares attributed the shift of the absorption spectrum associated with the bleachable color centers to absorption by excess Pb^{2+} ions but did not speculate on the nature of the center in the colored state. Neeley, Gruber, and Gray[39] reported the identification of an F center (electron trapped at an oxygen vacancy) in thoria single crystals by EPR techniques. The crystals were grown from a lead flux and were optically clear and had a very clean EPR spectrum before irradiation. Irradiation at 77°K with 2 MeV electrons, Co^{60} gamma rays, or x-rays produced a sharp EPR line and a yellowish color. The yellow color was

bleached rapidly by ultraviolet light. The angular variation of the EPR line was slightly anisotropic and the g values were slightly less than two. Neeley et al[39] attributed the center to electrons trapped at oxygen vacancies needed for charge compensation of 3+ impurities and from the natural abundance of oxygen vacancies in thoria. Their conclusion was supported by the observation that the addition of Er^{3+} and La^{3+} to the thoria crystals increased the number of centers in proportion to the number of 3+ ions added. The anisotropy and g values agree quite well with one of the lines observed by Neaves and Tint[32] in OR2. It appears as if the line observed by Neeley et al is the same as one of the ıp lines which anneals at 149°C as observed by Neaves and Tint. However, the retrap line observed by Neaves and Tint was not directly produced by irradiation; it was seen only after the irradiated sample had been warmed through the -103°C glow peak and did not reach full saturation value until the sample had been warmed through the -14°C glow peak. There is the possibility that the sample used by Neeley et al warmed between irradiation and measurement such as during a transfer between an irradiation dewar and the microwave cavity. Neeley et al did report scanning the resonance spectrum at room temperature as well as at 77°K and 4.2°K after irradiation at 77° K. The bleaching of the EPR line by ultraviolet light at 77°K was observed by both groups of investigators.

It is very difficult to identify an F center on the basis of the above data alone. There are a number of defects that may involve a trapped electron having a narrow EPR line with suitable bleaching properties. For example: electrons can be trapped by Th atoms or foreign impurities at sites with high symmetry. The arguments of Neeley et al[39] with regard to the abundance of oxygen vacancies in thoria, and the enhancement of their EPR spectrum by the addition of 3+ lanthanides, plus the observations by other investigators, indicate that color centers are formed in thoria and that the presence of oxygen vacancies is a very important factor in the defect structure. Coloration of the crystals used here was not observed. This may be because the defect density was so low.

It is useful to consider the expected energy of an electron trapped at an oxygen vacancy in the thoria lattice. The lattice energy of polycrystalline thoria as determined from bulk modulus experiments has been reported as being about 2250 kcal/mole[53] which can be converted to about 97.5 eV. This is nearly an order of magnitude higher than for the alkali halides. The Madelung constant, which is dependent only on the lattice structure, is 5.03[54] for CaF_2 and will be taken as approximately the value for thoria. This is quite high compared with about 1.75 for the alkali halides. A high Madelung constant will imply a very tight binding of electrons trapped at a vacant lattice site. Seitz[54] has suggested that the potential of an electron trapped at an anion vacancy can be written, neglecting polarization, as:

$$E = \frac{-Ae^2}{r_o} \qquad (17)$$

where A is the Madelung constant, e is the charge of an electron and r_o is the nearest neighbor distance of the atoms. Using a value of 5 for the Madelung constant $2e^2$ for e^2 because the oxygen vacancy is initially doubly ionized, and using r_o = 2.425 Å[53] one obtains an energy of nearly 60 eV. Equation 17 transforms to $-e^2/r$ at large distances from the vacancy where the periodic Madelung potential can be neglected. Seitz points out that for a more reasonable estimate one should take the polarization of the vacancy into account so a second approximation would be:

$$E = \frac{-e^2}{kr_o} \tag{17a}$$

where k is the dielectric constant. In the absence of dielectric data, one can take the square of the index of refraction (n = 2.15)[40] so the potential depth becomes 2.5 eV. This would then be a rough estimate of the expected trap depth of an electron trapped at an oxygen vacancy. An energy of 2.5 eV is about twice as high as the thermal activation energy of the highest temperature glow peaks (see Figure 16 and Table IV). This may be as good agreement as can be expected from such a simple calculation. However, it is not required that an electron be thermally excited to the band before it can escape: it can tunnel to an excited state of the recombination center from some state intermediate between the ground state and ionized state of the trap.

Hence, these simple calculations and the strong connection between this investigation and the information in the literature make it reasonable to think of the trap responsible for the 149°C glow peak as being due to an electron trapped at an oxygen vacancy.

E. DISCUSSION OF MODELS

In this section, the information obtained from the experimental data, the data analyses, and reference to the literature will be used to construct specific models of the defect structure participating in the thermoluminescence. Portions of these models were discussed in the preceding sections. For example: from the measurement of the emission spectra it is obvious that any reasonable model must include a mechanism for recombination via rare earth ions. Also, the composite glow curves showed that the trapping states are nearly independent of the rare earths, and impurity analyses failed to show a clear relationship between particular impurities and the trapping states. On this basis and with the understanding of the correlation with EPR and the subsection immediately preceding this discussion, it is quite reasonable to identify the primary defect as being due to oxygen vacancies. The models to be discussed will be constructed with oxygen vacancies as the key defect. The first model also involves trapping states at Th sites and the alternative model involves different ionization states of the oxygen vacancy.

Figure 42(a) shows a glow curve with the peak temperature, activation energies, and other selected information for OR2. The glow curve was obtained after excitation to saturation and is essentially identical to the glow curve in Figure 5. All of the information shown has been discussed in detail in previous sections, but it is useful to reconsider the information as various models are discussed.

Consider an oxygen vacancy in the thoria lattice. Distortions of the lattice will occur in the neighborhood of the vacancy and will cause modified electronic energy levels, perhaps as in the pictorial representation in Figure 42(b). The figure is a plot of energy states vs. distance from the vacancy. Values for the energy differences and the distances are difficult to define although the discussion above would indicate the "depth" of the oxygen vacancy to be from 1.25 to 2.5 eV. The normal electron configuration of Th is the Radon core with four outer electrons $6d^2 7s^2$. Thorium is the first element in the actinide series so the 5f shell is unfilled. The electronic state for Th^{3+} is 5f;[55] that is, the 5f state is of lower energy than the 6d or 7s states. We shall consider Th^{3+} as a possible trapping state. In the thoria lattice, each Th atom is at the center of a perfect cube of 8 oxygen atoms. A 5f state such as for Th^{3+} in a cubic field has three modes, two of which are degenerate, and being close to the oxygen vacancy the symmetry is lowered so there are five energy levels. Further splitting may occur, such as by a local charge compensating impurity or the Jahn-Teller effect, so there may be seven energy states available. Some of these states would be expected to lie in the band while others would be in the band gap.

Thermoluminescence excitation was shown to be primarily a band gap process, so ultraviolet irradiation would promote electrons across the band gap and they would be free to move in the conduction band. This could take place in most any region of the crystal. These electrons will tend to move towards an oxygen vacancy. It is suggested that before reaching the oxygen vacancy the electrons are trapped in Th^{3+} states that are nearest neighbors or next nearest neighbors to the oxygen vacancy. In the thoria lattice, an oxygen vacancy will have four nearest neighbor Th atoms forming a tetrahedron, 12 next nearest Th neighbors, 12 third nearest Th neighbors and 16 fourth nearest Th neighbors. The Th^{3+} trapping states would be associated with the -103°C and -14° glow peaks. The glow peaks may represent different energy states of the same trapping site or they may be from different sites such as next nearest neighbors and nearest neighbors. Recall the ratio of glow from the -103°C peak to the glow from the -14°C peaks is about 3 and that there are 3 times as many next nearest neighbors as nearest neighbors. One might also consider the fourth nearest neighbors as being associated with the -103°C peak. These sites are of two species with different symmetry properties (12 sites of one species and 4 of another) that may explain the multiplicity of this peak at low dose. Otherwise, the splitting of this peak would represent a minor spread of states in variance from a particular axis with the oxygen vacancy. The large number of available states could account for the multiplicity and also for the retrapping observed from the -14°C peak.

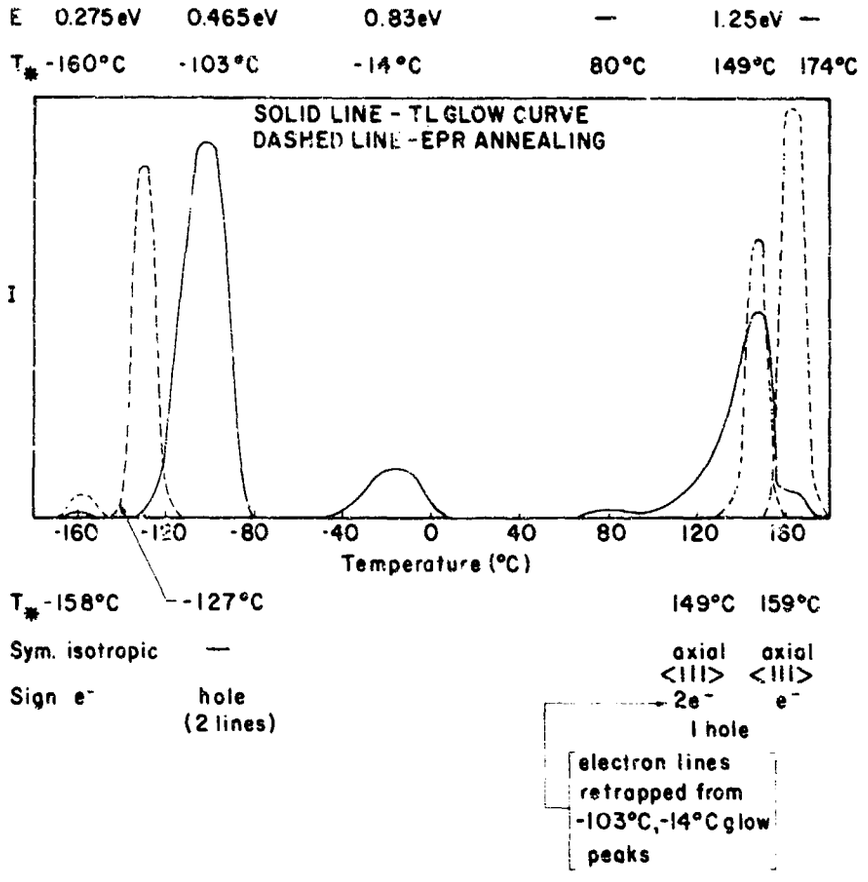

(A) Comparison of TL & EPR Properties

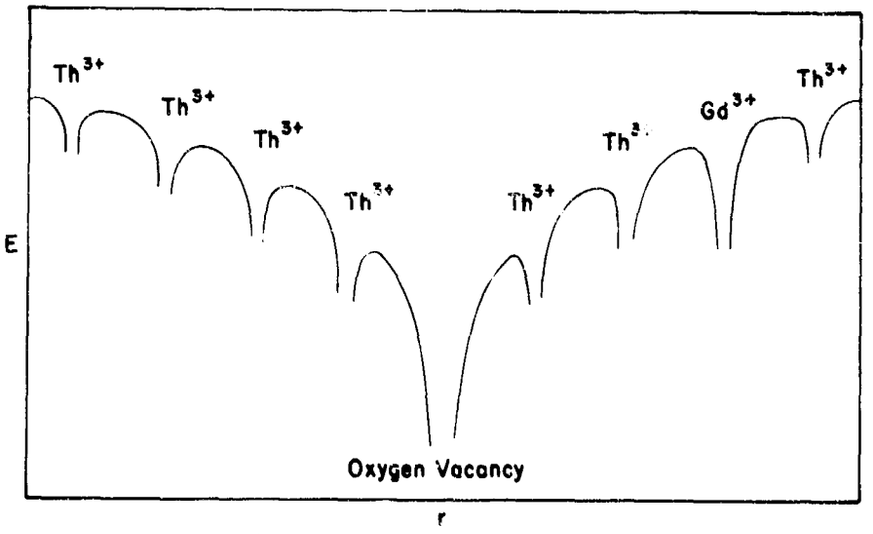

(B) Schematic of Th^{3+} Energy Levels in Neighborhood of Oxygen Vacancy

Figure 42.

Neaves and Tint[32] observed a Gd^{3+} spectrum at 77°K before irradiation. Ultraviolet irradiation bleached the spectrum but it was restored in two stages as the sample was warmed through -100°C and +100°C. Gadolinium would tend to enter the thoria lattice by replacing a Th atom near the oxygen vacancy, which in Figure 42(b) would be in the distorted region of the lattice. The bleaching of these sites at 77°K could be interpreted to mean that the Gd^{3+} ions are trapping electrons, creating Gd^{2+} which is a 5d state. The reappearance of the Gd^{3+} spectrum at -100°C and +100°C would be interpreted to mean that the trapped electrons are being thermally activated restoring the Gd^{3+}. No visible recombination of the electrons from the Gd was observed nor does it appear that there is any transfer to the rare earths responsible for the thermoluminescence. The restoration of the Gd spectra is over a wide temperature range and neither peak looks like one of the thermoluminescence peaks.

The -103°C and -14°C peaks were not directly observed by EPR. This could be because the lifetimes of the resonance states are so short that sufficient population cannot be built up for detection, or it may be that the lifetimes are so long that the excited resonance states become saturated.

As we heat the crystal through the -103°C glow peak, the trapped charge is freed. Some of the charge is retrapped (as observed by the growth of the EPR lines associated with the +149°C glow peak) and some of the charge recombines giving off thermoluminescence. Charge may leave the trap and go to the conduction band or it may tunnel to another trap or the excited state of a recombination center. The process is repeated as we heat through the -14°C peak. The 149°C peak is associated with the oxygen vacancy, i.e., it is an electron trapped at an oxygen vacancy and is the final trapping state for electrons initially trapped at Th sites. Two EPR lines that were close to each other in energy, symmetry, g factors, etc. were associated with the peak. One of these lines was also seen by Neeley et al and attributed to an electron at an oxygen vacancy. It is possible that two states are observed because of local variations of symmetry due to other impurities or defects and that the differences are not particularly important.

Thus it appears reasonable that the -103°C glow peak is due to trapping by the 3rd nearest neighbor Th atoms: the -14°C peak is due to trapping by the second nearest neighbors, and the 150°C peak represents trapping of the electrons at the oxygen vacancy. It does not appear to be possible to predict the relative magnitudes of the glow peaks, partly due to the retrapping and the poor efficiency of the thermoluminescent process. Since it is proposed that the electrons are trapped in three shells surrounding the vacancy, and each shell has a number of equivalent sites, self-retrapping and retrapping by deeper states must be expected. The thermoluminescence data showed strong evidence of retrapping in the -103°C and -14°C peaks by means of shifts of the peak temperature as a function of dose, and the EPR data and the thermoluminescence data showed that the 150°C peak derived all of its population from the lower temperature peaks.

The model discussed above is probably the most complete and sophisticated model available. Many of the experimental facts and observations are taken into account and several of the key factors correlate with the observations reported in the literature. All of the experimental facts are not explained and there remain several points of failure. The most puzzling experimental fact that cannot be explained is that the 149°C peak cannot be excited by irradiation at room temperature. For the model discussed above, this peak cannot be directly excited at 77°K because the electrons are trapped at Th sites on the way to the oxygen vacancy. However, at room temperature, the Th traps should be unstable and one should be able to populate the deeper traps. This was not possible and is unexplained. The model is also suspect because the 149°C peak does not appear in all samples, even when the lower temperature peaks are very similar to the peaks seen in OR2. Nor does the model account for the quadratic growth behavior of the -103°C peak at low dose conditions and the 149°C peak at moderate dose conditions.

The model discussed above does not account for all of the glow peaks, nor is it expected that any model will account for all peaks. The -158°C peak was correlated by Neaves and Tint[32] with an EPR line that was isotropic and had a g factor slightly less than 2, indicating a trapped electron. The very low annealing temperature and the expected tight binding of a trapped electron to an oxygen vacancy tend to rule out the possibility of this being an F center. The glow peak is well behaved and neither the glow nor the EPR line appears to be connected to the other peaks or lines. Tint[45] has proposed that this may be an oxygen vacancy with three trapped electrons (the resultant defect would have the same net spin as one electron). This idea can be extended by proposing that as the crystal is heated through the -158°C peak one trapped electron is removed. The remaining two electrons at the oxygen vacancy would form a defect that is electrically neutral and nonparamagnetic and hence undetectable by EPR. This would account for the fact that the -103°C and -14°C peaks were not detected by EPR. The -103°C and -14°C glow peaks could represent different configurations of the same trap and the progressively higher activation energies could reflect tighter binding of the electrons to the vacancy. Removal of an electron by heating through the -103°C and -14°C peaks would leave a rather tightly bound electron that is not activated until the glow peak at 149°C. On this basis, it is easy to explain the growth of the EPR lines associated with the 149°C peak. One could also speculate about the possibility of the hole, released at -130°C, combining with one of the two trapped electrons in an excited state such that additional thermal activation results in the -103°C glow peak or the -14°C peak. The major problem with this model is that it is unreasonable for states with two or three trapped electrons to be produced by irradiation while the state with one trapped electron is not produced. Nor can it be seen why the state with one trapped electron cannot be produced at room temperature.

Several other EPR lines or thermoluminescent glow peaks are not included in the model above. The 174°C glow peak was associated with an EPR line that had the characteristics of a

trapped electron but detailed thermoluminescence measurements could not be made because the peak was quite weak. Several EPR lines with the characteristics of trapped holes are also ignored. One of these lines annealed at -130°C and had a dosage curve that was nearly identical to the thermoluminescent dosage curve of the -103°C peak. It is very difficult to associate the release of a trapped hole with the thermoluminescent emission observed, especially since the thermoluminescent emission is essentially identical for all glow peaks from a sample. The coincidence of the dosage curves need not be given great importance; linear growth rates can be observed for a variety of processes.

Several reasonable models have been disucssed with respect to the experimental results. Neither model is able to account for all of the experimental data, and both models have shortcomings. The models are able to account for much of the data and they relate favorably to the information in the literature.

F. SUMMARY AND SUGGESTIONS FOR FUTURE WORK

The ultimate aim of a study of the thermoluminescence of a material is to contribute to the description and understanding of the defect structure of the material. There are many techniques for studying the defect structure of a material, none of which are able to measure all parameters. Thermoluminescence is also a limited method,but is a very useful tool over particular temperature regions and for certain types of defects. Thermoluminescence is a cyclic, reproducible process that depends on the orderly rearrangement of charge between defect states. Thermoluminescence resulting from ultraviolet excitation does not alter the defect concentration, i.e., defects are not created by the excitation or annealing of thermoluminescence as studied in this investigation. However, thermoluminescence is sensitive to changes of the defect concentrations produced by doping, heat treatment, or high energy bombardment. Thermoluminescence is able to extract information about all aspects of the cyclic process, i.e., the excitation, trapping, and recombination. This investigation yielded good evidence as to the processes taking place in each aspect in the crystals available with the defect concentrations available. Thermoluminescence is sensitive to the variation of many parameters and hence many parameters must be controlled and measured over a reasonable range. In some cases, the data showed very subtle differences or anomalies that were revealed by very careful measurement that are difficult to incorporate in a general model. Examples are the preferential filling of the traps observed from the excitation spectra data or the subtle differences of emission from the various peaks as observed from the emission spectra.

Some of the major conclusions about the thermoluminescence of ThO_2 as determined by this investigation are:

1. The glow curves are very similar to each other irrespective of impurity content and method of growth, indicating that the trapping states are due to stoichiometric defects or very small concentrations of impurities. No correlation between the thermoluminescent trapping states and specific impurities was determined.

2. The most important glow peaks after ultraviolet excitation at liquid nitrogen temperature have maxima at -160°C, -120°C to -100°C, -14°C, and 150°C.

3. Dosage studies indicated that most of the growth rates are linear although some peaks showed sublinear or quadratic behavior. The 150°C peak from the Oak Ridge crystals was the most important peak showing quadratic growth behavior.

4. Evidence of self-retrapping was observed for several peaks by the decrease of peak temperature with increasing dose. The temperature shifts are consistent with theory.[8,9]

5. It was observed from dosage studies that nearly all of the individual glow peaks in a crystal attained saturation after the same amount of irradiation indicating either the depletion of sources or the simultaneous filling of the traps.

6. The 150°C peak in OR2 was truncated and the 174°C peak was merely a shoulder. The EPR line associated with the 174°C peak was the largest line observed. This indicates that luminescence recombination centers are filled before all traps are emptied or that the efficiency for luminescent transitions decreases rapidly in this temperature region. Quenching of the fluorescence was observed in this temperature region, which tends to support the latter case.

7. The thermoluminescence emission from many of the samples is the characteristic line emission of particular rare earths. Less than 1 ppm of the rare earths were necessary for bright thermoluminescence. There were no major differences among the emission spectra of the glow peaks in a glow curve from the rare earth dominated cyrstals.

8. The fluorescence emission appears to be the same as the thermoluminescence emission in the rare earth dominated crystals. No degradation of the fluorescence was noted as a function of irradiation time which indicates that most of the rare earth ions do not change valence and therefore provide neither sources nor traps. One contrary observation was the conversion of Gd at 77°K in OR1 as reported by Neaves and Tint.[32]

9. The band gap is 5.75 eV and this energy is higher than previously observed. [26,27,28]

10. The maxima of the thermoluminescence excitation spectra and the ultraviolet cutoff coincide at about 215 nm, indicating that some trap excitation involves a band gap transition. Some indications of preferential excitation were observed. The spectra had a long wavelength tail that varied among crystals that is probably due to impurities. The excitation spectra of the fluorescence does not coincide with the excitation of the thermoluminescence.

11. Excitation of the thermoluminescence due to the radioactivity of thorium was observed. The rate of self-excitation is much smaller than the rate of excitation by ultraviolet irradiation used here. The self-excitation was not an important factor in this study except in some cases of very low ultraviolet dose.

12. The thermal activation energy and frequency factor analyses by three methods showed good agreement between crystals and variations between methods of analysis. The differences between methods is considered to be a consequence of peak multiplicity and retrapping. The thermal activation energies had values such as 0.2 eV for the -160°C peak to about 1.25 eV for the 150°C peak. It is believed that the initial rise analysis yields the most appropriate values of E.

13. The charge in the traps can be optically released by a broad band of light. There is no sharp bleaching spectrum.

14. The traps responsible for the 150°C glow peak are populated by charge released from the -103°C and -14°C glow peaks in proportion to the relative strengths of the latter peaks.

15. The traps responsible for the 150°C glow peak cannot be directly populated by ultraviolet irradiation even at room temperature where the -103°C and -14°C peaks are unstable. The EPR study indicated that the associated traps are bleached by ultraviolet irradiation at 77°K so it is quite likely that these traps cannot be directly excited at any temperature.

16. The EPR line associated with the 150°C peak agrees quite well with a previous investigation[39] in which the line was associated with an oxygen vacancy. On this basis and by other considerations such as the similarity of glow peaks from other crystals, it seems probable that oxygen vacancies or complexes including oxygen vacancies provide the major trapping states.

17. The principal model discussed suggests that an oxygen vacancy forms the trap for the 150°C peak and the -14°C and -103°C peaks are due to electrons trapped at neighboring Th atoms. It is suggested that electrons excited by the irradiation are trapped by the Th atoms as the electrons move towards the oxygen vacancy. Heating releases these electrons to recombine and/or be trapped by the oxygen vacancy. It is suggested that the luminescence associated with the recombination is accomplished by a tunneling or resonance transfer of energy to neighboring rare earth ions. The self-retrapping and possibly the relative ratios of the low temperature peaks can be predicted on the basis of this model. We could not adequately determine the nature of the sources or recombination centers. Nor could we determine the location of the rare earth states relative to the bands, the migration of the holes in the valence band after excitation and trapping, and the details of hole recombination. More experimental evidence and a more sophisticated model are required for a complete description of the cyclic process.

There are several specific directions in which the study should be extended. The thermoluminescence should be studied as a function of oxygen content in a careful and thorough manner. The high temperature oxidation or reduction and the quenching must be done carefully to avoid contamination or some other creation of defects. This type of study may confirm that oxygen vacancies are involved in the trapping and may give support or provide alternatives to the models proposed above. Spin resonance data are needed on more crystals representing varied defect concentrations to help in establishing the proposed intrinsic nature of the excitation process and trapping states. Resonance data on samples doped with rare earths could provide more information about the symmetry of the recombination centers as well as the traps and perhaps yield information about the transfer of energy from the traps to the luminescent ions. It is important that the EPR measurements be extended to 4.2°K since many electronic states having an unpaired electron, including most of the rare earths, cannot be seen at higher temperatures. At 4.2°K one could explore the possibility of charge conversion upon irradiation. It is very important that further studies be made by EPR and thermoluminescence to determine a detailed picture of the filling of the 150°C glow peak. The explanation of the filling of this peak remains as the most difficult problem in the interpretation. Careful comparison of the excitation and emission of the fluorescence with the excitation and emission of the thermoluminescence may result in detailed identification of the states participating in the thermoluminescence and the symmetry[10] of the rare earth environment. More detailed study of the crystals currently available that are doped with rare earths would be useful for comparison with the undoped crystals. It might also be useful to excite the thermoluminescence or fluorescence with x-rays to confirm the correlation with the work of Neeley et al[39] and to check further the role of the rare earths in the excitation.

REFERENCES

1. A. Halperin and R. Chen, "Thermoluminescence of Semiconducting Diamond," Phys. Rev., 148, 839 (1966).

2. J. H. Schulman, "Survey of Luminescence Dosimetry," *Luminescence Dosimetry, Proceedings of International Conference on Luminescence Dosimetry,* Stanford University (1965), Edited by Frank H. Attix, Published by U.S. Atomic Energy Commission, Division of Technical Information (1967).

3. P. D. Townsend, C.D. Clark, and P. W. Levy, "Thermoluminescence in Lithium Fluoride," Phys. Rev., 155, 908 (1967).

4. J.R. Cameron, N. Suntharalingam, and C. Wilson, "Supralinearity of Thermoluminescent Phosphors," *Proceedings of Second International on Luminescence Dosimetry,* Gatlinburg, Tenn., (1968), Published by U.S. Atomic Energy Commission and Oak Ridge National Laboratory, Division of Technical Information (Conf. 680920).

5. A. Halperin and M. Schlesinger, "Effect of Thermal Pretreatment on the Thermoluminescence of KC1 Crystals," Phys. Rev., 113, 762 (1959).

6. A. Halperin and A.A. Braner, "Evaluation of Thermal Activation Energies from Glow Curves," Phys. Rev., 117, 408 (1960).

7. Ch. B. Luschik, Dok. Akad. Nauk. S.S.R. 101, 641 (1955).

8. P.L. Land, "A New Method for Determining Electron Trap Energies from Thermoluminescence or Conductivity Glow Curves," J. Phys. Chem. Solids, 30, 1681 (1969).

9. P.L. Land, "Equations for Thermoluminescence as Derived from Simple Models," J. Phys. Chem. Solids, 30, 1693 (1969).

10. J.L. Merz and P.S. Pershan, "Charge Conversion of Irradiated Rare-Earth Ions in Calcium Fluoride I and II," Phys. Rev., 162, 217 (1967).

11. J.T. Randall and M.H.F. Wilkins, "Phosphorescence and Electron Traps I and II," Proc. Roy, Soc., A184, 366 (1945).

12. D. Curie, *Luminescence in Crystals,* Metheun and Co. Ltd., London (1963).

13. G.F.J. Garlick, "Luminescence," Handbuck Der Physik, 26, 1 (1958).

14. *Proceedings of Second International Conference on Luminescence Dosimetry,* Gatlinburg, Tenn. (1968), Published by U.S. Atomic Energy Commission and Oak Ridge National Laboratory, Division of Technical Information (Conf. 680920).

15. D.J. McDougall, editor, *Thermoluminescence of Geological Materials,* Academic Press, London (1968).

16. J.A. Crawford, "Research Topic for Small Colleges: Thermoluminescence," Am. J. Phys., 34, 235 (1966).

17. P.L. Land and E.D. Wysong, "Appartus for Thermoluminescence Measurements," *Proceedings of Second International Conference on Luminescence,* Gatlinburg, Tenn. (1968), Published by U.S. Atomic Energy Commission and Oak Ridge National Laboratory, Division of Technical Information (Conf. 680920).

18. E. Rohner and M.J.O. Strutt, "Automatic Spectrometer Using Interference Filters," Rev. Sci. Instr., 28, 1074 (1957).

19. R.W. Vest and W.C. Tripp, *Electrical Behavior of Refractory Oxides IV,* Technical Documentary Report, ARL 66-0220 (1966).

20. Sauereisen Cement Co., Pittsburgh, Pennsylvania.

21. R.L. Christensen and I. Ames, "Absolute Calibration of a Light Detector," J. Opt. Soc. Am., 51, 224 (1961).

22. W.E. Danforth, "Thorium Oxide in Electronics," *Advances in Electronics,* Vol. 5, Academic Press, New York (1953).

23. I.E. Campbell, Ed., *High Temperature Technology,* John Wiley & Sons, New York (1956).

24. F.W. Norton, *Refractories,* 3rd. Ed., McGraw-Hill, New York (1949).

25. J.B. Wachtman, "Mechanical and Electrical Relaxation in ThO_2 Containing CaO," Phys. Rev., 131, 517 (1963).

26. O.A. Weinreich and W.E. Danforth, "Optical Properties of Crystalline Thoria," Phys. Rev., 88, 953 (1952).

27. J.L. Bates, *The Absorption Spectra of Thorium Dioxide,* AEC Report, BNWL-457 (1967).

28. R.C. Linares, "Growth and Properties of CeO_2 and ThO_2 Single Crystals," J. Phys. Chem. Solids, 28, 1285 (1967).

29. E.H. Greener, W.M. Hirthe, and E. Angino, "Thermoluminescence of Thoria," J. Chem. Phys., 36, 1105 (1962).

30. C.B. Finch, L.J. Nugent, G.K. Werner, and M.M. Abraham, "Self-Excited Thermoluminescence and Optical Bleaching in Rare Earth Doped Thorium Dioxide Crystals," Seventh Rare-Earth Research Conference, San Diego, Calif. (Oct. 1968) (Unpublished).

31. A.K. Trofimov, "Luminescence of Lanthanides in ThO_2" Izv. Akad. Nauk. S.S.S.R., Ser. Fiz., 25, 460 (1961).

32. A. Neaves and G.S. Tint, *Defect Structure of Ionic Materials by Electron Paramagnetic Resonance and Nuclear Magnetic Resonance,* Technical Documentary Report, ARL 69-0071 (1969).

33. M.M. Abraham, R.A. Weeks. G.W. Clark, and C.B. Finch, "Electron Spin Resonance of Rare Earth Ions in Thorium Oxide," Phys. Rev., 137, A138 (1965).

34. M.M. Abraham, E.J. Lee, and R.A. Weeks, "Paramagnetic Resonance of Gd^{3+} in ThO_2 Single Crystals," J. Phys. Chem. Solids, 26, 1249 (1965).

35. M.M. Abraham, C.B. Finch, and G.W. Clark, "Electron Spin Resonance of Tripositive Curium in ThO_2 and CeO_2," Phys. Rev., 168, 933 (1968).

36. M.M. Abraham, C.B. Finch, R.W. Reynolds, and H. Zeldes," ESR Spectrum of Divalent Europium in Thorium Dioxide," Phys. Rev., 187, 451 (1969).

37. S.A. Marshall, "Isotopic Shift in the Electron Spin Resonance Absorption Spectrum of Gd^{3+} in Thorium Dioxide," Phys. Rev., 159, 191 (1967).

38. W. Low and D. Shaltiel, "Paramagnetic Resonance Spectrum of Gadolinium in Single Crystals of Thorium Oxide," J. Phys. Chem. Solids, 6, 315 (1958).

39. V.I. Neeley, J.B. Gruber, and W.J. Gray, "F Centers in Thorium Oxide," Phys. Rev., 158, 809 (1967).

40. C.B. Finch and G. Wayne Clark, "Single Crystal Growth of Thorium Dioxide from Lithium Ditungstate Solvent," J. Appl. Phys., 36, 2143 (1965).

41. Norton Co. Chippawa, Ontario.

42. Electronic Space Products, In., 854 So. Robertson, Los Angeles, Calif.

43. E.T. Rodine and P.L.Land, "Fluorescence of Rare Earth Ions in ThO_2," (to be published).

44. J. Nahum and A. Halperin, "Thermoluminescence and the Relation Between Thermal and Optical Activation Energies in Diamond," J. Phys. Chem. Solids, 24, 823 (1963).

45. G.S. Tint, PhD Dissertation, Department of Physics, Temple University, Philadelphia, Penn., (unpublished) 1970.

46. W. Hayes and J.W. Twidell, "The Self-Trapped Hole in CaF_2 ," Proc. Phys. Soc. (London), 79, 1295 (1962).

47. John E. Wertz and Peteris Auzins, "Crystal Vacancy Evidence from Electron Spin Resonance," Phys. Rev. 106, 484 (1957).

48. J.E. Wertz, G.S. Saville, L. Hall, and P. Auzins, "Point Defects in Magnesium Oxide," Proc. Crit. Ceram. Soc., 1, 59 (1964).

49. R.C. Linares, "Fluorescent Properties of Trivalent Rare Earths in Fluorite Structure Oxides," J. Opt. Soc. Am., 56, 1700 (1966).

50. W.L. Wanmeker, A. Bril and J.W. terVrugt, "Sensitization of Tb^{3+} Luminescence by Sn^{2+} and Cu^{+} in Alkaline Earth Phosphates," Appl. Phys. Letters, 8, 260 (1966).

51. C.G.B. Garrett and W.K. Kaiser, "Terbium and Cerium Activated Calcium Fluoride Optical Maser Material," U.S. Patent 3.079.347 (1963).

52. W.L. Wanmaker, A. Bril, and J.W, terVrugt, "Fluorescent Properties of Terium-Activated Alkaline Earth Alkaline Borates," J. Electrochem. Soc. 112, 1147 (1965).

53. Rinoud Hanna, "Lattice Energy of Some Cubic Crystals," J. Phys. Chem. 69, 2971 (1965).

54. Frederick Seitz, *The Modern Theory of Solids*, McGraw-Hill, New York (1940).

55. B.G. Wybourne, *Spectroscopic Properties of Rare Earths*, Interscience Publishers, New York (1965).

Unclassified
Security Classification

DOCUMENT CONTROL DATA - R & D

(Security classification of title, body of abstract and indexing annotation must be entered when the overall report is classified)

1. ORIGINATING ACTIVITY *(Corporate author)*
SYSTEMS RESEARCH LABORATORIES, INC.
7001 Indian Ripple Road
Dayton, Ohio 45440

2a. REPORT SECURITY CLASSIFICATION

2b. GROUP

3. REPORT TITLE

THERMOLUMINESCENCE OF THORIUM OXIDE SINGLE CRYSTALS

4. DESCRIPTIVE NOTES *(Type of report and inclusive dates)*
Scientific. Interim.

5. AUTHOR(S) *(First name, middle initial, last name)*

Elward T. Rodine

6. REPORT DATE	7a. TOTAL NO. OF PAGES	7b. NO. OF REFS
August 1970	128	55

8a. CONTRACT OR GRANT NO.
AF33615-69-C-1017
b. PROJECT NO. 7021
c. DoD Element 61102F
d. DoD Subelement 681306

9a. ORIGINATOR'S REPORT NUMBER(S)

9b. OTHER REPORT NO(S) *(Any other numbers that may be assigned this report)*
ARL 70-0138

10. DISTRIBUTION STATEMENT

1. This document has been approved for public release and sale; its distribution is unlimited.

11. SUPPLEMENTARY NOTES

TECH OTHER

12. SPONSORING MILITARY ACTIVITY

Aerospace Research Laboratories (ARZ)
Wright-Patterson AFB, Ohio 45433

13. ABSTRACT

This report contains the results of measurements of the thermoluminescence (TL) between liquid nitrogen temperature and 300°C of a large number of ThO_2 single crystals. These results indicate that the same traps occur commonly in crystals grown by different methods and which differ considerably in purity. The maxima of the TL excitation spectra and the ultraviolet cutoff are shown to coincide, indicating that some trap excitation involves a band gap transition and that the band gap is 5.75 eV. The TL emission spectra observed here are quite broad in some cases but in other cases they are the sharp line spectra of particular rare earths. The flourescence emission for some of these ThO_2 crystals appears to be identical to the TL emmision. Dosage studies show cases of linear and quadratic growth of TL with dose. Excitation due to the radioactivity of thorium is observed in some of these crystals. Energy and frequency factor analysis of the trapping states is performed, and comparison is made between the results obtained by applying the methods of initial rise, inflection points, and halfwidths. The TL experiments are correlated with EPR measurements. This investigation shows that as few as 10^{10} optical transitions are necessary for a resolvable glow peak and that concentrations of rare earth impurities of less than 1 ppm may result in bright TL. There are strong indications that the trapping states are due to intrinsic defects involving oxygen vacancies, and several models are proposed and correlated with the experimental results.

DD FORM 1 NOV 65 1473

Unclassified
Security Classification

Security Classification

14. KEY WORDS	LINK A		LINK B		LINK C	
	ROLE	WT	ROLE	WT	ROLE	WT
Thermoluminescence						
Thorium Oxide						
Refractory Oxides						
Point Defects						
Rare Earth Emission						

Security Classification